Cellular Interaction with Novel Biomaterials

CHRISTOPHER DAVID GRAHAM

Doctor of Philosophy

ASTON UNIVERSITY

October 1998

Aston University

Cellular Interaction with Novel Biomaterials

Chistopher David Graham

Doctor of Philosophy
1997

Summary

The objective of this thesis is to report the behaviour of mammalian cells with biocompatible synthetic polymers with potential for applications to the human body.

Composite hydrogel materials were tested as possible keratoprosthetic devices. It was found that surface topography is an important consideration, pores, channels and fibres exposed on the surface of the hydrogels tested can have significant effects on the extent of cell adhesion and proliferation. It is recommended that the core component be fabricated out of one of the following to provide a non cell adhesive base; AMO:EEMA:MEMA, THFFMA:NVP:PU, THFFMA:AMO:CAB, or Acrylamide:HPA:PU:THFFMA:AMO. The haptic periphery fabricated out of one of the following would provide a cell adhesive composite; THFFMA:AMO:PU (polymerised around NaCa alginate), AMO:EEMA:MEMA:THFFMA with hydroxyapatite, AMO:EEMA:MEMA:THFFMA with dextrin and dextran, or AMO:EEMA:MEMA:THFFMA with hydroxapatite whiskers.

The presence of vitronectin in the ocular tissue appears to lead to higher cell adhesion to the posterior surface of a contact lens when compared with the anterior surface. Group IV contact lenses adhere more cells than Group II contact lenses which may indicate that more protein (including vitronectin) is able to adhere to the contact lens due to the Group IV contact lens properties of high water content and ionic hydrogel matrix.

Artificial lung surfactant protein analogues were found to be non cytotoxic but also decreased cell proliferation when tested at higher concentrations. Poly(lysine ethyl ester adipamide) [PLETESA] had the most favourable response on cell proliferation and commercial styrene/maleic anhydride (pMA/STY sp^2) the most pronounced inhibitory response. The mode of action that decreases cell proliferation appears to be through membrane destabilization. Tissue culture well plates coated with PLETESA allowed cells to adhere in a concentration dependent manner, vesicles possibly of PLETESA were observed in solution in PLETESA coated wells.

Polyhydroxybutryate (PHB) and polyhydroxyvalerate (PHV) blends that contained hydroxyapatite were found to be the most cell adhesive material of those materials tested. The blends that were most susceptible to degradation adhered the most cells in initial stages of degradation. The initial slight increase in cell adhesion may be due to the increased rugosity of the material. As the degradation continued the number of cells adhering to the samples decreased, this may indicate that the polarity was inhibitory to cell adhesion during the later stages of degradation.

Keywords: biomaterial, cell adhesion, cell proliferation, cytotoxicity

Acknowledgements

I would like to thank my parents for their support and to thank the staff and post doctorates of the Biomaterials Research Unit for help and advice in production of this thesis. These include Vincent Rebeix for computer support, Sue Rudd for chasing up lose ends and in particular, Steve Tonge, Mohammed Yasin and Brian Tighe for countless hours spent reading the draft copies.

I would like to acknowledge the financial support of the Engineering and Physical Sciences Research Council

Index

List of Tables

List of Figures

List of Plates

Abbreviations

Antibody	Ab
Acrylmorpholine	AMO
Azo-bis-isobutyro-nitrile	AZBN
Cellulose acetate butyrate	CAB
Dextrin	DEX
Dipalmitoyl phosphatidyl choline	DPPC
Ethylenediaminetetraacetic acid	EDTA
Ethoxy ethyl methacrylate	EEMA
Equilibrium water content	EWC
Fibronectin	Fn
Foetal bovine serum	FBS
Hydroxyapatite sphere	Hap
Hydroxyapatite whiskers	Hap W
HEPES buffered solution	HBS
2-hydroxyethyl methacrylate	HEMA
Hydroxy propyl acrylate	HPA
Methacrylic acid	MA
Methoxy ethyl methacrylate	MEMA
Magnesium chloride	MgCl
Methyl methacrylate	MMA
Manganese chloride	MnCl
N-vinyl pyrrolidone	NVP
Phosphate buffered saline	PBS
Poly(hydroxybutyrate)	PHB
Poly(hydroxyvalerate)	PHV
Poly(lysine ethyl ester adipamide)	PLETESA
Styrene/maleic anhydrate copolymer	PSTY/MA
Polyurethane	PU
Standard deviation	SD
Styrene maleic anhydride	STY/MA
Tissue culture polystyrene	TCPS
Tetrahydrofurfuryl methacrylate	THFFMA
Vitronectin	Vn

CHAPTER ONE
Literature Review

1.1 Introduction

Materials that are intended for biocompatible usage are usually tested extensively for their chemical and physical properties at the design stage, yet, cytotoxicity studies although carried out are understated in their importance, sometimes only carried out after materials have been developed. The interaction of cells with materials *in vitro* prior to use in animal trials should be investigated fully because animal trials are expensive, time consuming and can be subject to ethical debate. The resources spent investigating inappropriate materials that have reached animal trails could be reduced if *in vitro* cell culture studies are employed first. For example, the materials described in this thesis for the keratoprosthetic device would have been tested in an animal model solely dependent on the materials physical parameters if the cell culture studies described in this thesis had not been carried out. *In vitro* cell culture models would give an indication of the possible effect the materials and their residual monomers would have when exposed to cells and may allow unsuitable materials during the design procedure to be eliminated before animal trials are embarked.

Investigation of novel biomaterials needs a balanced approach that researches the chemical, physical and biological interactions in a co-ordinated manner. To produce safe and reliable biocompatible products there is a greater need to understand all the factors involved in the interaction between the body and synthetic materials. The aim of this thesis is to report the behaviour of mammalian cells with potentially biocompatible materials in a variety of projects. The project researchers are involved in the investigation of the interaction of synthetic polymers with the body and the work presented here is planned to facilitate the future development and the design of their research by providing the researchers with an indication of how cells interact with certain synthetic materials.

Cells can be used as probes to investigate the propensity of materials to support cell adhesion and proliferation. In addition, cell culture can be used as a simple test for cytotoxicity of materials and their eluted components. Here, cell culture has been used with a number of materials to investigate the following:

- Cell adhesion to hydrogels for production of a non-cell adhesive core and cell adhesive skirt of a keratoprosthetic device.

- The propensity for the cell adhesive protein vitronectin to induce cell adhesion on hydrogels used for contact lenses. In addition, to observe how *in vitro* experimentation differs from the *in vivo* situation.

- Investigation of the cytotoxicity of a novel artificial surfactant, upon alveolar cells, proposed as an inexpensive synthetic lung surfactant for premature babies who do not produce lung surfactant.

- The potential for cells to be used as an indicator of the extent of degradation caused by physiological conditions on polyhydroxybutyrate and polyhydroxyvalerate blends containing polysaccharide fillers. This is because cells have the tendency to have different cell adhesion to materials with only slightly different surface topology.

1.2 Cell Adhesion Theory

The two main theories for cell adhesion are the contact hypothesis and colloidal stability theory:

The contact hypothesis states that 'close range intermolecular forces include not only dipole forces and electrostatic forces but also hydrogen bonds and hydrophilic bonds and that all these factors contribute to cell adhesion.[1] In addition, the forces involved in close interfacial contact are also assumed to contribute to surface energy. Therefore surfaces should be graded according to surface energy parameters as measured by the wettability of various liquids, with cells adhering more efficiently to hydrophilic than hydrophobic surfaces.[2,3] If a drop of water is placed on the surface of a solid there will be the creation of a liquid-solid interface with a resulting interfacial energy. If the surface energy is high then there will the tendency for the liquid to spread, the higher the energy the lower the contact angle.

The colloidal stability theory for cell adhesion (DLVO theory) states that there is a balance between long range electrostatic repulsion from negative charge groups on the cell surface and electromagnetic attraction due to fluctuations in dipole moments both on the cell surface and in the intervening medium.[2] This can affect cells suspended 1-10nm above the surface.[2,3]

It is generally agreed that hydrophilic surfaces (wettable) are better in providing adhesion than hydrophobic (non wettable surfaces).[4] Fitton states that there is a general agreement that the more hydrophobic surfaces are, then the greater will be the denaturation of adsorbed proteins. 'This is most probably due to the fact that proteins do not desorb as easily as from hydrophobic surfaces, due to greater conformational changes in adsorbed proteins'. Fitton also states that 'Hydrophilic surfaces have polar forces at the surface which hydrogen bond with water and the water molecules orient around the polar groups. Hydrophilic surfaces tend to cause an 'ice-like' configuration of water molecules at the surface'.[5]

However, wettability is not the sole criteria for cell adhesion. A number of physio-chemical properties have also been put forward as being involved in mediating cell behaviour; rugosity, polarity (electrostatic repulsion between charged groups), surface charge, hydrogen bonds and chemical group expression such as between amide bonds.[2]

The charge on a material can have a significant influence. Although cells are able to attach and grow on glass if it contains a slight negative charge positively charged polymer surfaces will also bind to the cell membrane increasing cell adhesion in culture systems.[6] However, it should be noted that it is believed that surfaces with a high positive charge are toxic to cells, the cytotoxicity produced by positive charge is thought to be able to disrupt the cell membrane.[5] This can be measured by the zeta (ζ) potential, which can be measured by the electric potential recorded between two electrodes. For example, Hela 33 cells have been found to adhere to materials with a ζ potential of > -60mV and are unable to adhere or to proliferate at positive ζ potentials.[7]

1.3 The Mechanism of Cell Adhesion

Cells contained in suspension above a surface will first contact the surface with microextensions of the cell membrane.[8] These cytoplasmic microextensions can help to overcome electrostatic forces particularly if the negatively charged cell encounters a negatively charged surface. The microextensions from the cell develop into protuberances called filopodia. Once in contact with a material the filopodia start to extend and spread over the material and the spaces between filopodia are filled with cytoplasm transforming into sheets of cytoplasm called lamellapodia.

The points of contact with a surface are called focal contacts and consist of approximately 1-2% of the total cell protein and 5-10% of the polysaccharide, most of which are in the form of glycosaminoglycans. It is at focal attachments that extracellular matrix proteins establish a bridgehead where cells can stick and remain attached to the surface, Figure 1.1. These proteins act as mediators and foundations for further cell adhesion. If a surface has already been coated with either extracellular matrix proteins artificially adsorbed or secreted from cells that had previously been in contact with the surface, or from serum proteins that have adsorbed to the surface, this facilitates the process of cell adhesion.[9] When cells form a confluent layer they do so through a variety of adhesion mechanisms. Gumbiner and Lauffenburger *et al.* provide a good review of these cell adhesion mechanisms and how they are associated with cell motility.[10,11]

Figure 1.1 Diagram of the possible organisation of cell adhesion to materials

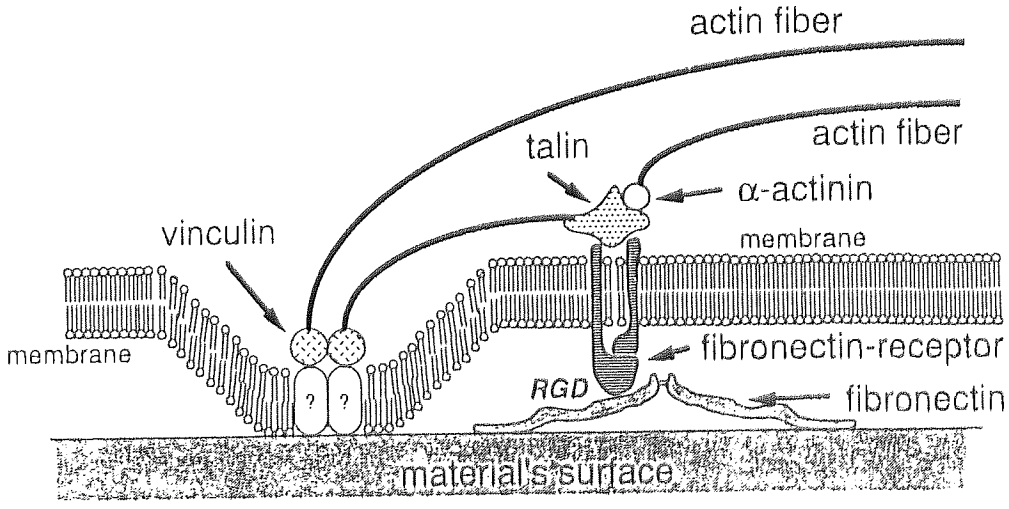

1.4 Cell Motility

When cells migrate, the leading edge of the cell extends filopodia, which when in contact with a surface may set down focal attachments, Figure1.2.[12] The cell gradually creeps forward thickening out the filopodia and as the endoplasm streams forward it becomes rigid and the filopodia are engulfed by endoplasm to form a sheet like lamellapodium. The cell does not adhere solidly to the surface, but only at the focal attachments. These are maintained until they reach the end of the cell where they are broken off.[11] Often parts of the extracellular matrix of the cell are left behind, as can be seen in Figure 1.2. The usual rate of cell progression is 0.5-4.6μm per minute, although this can be modified by temperature and the rate of cell metabolism.

Figure 1.2 Scanning electron micrograph of a cultured cell spreading

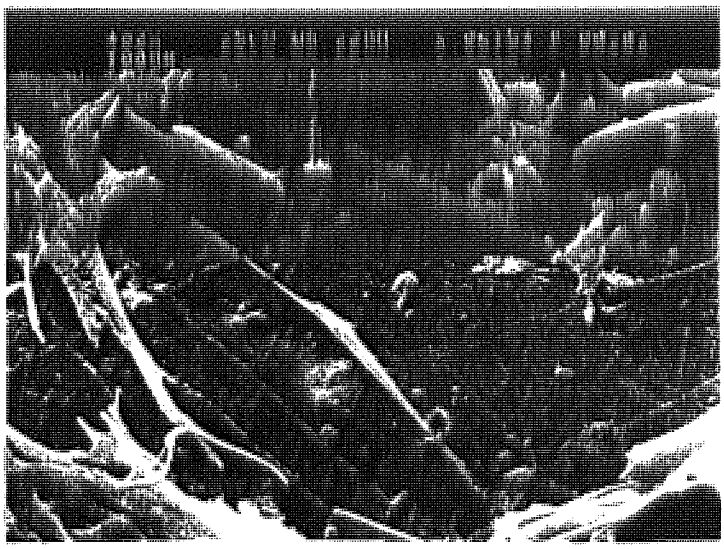

1.5 Surface Energy

The concept of surface energy can be used to describe the propensity of a material to spread water on its surface. The total surface energy can be shown as:

$$\gamma_t = \gamma_p + \gamma_d$$

γ_p polar component of surface energy (polar force of the surface free energy of a surface)

γ_d dispersive component of surface energy (or non-polar component)

γ_t total surface energy

It is generally agreed that the surface free energy of a polymer is important in determining the biocompatibility of that material. Materials that are wettable or hydrophilic are generally more cell adhesive than hydrophobic or non-wettable materials. For example, untreated polystyrene does not adhere cells significantly, it has a polar component of surface energy (γ_p) of 1.9 dynes/cm^2 and a dispersive component of surface energy of (γ_d) of 40.2 dynes/cm^2. When more cell adhesive materials, such as gas plasma treated polystyrene are measured, it is observed that although γ_d is very similar (for gas plasma treated polystyrene 33.7 dynes/cm^2) γ_p increases markedly (for gas plasma treated polystyrene 32.9 dynes/cm^2). This can be explained in part by the Wenzel effect; as γ_p increases, rugosity also increases and this allows the wettability of a material to increase.[2] Increasing the number of hydroxyl or carboxyl groups on a surface of a material, used as an alternative to utilizing gas plasma treatment, will increase the surface energy of the material, yet, not affect the rugosity of the surface.[13]

Lydon *et al.* stated that non polar polymers with low surface energy may still support cell attachment and spreading, possibly due to the surface morphology of the material, where materials that exhibit unexpected cell adhesion possess crystalline morphology, e.g. polyhydroxybutyate and polyhydroxyvalerate blends containing polysaccharides.[14]

A parallel can be found between fractional polarity and wettability in cell adhesion:

$$\text{Fractional Polarity} = \frac{\gamma_p}{\gamma_p + \gamma_d}$$

Lydon *et al.* states that there is a strong correlation between the equilibrium water content (EWC) and fractional polarity. Polystyrene has a very low fractional polarity and has a low cell adhesive potential, whereas tissue culture polystyrene has a higher fractional polarity and is more effective at cell adhesion.[14]

Wettability of a material can be determined by measurement of the contact angle that the material makes with water. However, measurement of the wettability of a hydrogel is harder than of a conventional polymer because of dehydration in the

hydrogel, causing movement of water and water-soluble compounds, such as oxygen, between the hydrogel and water that produces variability in contact angle measurement.

1.6 Biomaterials

The definitions of a biomaterial and of biocompatibility are dependent on how the material is planned to be incorporated and tolerated *in vivo*. For example, the minimum interfacial energy hypothesis defines a biomaterial as a material that exhibits maximum biocompatibility and possesses a low interfacial tension with the biological system, however, this hypothesis will not hold true for every material classified as a biomaterial. Here in this thesis a biomaterial is defined as a material intended to interface with a biological system and to treat, augment or replace any tissue, organ or function of the body. Biocompatibility, may be divided into cytotoxicity, concerned with the leaching of toxic chemicals from the material and cytocompatibility, concerned with electrochemical, micromorphological and physical characteristics of material surfaces.[5] In this thesis I will define a biocompatible material, although the definition will be limited to cell response, as a material that may or may not be cell adhesive, but does not exhibit a cytotoxic response or release cytotoxic materials into cells that are in contact with the material or release cytotoxic materials into the medium.

Cytotoxicity is not easily defined, the definition can range from cell death to metabolic abnormalities. Survival can be an instantaneous measurement; it is usually the integrity of the plasma membrane and the long term continuance of a cell line, however, the definition again varies depending on the study involved.

1.7 Considerations on Assessing Cytotoxicity

Test materials for clinical trials are generally implanted into animals. However, this type of *in vivo* test is expensive, time consuming and the UK Home Office licence to undertake such testing is restricted to limit the excessive use of animal experimentation.

Cytotoxicity assays that use cells can be divided into two groups; immediate or short term response and long term survival measuring self renewal capacity or survivability. The short term assay determines the viability of cells after some form of shock. Most viability tests rely on membrane integrity, with non viable cells with damaged membranes taking up a dye to which viable cells are impermeable. Short term tests only demonstrate whether cells are dead at the time of the assay. Cells frequently will go into a decline that would not be detected by such a short term assay e.g. neoplastic drugs may only show their effects after hours or even days later. Long term tests are often used to determine the metabolic or proliferative capacity of cells after exposure to a toxic influence. While *in vitro* tests give a quantitative evaluation over short periods of time and can take the place of *in vivo* testing in initial studies, they are not a complete substitution because the *in vitro* assay is a purely cellular event and does not involve a multicellular organism. Individual cells are unable to perform elimination of metabolites and toxic materials, as there are no clearance systems such as vascular and renal systems. Compared with the situation *in vivo*, there can be

significant differences in drug exposure time, rate of change of concentration, cell metabolism, tissue penetration, clearance and excretion. Many substances become toxic or concentrated only after metabolism by the liver. It must therefore be shown that drugs reaching cells *in vitro* are in the same form as those reaching cells *in vivo*. A toxic response *in vitro* can only be measured in terms of cell survival, cell division or metabolism changes. Whereas *in vivo* the tissue may have an alternative response including, inflammatory reaction or fibrosis, e.g. long term *in vivo* inflammation reaction to polyglycolic acid. In addition, cell strains *in vitro* have a finite life span before they become adapted to the *in vitro* conditions and become atypical cells compared with the source tissue present *in vivo*.

1.8 ISO 10993 Guidelines

The investigation of the materials assessed in this thesis used ISO 10993 guidelines to help define a scheme for testing *in vitro* cellular cytotoxicity for materials that are "in contact with a device".[15] The assessment evaluation involves; assessments of cell damage by morphological means, measurements of cell damage and measurements of cell growth.

It is required that a number of strict conditions are applied to validate the assessment and ensure that the control conditions are maintained.[15] Materials require at least one surface to allow the material to lay parallel in the well plate and to allow cells to settle evenly over a material. Materials that are packaged in sterile conditions before aseptic implantation are to be handled aseptically. Mammalian cell cultures used as the cell source are examined to determine morphology and contamination throughout the tests and appropriate incubation and buffering systems are to be used. It is recommended that for direct contact studies mouse fibroblast cell lines can be used.[4]

Negative controls should be incorporated into the assay to give an indication of the potential background response of the cells. In addition, a positive control material, with a reduced propensity for cells to adhere and to proliferate onto its surface should be incorporated into the assay. The positive control shows that an inhibitory response can be induced in the cell line used. If the cells are more resistant to cytotoxic shock than cells encountered *in vivo*, a false indication of the cytotoxicity of the material would be given. If, however, there are evident differences between the control and materials tested in the results then the test may be either invalid or inappropriate.

Membrane damage can be used to measure cell viability, estimated by colorimetric measures, such as by the use of Exclusion Dye (dead cells stain) techniques, e.g. Trypan Blue, or Supravital Dye (live cells stained) e.g. Neutral Red.[16] Depending on the fraction of the cell population stained, the dyes can give a quantitative indication of the number of living cells. Cell populations that display a viability of lower than 70% after contact with a substrate may indicate cytotoxicity.

CHAPTER TWO
Cellular Adhesion to Keratoprosthetic Components

2.1 Aim

The aim of this chapter is a preliminary review to investigate the cell adhesion, cell proliferation properties and cytotoxicity of a number of hydrogels for possible incorporation into keratoprosthetic devices. Two components are needed to produce a functioning keratoprosthesis, a clear optical core that is non-cell adhesive and a peripheral (haptic) skirt that supports cell adhesion and integration. The design envisaged would consist of a full thickness contact lens for the core with a porous hydrogel skirt made to resemble the Strampelli Osteo-Odonto-Keratoprosthesis (OOK).

2.2 Introduction

2.2.1 Keratoprosthetic Implants

Keratoprosthetic devices are used when it is not feasible to carry out a corneal transplant e.g. when there is a possible risk of rejection or when the anatomic integrity of the eye has been damaged. The use of artificial implants also eliminates the risk of transmission of infectious disease such as Human Immunodeficiency Virus (HIV) and Hepatitis B. Typically, the implant consists of a visual optical core supported in the cornea by a haptic peripheral component.

Existing keratoprosthetic devices are designed predominately to resemble a mushroom shaped device. Some designs have the haptic skirt threaded into the optical core whilst in other designs the skirt is more permanently fixed. The current trend is to use polymeric materials for both components of the keratoprosthetic device e.g. HEMA. However the haptic skirt construction varies depending on the design and often incorporate fibrous synthetic materials or osseous autologous biological material to improve tissue integration.[17]

A keratoprosthetic device (Kpro) must be securely attached to the surrounding cornea. The Kpro also requires the periphery of the device (constructed of a porous material) to be penetrated by stromal fibroblasts which will proliferate and synthesize connective tissue proteins. This allows natural healing and anchorage to take place.[18]

The material for the central optical core must allow full light transmission, ideally with ultraviolet filtering. Typically, the field of vision provided by the optical core is 30°.[19] It must also exhibit an elastic and tensile strength similar to that of the cornea. The optical core needs to protrude from the front and back of the cornea for vision to be maintained and to avoid the overgrowth of keratocyte cells or the downgrowth of epithelial cells. Long-term success of keratoprosthetic devices requires that the perforating plastic optical core is stabilized within the cornea.[17] A Kpro has to pass through the eyelid of the patient hence, there is often a need to remove the crystalline lens, iris, tarsis and partial removal of the vitreous body. In addition, the ocular muscles that create tension in the eyelid need to be excised and the eyelid has to be sutured.[19]

Not only does the peripheral portion of a keratoprosthesis need to stabilise the optical cylinder so as to maintain the optic core in a correct position in the cornea, the periphery needs to be flexible and resistant to stresses and also act as a barrier to epithelial down growth. The haptic component, however, is also required to be sufficiently porous to allow keratocyte ingrowth so that adhesion, migration and replication of host epithelium can take place. The periphery must not interfere with the normal metabolic actions of the cells making up the eye and elicit, at the most, only a limited inflammatory response. The peripherary must encourage the ingrowth of fibrous tissues from the adjacent rim of the host cornea and support the tissues continued viability.

Virtually all keratoprosthetic devices have suffered from complication, usually at the plastic-tissue interface. Typical KPro complications are; tissue necrosis "corneal melting" around the perforating impervious plastic optical core, due to enzymatic degradation of stromal collagen.[17] Leakage of aqueous humour around the KPro. Downgrowth of surface epithelium with subsequent implant encapsulation and extrusion or epithelization of the anterior chamber. Fibrous or inflammatory retroprosthetic membrane formation with or without opacification of the visual axis.[20]

Gradual ulceration (melting) is most likely to be the direct result of the local release of proteolytic enzymes such as collagenases and proteases probably released from polymorphonuclear leukocytes.[21] If this inflammation is severe, leukocytes can also pass into the tear film from dilated conjunctival capillaries. If at the same time, the inflammation has caused an epithelial defect in the cornea, the leukocytes in the tear film can adhere in large numbers to the naked stromal surface within the defect. The subsequent release of proteolytic enzymes at the site of keratoprosthetic attachment can cause digestion of the basal membrane and lead to keratoprosthetic extrusion and stromal perforation.[22]

Keratoprosthetic implants have been shown to have more success when the anterior prosthetic surface is covered by autologous materials e.g. the conjunctiva or buccal mucosa [19] Surface coating allows poly methyl methacrylate (pMMA) to escape recognition as a foreign body and in theory, the inflammatory response may be reduced. This leads to a minimization of necrotic tissue. Coating with a biological substrate such as collagen also demonstrates less post-operative necrosis in adjacent tissue.[20] In addition, collagen coated implants are surrounded by a more orderly lamellar stroma with collagen fibrils connecting keratocyte cell surfaces to coated surfaces and uncoated stromal fragments preferentially remaining attached to the coated surface of the keratoprosthesis.[20]

Coating appears to improve Kpro device attachment as the coating acts to smooth the "rough" artificial substrate surface and decrease implant antigenicity. Uncoated Kpro's have a greater inflammatory response than coated KPro, where inflammatory cells are most highly concentrated in the stroma, immediately adjacent to uncoated implants.[20] Patients with edema or scarring of the cornea but with little inflammation exhibit favourable prognosis with a corneal prosthesis.[23,24]

The body's response to implant material is the production of capsular or scar tissue in an attempt to isolate the implant. "Absence of a capsule around a porous polymer

confirms that there is no physical impedance to cellular invasion and therefore the creation of a tight junction between host tissue and implant indicates that extrusion of the implant over time is unlikely".[23]

2.2.2 Osteo-Odonto-Keratoprosthesis

The Osteo-Odonto-Keratoprosthesis (OOK) is a keratoprosthetic device using autologous biological materials. Created by Strampelli in 1963, Strampelli theorized that the materials would be better tolerated than artificial material used previously as only biological materials from the host were in direct contact with tissue. In addition, he theorized that toxicity to plastic materials could contribute significantly to the extrusion of corneas.[17] The Osteo-Odonto-Keratoprosthesis is employed when corneal transplantation is not feasible due to risk of rejection, such as in alkali burns or dry eye conditions.

The prosthetic device comprises of a section of the patient's tooth moulded into a disc supporting an acrylic optical cylinder, Figure 2.1. The acrylic lens cylinder is typically 9mm in length with 3.5mm of the cylinder extending behind the posterior surface of the cornea. A 2.5mm diameter lens is sufficient to give a sufficient optical image.

Figure 2.1 Schematic of a keratoprosthetic device (Doane, M.G., Dohlman, C.H. and Bearse, G., 1996, Fabrication of a keratoprosthesis. Cornea, 15, 2, 179-184)

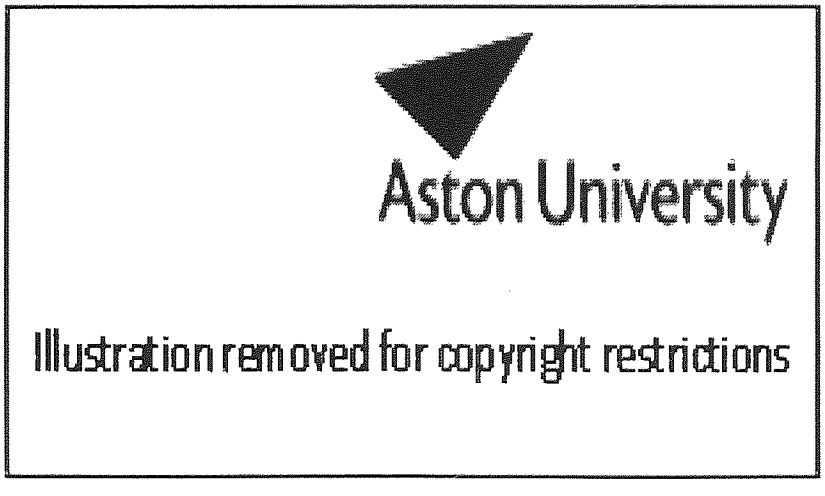

The steps in OOK insertion are described in Marchi et al:[25]

1. The osteodental acrylic lamina (ODAL) is prepared by removing a monocuspid tooth, preferably a canine, with part of the maxillary bone and some of the tooth's apical root still remaining. The apical part of the tooth is removed with the remaining tooth cross-sectioned to obtain a lamina of the alveolar bone and half of the dental root. The tooth is further modelled to fit the optical cylinder of the keratoprosthetic device so that the optical cylinder fits through the tooth periphery. The tooth and optical cylinder composite are then placed in a surgically created pocket in the lower eyelid for three months.

2. The corneal epithelium of the eye is removed and the eyeball is covered with a buccal mucosa strip from the upper or lower lip.

3. The ODAL is removed from the cutaneous pocket and cleansed of cellular tissue adhering to the optical cylinder, leaving tissue incorporated only over the tooth root surface.

4. The ODAL is implanted on the bulbar surface. The buccal mucosa and cornea are cut to create a pocket for the ODAL which is then sutured into place. The anterior portion of the cylinder is passed through the hole within the buccal mucosa. Moderate pressure is exerted through coverage of the eye with bandages and a temporary tarsorrhaphy (protective contact lens), lasting for a three day period, is utilized to allow the tissues to integrate. The pocket is designed to provide a secure environment that also allows autologous biological material to coat the synthetic materials. This coating is thought to improve the biocompatibility of the Kpro when it is implanted into the cornea.

The structure of spongy bone ensures a strong interlocking fit with the buccal mucosa. The interconnected pores provide a framework onto which tissue can be organized. The arrangement of spaces in the bone facilitates the rapid in-growth of fibroblasts and keratocytes and creates an interlocking network of soft connective tissue and vascular systems. Eventually this allows the host corneal epithelium to grow over and adhere to the anterior surface creating a wettable surface. The peridontal ligament that attaches the autologous tissue to the KPro is a crucial component of the system because it forms an impervious barrier to cellular infiltration and more importantly inhibits cell proliferation.

Strampelli's OOK has the advantage of ensuring long-term tolerance and acceptance of an acrylic lens. However, the technique utilizes complex surgery and involves the loss of a tooth. Implantation is also dependent on the integration of dental alveolar with the mucous epithelium. In addition, the OOK can lead to an incidence of pronounced corneal infiltration with vascularisation, corneal abscess formation and the extrusion of the implant.

There is additional concern that the bone used in the procedure is liable to reabsorption and one OOK extruded after 12 years was shown to have extensive bone resorption.[23] The resultant fear of bone reabsorption has initiated attempts to

replace the tooth components with glass ceramic by Blencke *et al.* although no discussion on the long term results have been noted.[26]

Figure 2.2 Illustration of a keratoprosthetic implant assembled in a corneal graft.

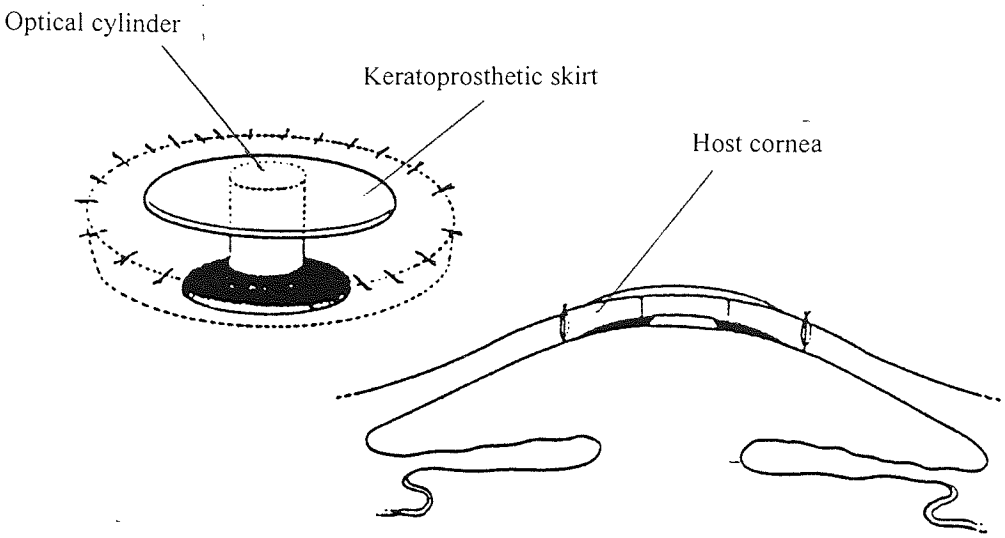

2.2.3 Hydrogels used in Keratoprosthetic Implants

Hydrogels are cross-linked hydrophilic polymers swollen with water which can be fabricated to be flexible and elastic, have good tensile properties or be optically clear. Non porous hydrogels are impervious to the ingrowth of stromal keratocytes and epithelial cells[1]. Hydrogels may however, suffer from the problem of limited resistance to mechanical deformation, such poor tear strength may be caused by the plastizing effect of the water held within the polymer network.[29]

Two components are needed to produce a functioning keratoprosthesis, a clear optical core that is non-cell adhesive and a peripheral (haptic) skirt that supports cell adhesion and integration. Poly (2-hydroxyethyl methacrylate) or p(HEMA) has been used as the central core of keratoprosthetic devices because of its favourable usage as a contact lens and as an intraoccular lens material.[17,27] Poly (2-hydroxyethyl methacrylate) is a non-ionic hydrophilic polymer with favourable physical properties and low cytotoxicity. Poly(HEMA) has the advantages of excellent transmission of light, elasticity, moderate hydrophilic properties and can be made into porous sponges.[29] In addition, Lydon *et al.* reports that certain fibroblastic cells (Chinese Hamster Ovary) are non cell adhesive to p(HEMA).[14] However, long term studies with p(HEMA) implanted subcutaneously in rats, hamsters and guinea pigs appear to show the material to be tumourgenic and susceptible to calcification.[28] There is also the problem of mechanical strength, thus the need to study different hydrogel materials to find a material that exhibits improved optimal properties for inclusion into a keratoprosthetic device.[29]

2.3 Materials

2.3.1 Cell Culture

The 3T3 Swiss Mouse Embryo (ECACC 88031146) cell line used was maintained in Dulbecco's Modified Eagle Medium (DMEM), with 10% foetal bovine serum (Life Technologies) and 400mM/L L-glutamine (Sigma) added to supplement growth. Cells for experimentation were used between passage number 2 and 6 and the cells were sub-cultured at $1x10^4$ cells/ml when confluent. The growth rate 3T3 Swiss Mouse Embryo at the time of use was determined as being $0.23h^{-1}$, Figure 2.3.

Figure 2.3 Growth Curve of 3T3 SME Cell Line

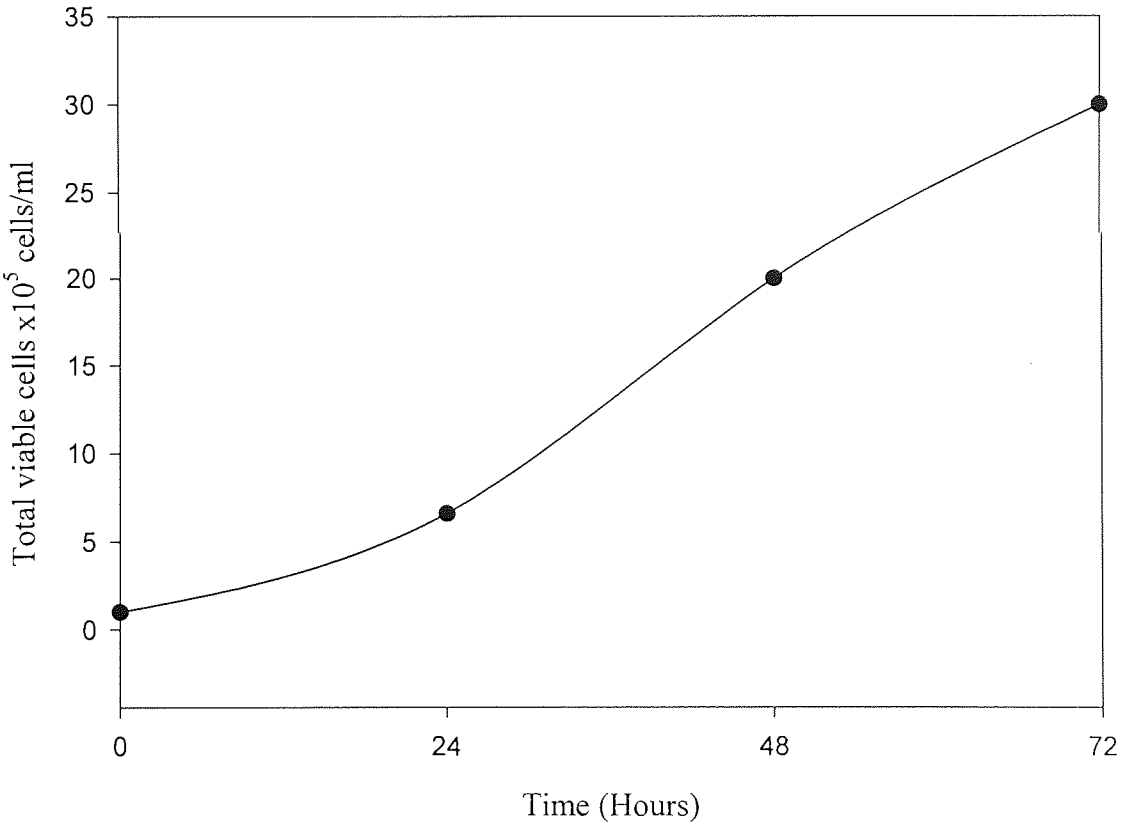

2.3.2 Material Testing for Cell Numbers and Cell Viability

14mm diameter samples were cut from a sheet of the material with a cork borer (number 6) and autoclaved (121°C/15 minutes/2 bar) in distilled water. This was followed by soaking in 1% (v/v) solution of Tween 20 (Sigma) for one hour. The samples were washed aseptically with sterile distilled water before being placed in a well of a tissue culture plastic well plate. The samples were seeded with 1ml of $1x10^5$ cells/ml of 3T3 Swiss Mouse Embryo cells from a confluent culture. Samples were left for 24 hours in a Gallenkamp CO_2 incubator at 37°C and 5% CO_2/95% air atmosphere. Controls included gas plasma treated polystyrene and p(HEMA) to determine the background response of the 3T3 cell growth to a positive and negative control substrate.

After the incubation period, samples were removed from the well plate and washed with sterile phosphate buffered saline pH7.4 (without Ca^{2+} and Mg^{2+}) before being placed into a new well. 1ml of 0.25% trypsin/EDTA solution (Sigma) was added to the well and left to incubate with the sample for ten minutes within the Gallenkamp CO_2 incubator at 37°C and 5% CO_2/95% air atmosphere. Trypsin was neutralized by the addition of 1ml of DMEM (Life Technologies). Cell viability was determined by the Trypan Blue Exclusion test, adding 250µl of cell suspension to 100µl of trypan blue solution (Sigma) before loading the sample onto a haemocytometer, cell counts were taken and the percentage of viable cells calculated. Samples for cell counts were the means of four replicates.

2.3.3 Scanning Electron Microscopy

Samples were prepared for scanning electron microscopy using the same protocol detailed in 2.3.2, however, the incubation period was 72 hours. Cells were fixed with 2% glutaraldehyde (Sigma) in 0.1M sodium cacodylate buffer for thirty minutes. Followed by dehydration through a graded ethanol series (50% v/v ethanol 10 minutes x 3, 70% v/v ethanol 10 minutes x 3, 100% v/v ethanol 10 minutes x3). Samples were dried under liquid freon 113 in a Polaron E3100 II critical point dryer, mounted on aluminium SEM stubs (Biorad) and gold coated in a Polaron splutter coating unit at 1kV and 20mA. Samples were then observed with a Cambridge Stereoscan electron microscope at accelerating voltages of 15-25kV.

2.4 Results

44 hydrogels of different composition were seeded with 3T3 Swiss Mouse Embryo cells as described in 2.3.2. In addition, the hydrogel samples underwent scanning electron microscopic investigation as described in 2.3.3.

The semi quantitative evaluation, of the extent of cellular adhesion and proliferation used the following scaling when fibroblast cells were viewed with a scanning electron microscope (SEM):

0	No cell adhesion
*	Cells were rounded no indication of proliferation
**	Cells adhered and starting to proliferate
***	Increased numbers of cells adhered and proliferating
****	Classical fibroblast morphology proliferating over the whole surface

Quantitative evaluation counted the number of viable and non viable cells under a haemocytometer. Ten counts were taken for each sample and four samples tested for each material. The mean viable cell number and viability of each material was calculated along with the standard deviation. To compare different materials all results of viable cell numbers and cell viability were converted to an index of 100. With the viable cell number and viability of the tissue culture plastic control taken as 100.

2.4.1 Membrane Codes

Dextrin (DEX) was used to produce pores 38-68μm in size and dextran with an average molecular weight of 19,500 was used to produce channels. When the samples were soaked for one week after polymerization any polysaccharides were dissolved out of the hydrogels. Na Ca alginate was added to some of the hydrogels during production to produce an interwoven network of fibres throughout the polymer. Polymer content descriptions are found in Table 2.1.

Table 2.1 Polymer Codes

Code	Hydrogel	Composition	EWC
A1	NVP:MMA:CAB:DEX	45:23:12:20	54.4
A2	THFFMA:NVP:PU:DEX	35:35:10:20	49.7
A3	THFFMA:NVP:PU:DEX	30:35:15:20	45.5
A4	THFFMA:NVP:CAB:DEX	30:30:20:20	43.7
A5	THFFMA:AMO:PU:DEX	35:35:10:20	34.8
A6	THFFMA:AMO:PU:DEX	30:35:15:20	33.0
A7	THFFMA:AMO:CAB:DEX	30:30:20:20	28.3
A8	THFFMA:NVP:PU	41.6:41.6:16.8	20.2
A9	THFFMA:NVP:PU	36.6:41.6:21.8	45.4
A10	THFFMA:NVP:CAB	36.6:36.6:26.8	40.0
A11	THFFMA:AMO:PU	41.6:41.6:16.8	29.9
A12	THFFMA:AMO:PU	36.6:41.6:21.8	47.9
A13	THFFMA:AMO:CAB	36.6:36.6:26.8	23.9
A14	THFFMA:AMO:PU	30:50:20	30.4
A15	THFFMA:AMO:PU:DEX	24:40:16:20	41.6
A16	THFFMA:AMO:PU (Polymerised around NaCa alginate)	30:50:20	N/A
A17	THFFMA:AMO:PU:DEX (Polymerised around NaCa alginate)	24:40:16:20	N/A
A18	THFFMA:AMO:PU	25:60:15	53.7
A19	THFFMA:AMO:PU:DEX	21.25:51:12.75:15	50.0
A20	THFFMA:AMO:PU (Polymerised around NaCa alginate)	25:60:15	N/A
A21	THFFMA:AMO:PU:DEX (Polymerised around NaCa alginate)	21.25:51:12.75:15	N/A
A22	Poly(acrylamide):HPA:PU:THFFMA:AMO	10:10:10:30:40	N/A
A23	AMO:EEMA:MEMA	50:25:25	46.7
A24	AMO:EEMA	50:50	N/A
A25	AMO:MEMA	50:50	N/A
A26	AMO:EEMA:MEMA	20:40:40	7.9
A27	EEMA	100	2.0
A28	MEMA	100	3.3
A29	AMO:EEMA:MEMA:THFMA	25:25:25:25	8.6
A30	AMO:EEMA:MEMA:THFMA:Dextrin:Dextran	25:25:25:25	N/A
A31	AMO:EEMA:MEMA:THFMA:Hap(36μm)	25:25:25:25	N/A
A32	AMO:EEMA:MEMA:THFMA:HA(100μm)	25:25:25:25	N/A
A33	AMO:EEMA:MEMA:THFMA:HA(250μm)	25:25:25:25	N/A
A34	THFFMA:AMO:Pu:Dextrin:Dextran	37:42:21:10:4	N/A
A35	THFFMA:AMO:PU:Hap(36μm)	37:42:21:10	N/A
A36	THFFMA:AMO:PU:Hap(100μm)	37:42:21:10	N/A
A37	THFFMA:AMO:PU:Hap(250μm)	37:42:21:10	N/A
A38	THFFMA:AMO:PU:Dextrin:Dextran	30:50:20:10:4	N/A
A39	THFFMA:AMO:PU: Hap(36μm)	30:50:20:10	N/A
A40	THFFMA:AMO:PU: Hap(100μm)	30:50:20:10	N/A
A41	THFFMA:AMO:PU: Hap(250μm)	30:50:20:10	N/A
A42	AMO:EEMA:MEMA:THFFMA:Hap W	25:25:25:25:10	N/A
A43	THFFMA:AMO:PU:Hap W	37:42:21:10	N/A
A44	THFFMA:AMO:PU:Hap W	30:50:20:10	N/A

Table 2.2 Keratoprosthetic skirt component cell viability and total cell viability of cells stripped off hydrogel candidates for a haptic periphery compared with an index of 100 (TCPS cytotoxicity and cell numbers supported by the polymer = 100)

Code	Hydrogel	Cell numbers (Index 100) ± S.D.	Cytotoxicity (Index 100)	Extent of cell adhesion
TCPS	N/A	100±2	100	****
A1	NVP:MMA:CAB:DEX	44±2	100	*
A2	THFFMA:NVP:PU:DEX	6±0.5	101	*
A3	THFFMA:NVP:PU:DEX	42±2	101	*
A4	THFFMA:NVP:CAB:DEX	2±0.3	101	*
A5	THFFMA:AMO:PU:DEX	26±1	96	*
A6	THFFMA:AMO:PU:DEX	15±0.1	101	*
A7	THFFMA:AMO:CAB:DEX	36±2	97	*
A10	THFFMA:NVP:CAB	5±0.6	101	*
A15	THFFMA:AMO:PU:DEX	75±2	95	*
A16	THFFMA:AMO:PU (Polymerised around NaCa alginate)	39±2	100	**
A17	THFFMA:AMO:PU:DEX (Polymerised around NaCa alginate)	23±2	98	**
A19	THFFMA:AMO:PU:DEX	34±2	93	*
A20	THFFMA:AMO:PU (Polymerised around NaCa alginate)	19±2	93	**
A21	THFFMA:AMO:PU:DEX (Polymerised around NaCa alginate)	28±3	90	**
A30	AMO:EEMA:MEMA:THFMA:Dextrin: Dextran	48±3	100	**
A31	AMO:EEMA:MEMA:THFMA: Hap(36μm)	61±4	97	*
A32	AMO:EEMA:MEMA:THFMA: HA(100μm)	55±2	100	*
A33	AMO:EEMA:MEMA:THFMA: HA(250μm)	57±3	102	**
A34	THFFMA:AMO:Pu:Dextrin:Dextran	45±3	98	*
A35	THFFMA:AMO:PU:Hap(36μm)	48±3	100	*
A36	THFFMA:AMO:PU:Hap(100μm)	62±8	101	*
A37	THFFMA:AMO:PU:Hap(250μm)	73±4	101	*/*** holes
A38	THFFMA:AMO:PU:Dextrin:Dextran	50±2	101	**
A39	THFFMA:AMO:PU: Hap(36μm)	32±3	99	*
A40	THFFMA:AMO:PU: Hap(100μm)	39±2	97	*
A41	THFFMA:AMO:PU: Hap(250μm)	65±2	102	*
A42	AMO:EEMA:MEMA:THFFMA:Hap W	46±1	100	**
A43	THFFMA:AMO:PU:Hap W	85±2	99	**
A44	THFFMA:AMO:PU:Hap W	76±2	99	**
HEMA	N/A	33±3	99	*

Table 2.3 Keratoprosthetic core component cell viability and total cell viability of cells stripped off hydrogel candidates for the optical core compared with an index of 100 (TCPS cytotoxicity and cell numbers supported by the polymer = 100)

Code	Hydrogel	Cell numbers (Index 100) ± S.D.	Cytotoxicity (Index 100)	Extent of cell adhesion
TCPS	N/A	100±2	100	****
A8	THFFMA:NVP:PU	32±2	99	*
A9	THFFMA:NVP:PU	39±2	101	*
A11	THFFMA:AMO:PU	11±7	98	*
A12	THFFMA:AMO:PU	45±3	99	**
A13	THFFMA:AMO:CAB	30±1	101	*
A14	THFFMA:AMO:PU	42±2	94	*
A18	THFFMA:AMO:PU	30±2	96	**
A22	Poly(acrylamide):HPA:PU:THFFMA:AMO	31±2	97	*
A23	AMO:EEMA:MEMA	34±1	96	*
A24	AMO:EEMA	37±2	97	*
A25	AMO:MEMA	49±2	99	0
A26	AMO:EEMA:MEMA	77±2	101	*
A27	EEMA	82±2	100	**
A28	MEMA	71±2	101	*
A29	AMO:EEMA:MEMA:THFMA	67±2	100	**
HEMA	N/A	33±3	99	*

2.4.2 Cell Viability

All core and periphery materials exhibited low cytotoxicity, this implied that contact with the substrate surface was non-toxic and that for all hydrogels there were negligible amounts of residual cytotoxic material, such as monomers from polymerization, released from the materials, Table 2.2 and Table 2.3. The cell counting method used, Trypan Blue Dye Exclusion, would give an overestimate of the viable cell numbers on the samples. As trypan blue will only indicate non-viable cells if the dye is able to penetrate damaged membranes. Those cells that are non-viable, but, with an intact membrane will not be penetrated by the dye and hence, will be determined to be viable. Dead cells should be washed off the materials during the washing stages of the assay. The washing stages were of the same duration and used the same volume of PBS for each assay. This should remove any cells suspended in solution and remove many of the dead cells in the well therefore it can be expected that the viability measurements will tend to be high.

2.4.3 Controls

The tissue culture polystyrene (TCPS) control material exhibited the highest degree of cell adhesion, the extent of spreading and proliferation of the cells followed classical fibroblastic morphology, Plate 2.1. HEMA the negative control, exhibited

a far lower level of cell adhesion with low levels of cell spreading and proliferation, Plate 2.2.

Plate 2.1 Scanning electron micrograph of 3T3 SME cells seeded on TCPS for 72 hours (magnification X29)

Plate 2.2 Scanning electron micrograph of 3T3 SME cells seeded on HEMA for 72 hours (magnification X29)

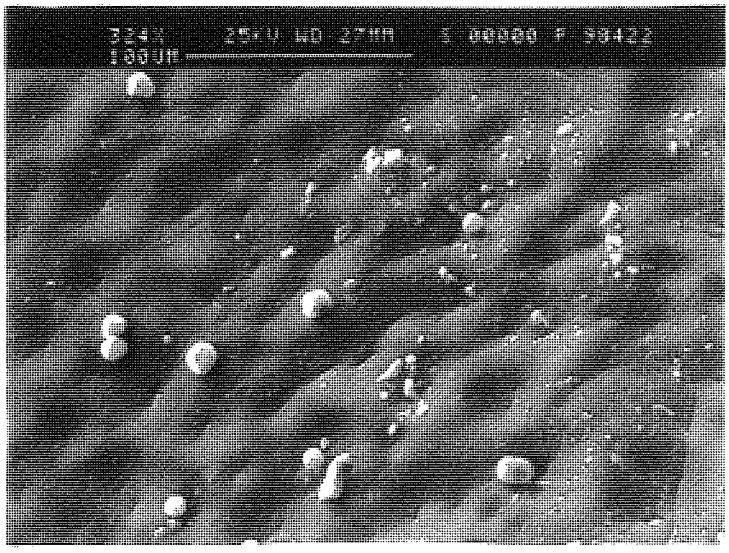

2.4.4 A1 as a Starting Material

SEM micrographs of materials A1 (NVP:MMA:CAB:DEX composition 45:23:12:20) and A4 (THFFMA:NVP:CAB:DEX 30:30:20:20) showed that when the 3T3 cells that had adhered to the hydrogels had become rounded and failed to exhibit a fibroblastic morphology, Plate 2.3. No difference in cell adhesion and proliferation was seen between samples on the SEM micrographs, however, the counts of cells recovered from samples indicated a slight difference, with A1 appearing to be slightly more effective at adhering cells (assuming normal distribution heteroscedastic t-test assuming unequal variance $P<0.05$). The dextrin incorporated into A4 appeared to have precipitated out of solution in the process of manufacture. This resulted in a low frequency of pores on the surface of the hydrogel after the dextrin had been dissolved. It should be noted that there was a substantial difference in NVP concentration (A1 45 per cent and A4 30 per cent).

Plate 2.3 Scanning electron micrograph of 3T3 SME cells seeded on A1 (NVP:MMA:CAB:DEX 45:23:12:20) for 72 hours (magnification X44)

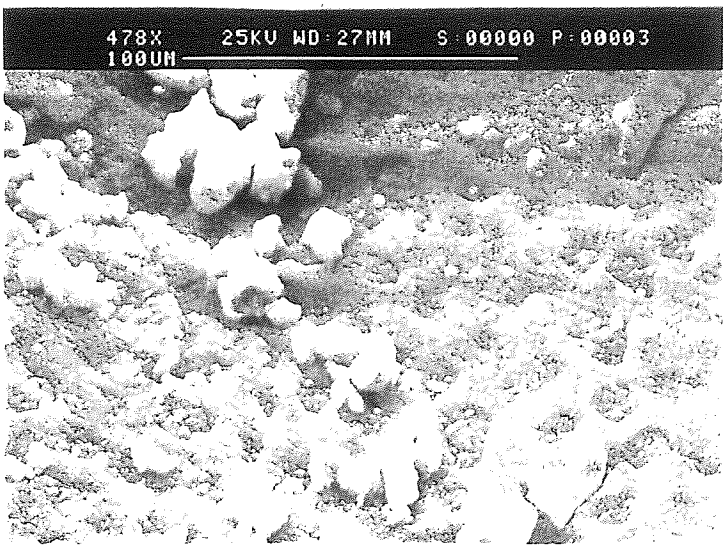

2.4.5 AMO and NVP

The AMO containing materials A5 (THFFMA:AMO:PU:DEX 35:35:10:20), A7 (THFFMA:AMO:PU:DEX 30:30:20:20) and A13(THFFMA:AMO:CAB 36.6:36.6:26.8) were more effective in adhering cells than NVP containing hydrogels A2 (THFFMA:NVP:PU:DEX 35:35:10:20), A4 (THFFMA:NVP:CAB:DEX 30:30:20:20) and A10 (THFFMA:NVP:CAB 36.6:36.6:26.8), assuming normal distribution heteroscedastic t-test assuming

unequal variance $P<0.05$, Figure 2.4. The SEM micrographs of these samples showed that these materials exhibited the same extent of cell spreading and proliferation.

Figure 2.4 Comparison of AMO Containing Materials (A5, A7, A13) versus NVP Containing Materials (A2, A4, A10) +/- S.D.

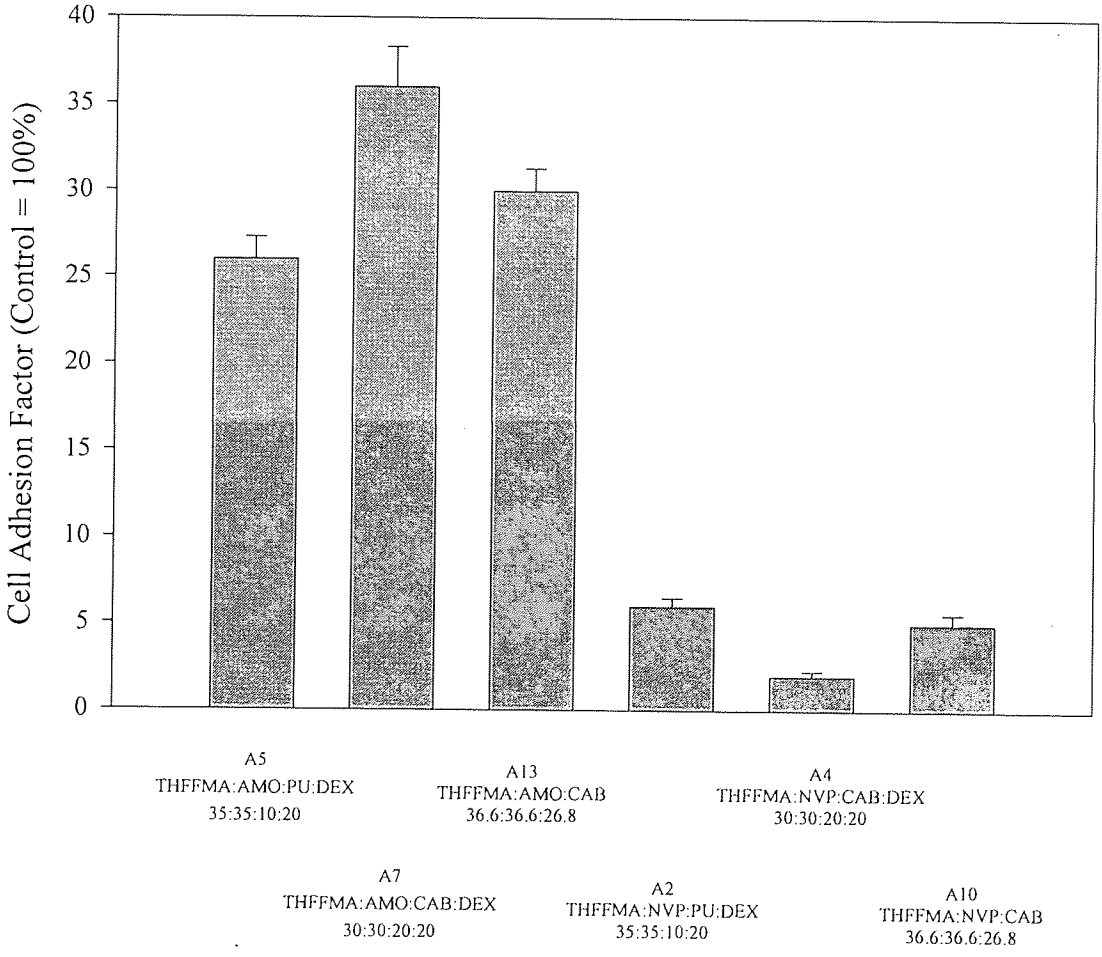

2.4.6 THFFMA

When the content of THFFMA was increased in a hydrogel, the numbers of adhered cells and the extent of their spreading and proliferation was reduced as seen in Figure 2.5 increasing THFFMA from 24 per cent to 41.6 percent. This trend was seen with A2 (THFFMA:NVP:PU:DEX 35:35:10:20), A3 (THFFMA:NVP:PU:DEX 30:35:15:20), A8 (THFFMA:NVP:PU 41.6:41.6:16.8), A9 (THFFMA:NVP:PU 36.6:41.6:21.8), A11 (THFFMA, AMO, PU

41.6:41.6:16.8), A12 (THFFMA:AMO:PU 36.6:41.6:21.8), A14 (THFFMA:AMO:PU 30:50:20) and A18 (THFFMA:AMO:PU 25:60:15). Heteroscedastic t-tests (assuming normal distribution and unequal variance) for A2 (35% THFFMA) versus A3 (30% THFFMA), A8 (41.6% THFFMA) versus A9 (36.6% THFFMA) and A18 (25% THFFMA) versus A11 (41.6% THFFMA) gave $P<0.05$, and $P<0.05$, $P=0.12$ and $P<0.05$ respectively.

Figure 2.5 The Effect of Cell Adhesion with Changes in AMO and THFFMA Concentration +/- S.D.

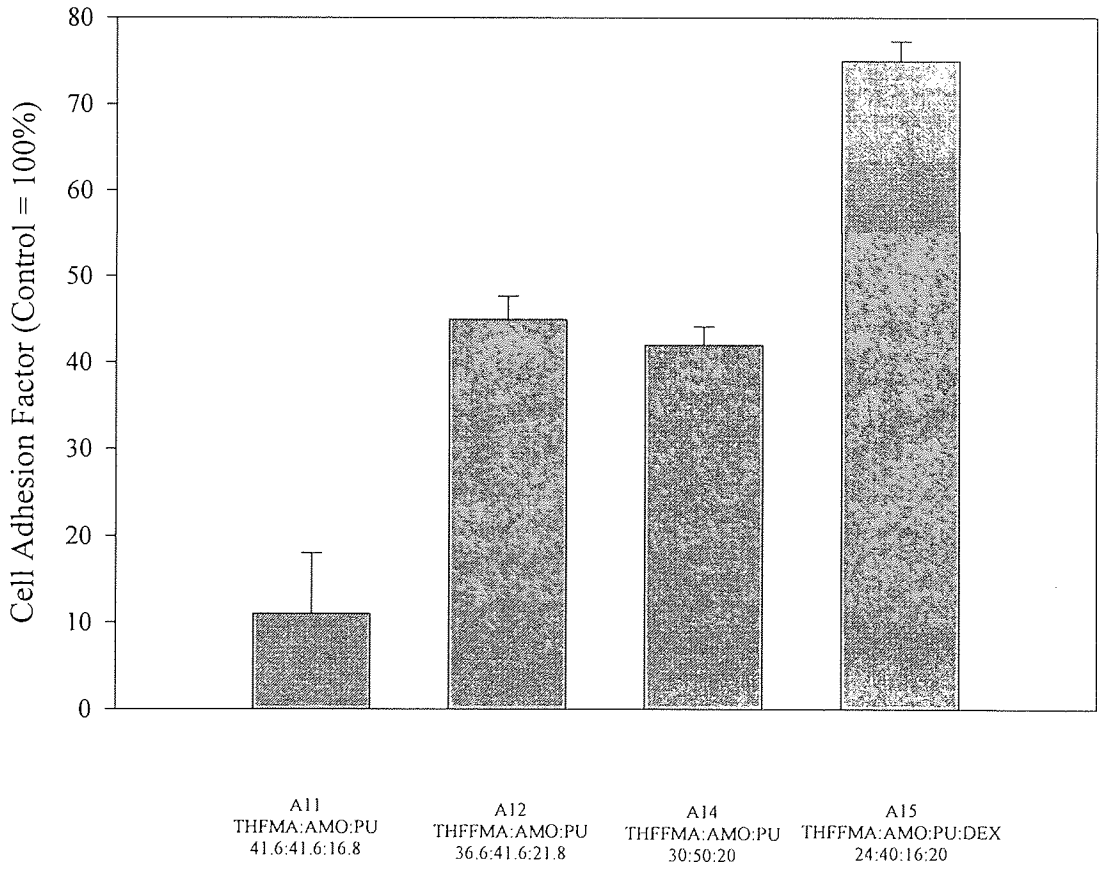

2.4.7 THFFMA in Combination with PU

As the concentration of PU was increased and the concentration of THFFMA was decreased, samples A11 (THFFMA:AMO:PU 41.6:41.6:16.8) and A12 (THFFMA:AMO:PU 36.6:41.6:21.8), the samples exhibited increased cell adhesion

and proliferation, Figure 2.6. This behaviour was also repeated with other pairs of materials A2 (THFFMA:NVP:PU:DEX 35:35:10:20) and A3 (THFFMA:NVP:PU:DEX 30:35:15:20) and samples A8 (THFFMA:NVP:PU 41.6:41.6:16.8) and A9 (THFFMA:NVP:PU 36.6:41.6:21.8). Heteroscedastic t-tests (assuming normal distribution and unequal variance) for A2 versus A3, A8 versus A9 and A11 versus A12 gave $P<0.05$, and $P<0.05$, 0.12 and $P<0.05$ respectively. However, as the concentration of THFFMA decreased and PU concentration increased with samples A5 (THFFMA:AMO:PU:DEX 35:35:10:20) and A6 (THFFMA:AMO:PU:DEX 30:35:15:20) the cell numbers recorded decreased. In A3 (THFFMA:NVP:PU:DEX 30:35:15:20) the surface morphology of the sample exhibited a "honeycombed" appearance, Plate 2.4.

Figure 2.6 The Effect of Cell Adhesion with Changes in PU and THFFMA Concentration +/- S.D.

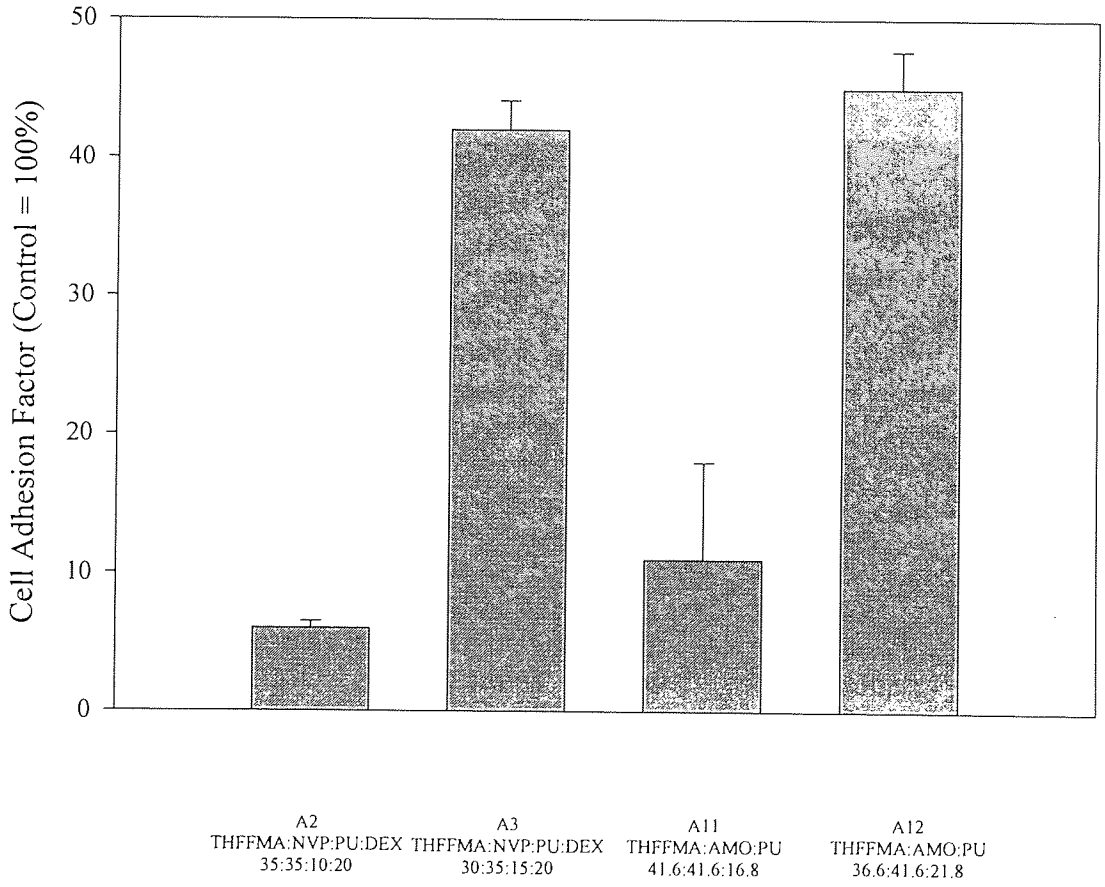

Plate 2.4 Scanning electron micrograph of 3T3 SME cells seeded on A3 (THFFMA:NVP:PU:DEX 30:35:15:20) for 72 hours (magnification X46)

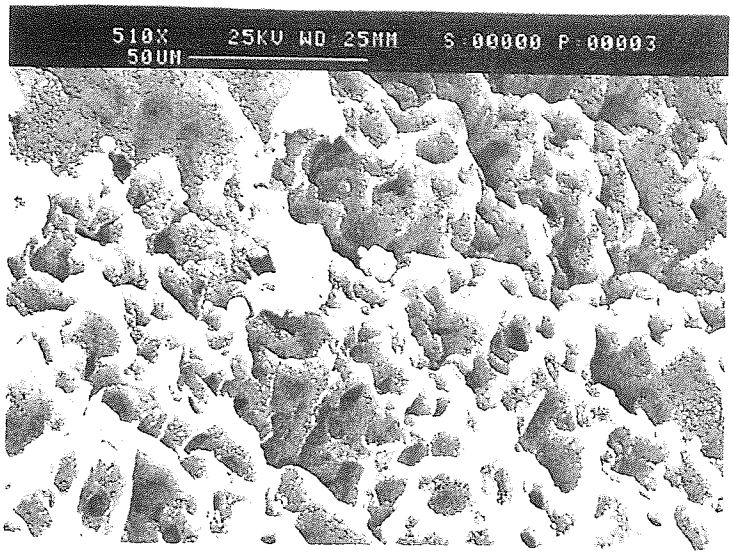

2.4.8 Changing THFFMA, AMO and PU Concentration

In samples of A15 (THFFMA:AMO:PU:DEX 24:40:16:20) the high cell counts observed were higher than those noted with A19 (THFFMA:AMO:PU:DEX 21.25:51:12.75:15) where SEM micrographs indicated that the dextrin in A19 had precipitated out of solution before making pores. However heteroscedastic t-tests (assuming normal distribution and unequal variance) for A15 versus A19, gave P=0.20 indicating the result was not statistically significant. By contrast the surface of A15 was very crumbly in appearance indicating that the dextrin in this sample had not precipitated out of solution and although A15 was mostly crumbly in appearance, there were also some parts of the sample which showed a smooth surface, Plate 2.5. On the smooth parts of A15 the morphological appearance of the cells was the same as that noted with A19. When THFFMA concentrations were decreased and when AMO concentrations increased within samples A14 (THFFMA:AMO:PU 30:50:20) and A18 (THFFMA:AMO:PU 25:60:15) cell numbers did not increase.

Plate 2.5 Scanning electron micrograph of 3T3 SME cells seeded on A15 (THFFMA:AMO:PU:DEX 24:40:16:20) for 72 hours (magnification X13.5)

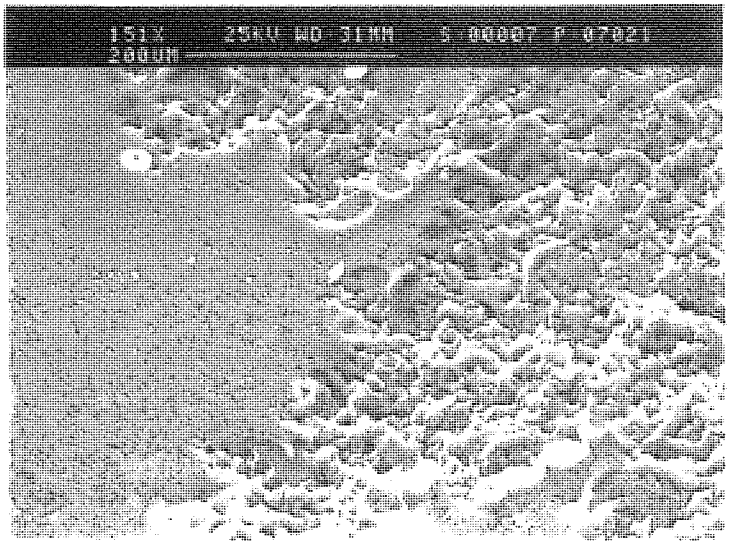

2.4.9 THFFMA in Combination with AMO:EEMA:MEMA

Addition of THFFMA to AMO:EEMA:MEMA, A29 (AMO:EEMA:MEMA:THFFMA 25:25:25:25), had the effect of reducing the number of adhered cells when compared with the hydrogel A26 (AMO:EEMA:MEMA 20:40:40). Heteroscedastic t-tests (assuming normal distribution and unequal variance) for A29 versus A26, gave $P<0.05$ indicating the result was statistically significant. Cell spreading as seen with scanning electron microscopy appeared to have improved slightly when THFFMA was incorporated into the sample.

2.4.10 EEMA and MEMA

A27 and A28 both contain a single polymer, (EEMA or MEMA respectively) in both cases this caused high cell numbers to adhere with EEMA giving a greater cell count than MEMA. However, heteroscedastic t-tests (assuming normal distribution and unequal variance) for A27 versus A28, gave $P=0.08$ indicating the result was not statistically significant The SEM micrographs of A27 and A28 showed that the polymers were not as smooth as expected with both hydrogels exhibiting rippled surfaces. When EEMA:MEMA were combined with AMO and THFFMA (A29) the combination produced a material with an irregular mosaic appearance, Plate 2.6 and similar samples that contained EEMA, MEMA and AMO (A23 and A26) also showed some surface irregularities.

Plate 2.6 Scanning electron micrograph of 3T3 SME cells seeded on A29 (AMO:EEMA:MEMA:THFFMA 25:25:25:25) for 72 hours (magnification X100)

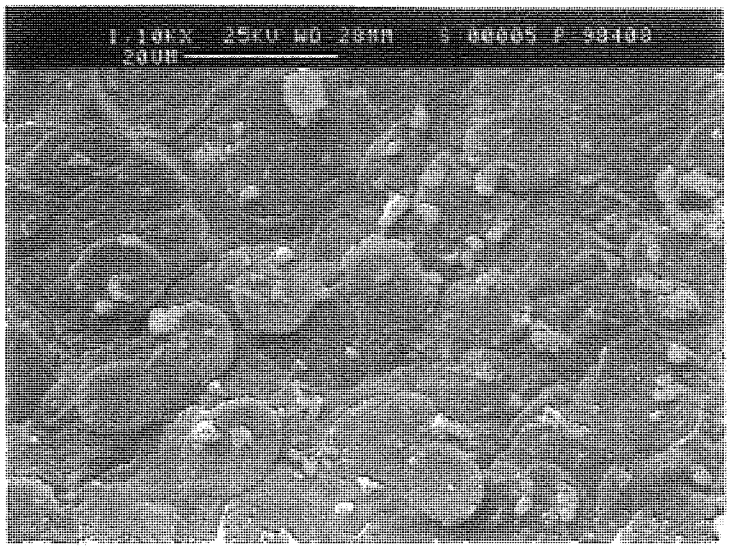

2.4.11 EEMA and MEMA versus AMO

When EEMA and MEMA were combined with AMO A24 (AMO:EEMA 50:50) and A25 (AMO:MEMA 50:50), the cell numbers recovered were markedly less than that observed when using EEMA or MEMA in the pure form and the extent of cell spreading and proliferation was also reduced. Heteroscedastic t-tests (assuming normal distribution and unequal variance) for A24 versus A27 and A25 versus A28, both gave $P<0.05$ indicating that the results were statistically significant. The critical point drying procedure, had resulted in a "bubbled up" surface with A25. Decreasing the proportion of EEMA and MEMA, A23 (AMO:EEMA:MEMA 50:25:25) and A26 (AMO:EEMA:MEMA 20:40:40), increased the number of cells recovered from samples, Figure 2.6. A26 also displayed a curious surface patterning of "stars" when viewed under the SEM, Plate 2.7.

Figure 2.7 The Effect of Reduction of EEMA & MEMA in a Hydrogel Containing AMO:EEMA:MEMA on Cell Adhesion +/- S.D.

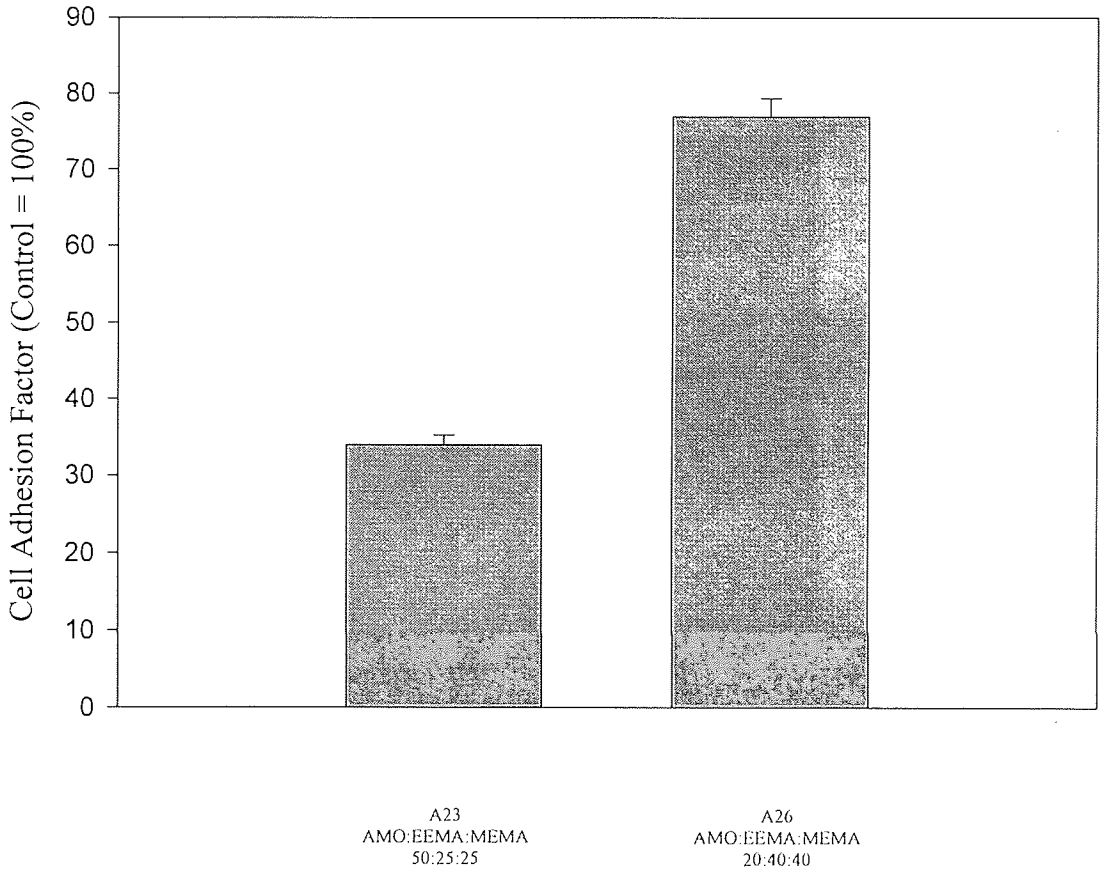

2.4.12 Poly(acrylamide) Containing Hydrogel

In sample A22 Poly(acrylamide):HPA:PU:THFFMA:AMO 10:10:10:30:40), low cell adhesion levels were exhibited with little cell spreading and proliferation.

2.4.13 CAB and PU

A comparison of CAB with PU and NVP showed that CAB resulted in the recovery of greater cell numbers from samples than in a material incorporating NVP inplace of CAB. PU containing materials exhibited higher cell counts than CAB, A9 (THFFMA:NVP:PU 36.6:41.6:21.8) and A10 (THFFMA:NVP:CAB 36.6:36.6:26.8), Figure 2.7. Heteroscedastic t-tests (assuming normal distribution and unequal variance) for A9 versus A10 gave $P<0.05$ indicating that the results was

statistically significant. However, it should be noted that A13 (THFFMA:AMO:CAB 36.6:36.6:26.8) contained slightly less AMO than A12 (THFFMA:AMO:PU 36.6:41.6:21.8) CAB was also seen to be more cell adhesive in A3 (THFFMA:NVP:PU:DEX 30:35:15:20) and A4 (THFFMA:NVP:CAB:DEX 30:30:20:20) when compared to PU although there was a slight difference in the concentration of NVP.

Plate 2.7 Scanning electron micrograph of 3T3 SME cells seeded on A26 (AMO:EEMA:MEMA 20:40:40) for 72 hours (magnification X215)

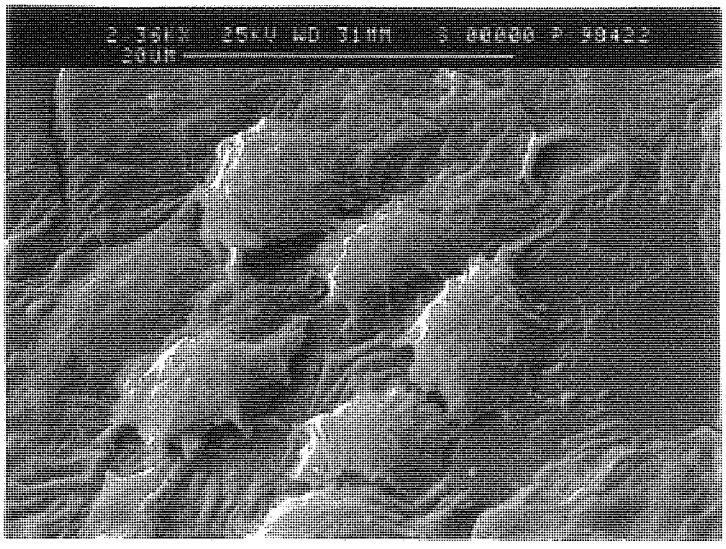

Figure 2.8 The Effect of the Addition of CAB to PU Containing Hydrogels on Cell Adhesion +/- S.D.

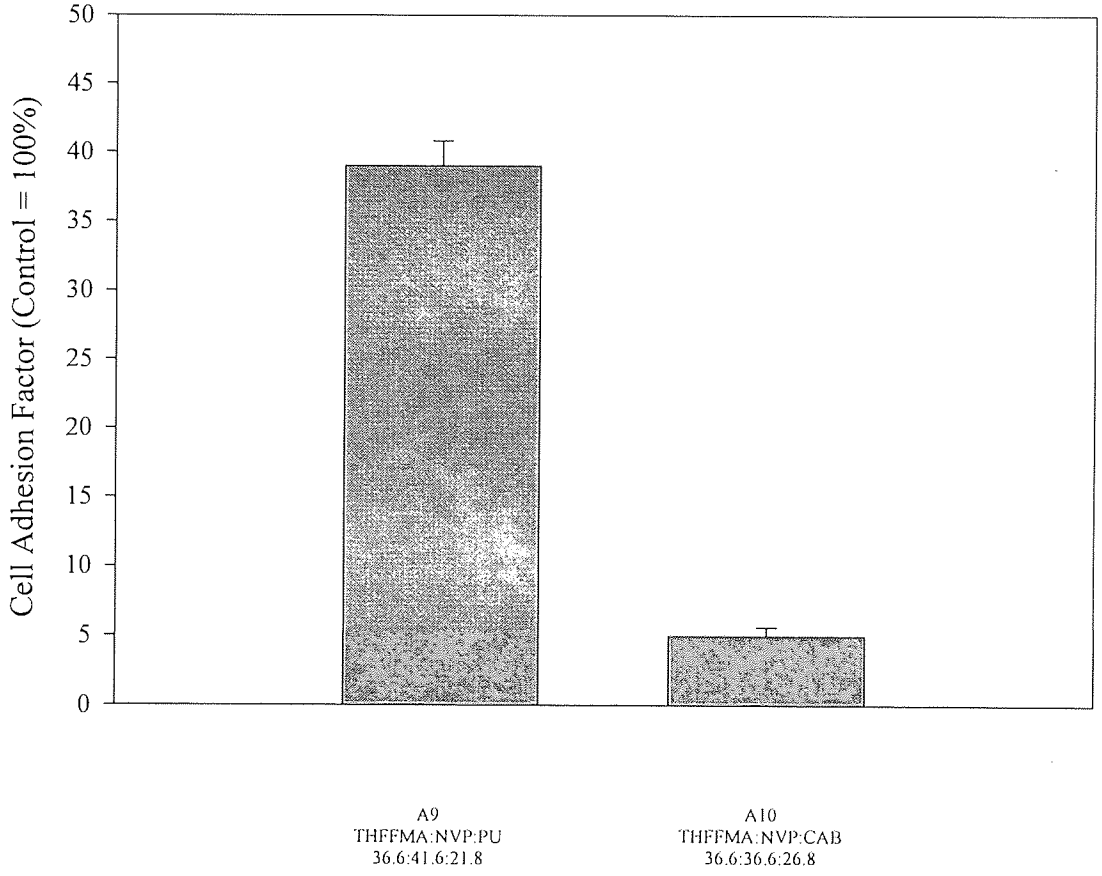

2.4.14 Pores

Haptic peripheral components were slightly improved by the incorporation of pores in the surface of the material. As can be seen with A7 (THFFMA:AMO:CAB:DEX 30:30:20:20) and A13 (THFFMA:AMO:CAB 36.6:36.6:26.8), Plates 2.8 and 2.9. The materials were of the same composition, however, A13 did not include pore producing dextrin. Although the appearance of the cells on A7 appeared similar to A13 there was a slight increase in the number of cells attached to A7 Heteroscedastic t-tests (assuming normal distribution and unequal variance) for A7 versus A13 gave $P<0.05$ indicating that the results was statistically significant. The samples A2 (THFFMA:NVP:PU:DEX 35:35:10:20) and A3 with added dextrin (THFFMA:NVP:PU:DEX 30:35:15:20) when compared to A8 (THFFMA:NVP:PU 41.6:41.6:16.8) and A9 (THFFMA:NVP:PU 36.6:41.6:21.8) with no dextrin added showed that the pores derived from dextrin produced a honey combed surface on the

hydrogel (more so on A3). This resulted in improved fibroblastic cell spreading and proliferation, while cell numbers were similar or lower on dextrin containing samples, the result was statistically significant for A2 V A8 ($P<0.05$) yet, was not statistically significant for A3 versus A9 $P=0.199$, Plate 2.4. The pores incorporated into A4 (THFFMA:NVP:CAB:DEX 30:30:20:20) did not seem to aid cell adhesion compared to the related material A10 (THFFMA:NVP:CAB 36.6:36.6:26.8) that lacked pores. Although the result was statistically significant $P<0.05$.

Plate 2.8 Scanning electron micrograph of 3T3 SME cells seeded on A7 (THFFMA:AMO:CAB:DEX 30:30:20:20) for 72 hours (magnification X29)

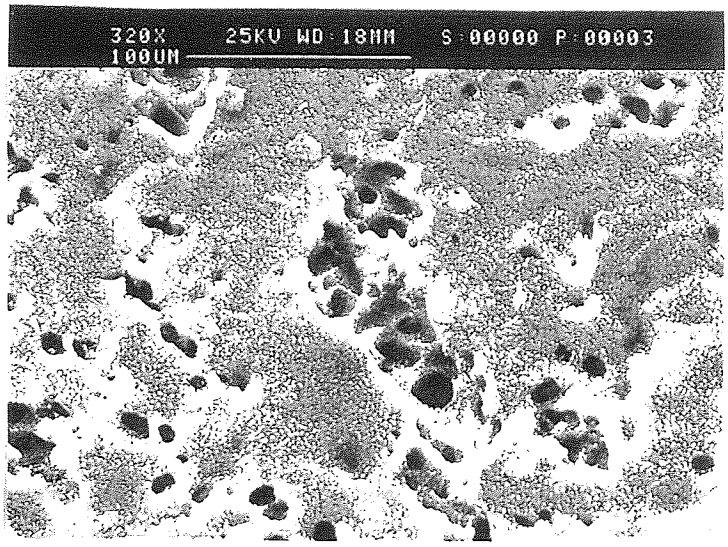

Plate 2.9 Scanning electron micrograph of 3T3 SME cells seeded on A13 (THFFMA:AMO:CAB 36.6:36.6:26.8) for 72 hours (magnification X22)

2.4.15 Pores and Channels

The addition of dextrin and dextran to produce pores and channels was investigated using A38 (THFFMA:AMO:PU:DEX:Dextran 30:50:20:10:4). Compared to A14 (THFFMA:AMO:PU 30:50:20), a hydrogel that did not contain pores and channels, i.e. A38 exhibited higher cell counts although not statistically significant. A38 also showed improved cell spreading and proliferation. However, A30 (AMO:EEMA:MEMA:THFFMA:DEX:Dextran 25:25:25:25) displayed an equal amount of cell spreading compared with A29 (AMO:EEMA:MEMA:THFFMA 25:25:25:25) which did not include pores and channels on the surface of the hydrogel. In addition, cell numbers from the materials were higher when pores and channels were absent. SEM micrographs indicated that the surface of A29 had a "mosaic" appearance not seen on other samples, Plate 2.10. While there was no difference in cell numbers between inclusion of pores and channels with A34 (THFFMA:AMO:PU:DEX:Dextran 37:42:21:10) and A12 (THFFMA:AMO:PU 36.6:41.6:21.8), cell spreading and proliferation was seen to be improved with A12 a material without pores and channels (statistically significant).

Plate 2.10 Scanning electron micrograph of 3T3 SME cells seeded on A29 (AMO:EEMA:MEMA:THFFMA 25:25:25:25) for 72 hours (magnification X29)

2.4.16 Hydroxyapatite

Hydroxyapatite improved cell adhesion significantly, (A35-A37 using THFFMA:AMO:PU:Hap 37:42:21:10 with hydroxyapatite particles of 36μm, 100μm and 250μm respectively), Figure 2.9. The SEM micrographs of cells from all samples were similar apart from cells seen on A37 (250μm hydroxyapatite

particle size). With A37 a significant amount of cell proliferation was seen in holes in the hydrogel surface where hydroxyapatite particles met. Over the surface of the hydrogel, a similar proliferation response was seen with the other materials A35 (36μm hydroxyapatite particle size) and A36 (100μm hydroxyapatite particle size).

Lower cell numbers were seen on hydroxyapatite particles embedded in a hydrogel based on A29 (AMO:EEMA:MEMA:THFFMA 25:25:25:25) and the hydroxyapatite containing materials A31 (AMO:EEMA:MEMA:THFFMA 25:25:25:25 Hap 36μm), A32 (AMO:EEMA:MEMA:THFFMA 25:25:25:25 Hap 100μm) and A33 (AMO:EEMA:MEMA:THFFMA 25:25:25:25 Hap 250μm). However, the cell numbers exhibited on A31-A33 were still higher than many other samples tested for the haptic peripheral, excluding A33, where cell spreading and proliferation was minimal. The holes at the edges of the particles on A33 gave good points of anchorage for cells, whilst on other hydroxyapatite containing samples in the series, the surface of the material often appeared smooth. The hydroxyapatite containing series A39 (THFFMA:AMO:PU:Hap 36μm 30:50:20:10), A40 (THFFMA:AMO:PU:Hap 100μm 30:50:20:10) and A41 (THFFMA:AMO:PU:Hap 250μm 30:50:20:10) compared less favourably with the other materials described above and the appearance of the surfaces of these materials (A39-A41) were smooth.

With the three series of hydrogel materials containing hydroxyapatite particles there appeared to be a trend of higher cell counts coming from samples using THFFMA:AMO:PU than those of the AMO:EEMA:MEMA:THFFMA series. The 250μm samples A37 (THFFMA:AMO:PU:Hap 37:42:21:10 with hydroxyapatite particles of 250μm) and A41 gave the highest cell counts. Cellular spreading and proliferation was best on hydrogels containing the largest particle sized hydroxyapatite. With A33 and A37 exhibiting the best response to cell adhesion of the hydrogels tested. On some hydroxyapatite containing samples the surface of the material often appeared smooth possibly indicating that hydroxyapatite particles had precipitated out of solution.

Figure 2.9 The Effect of an Increase in Cell Adhesion with Hydroxyapatite Concentation +/- S.D.

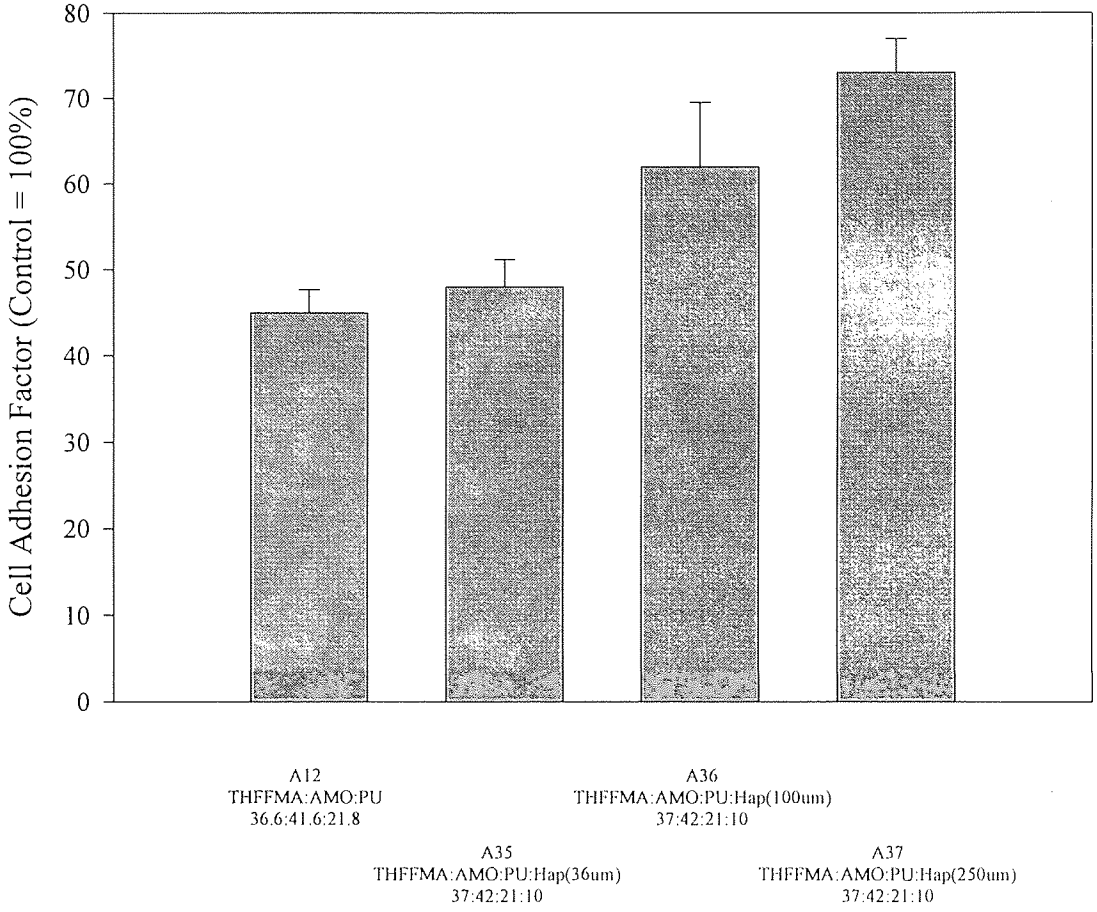

2.4.17 Hydroxyapatite Whiskers

Samples incorporating hydroxyapatite whiskers, A43 (THFFMA:AMO:PU:hap W 37:42:21:10) and A44 (THFFMA:AMO:PU:Hap W 30:50:20:10) compared favourably with a similar material without such whiskers A14 (THFFMA:AMO:PU 30:50:20). Higher numbers of cells were stripped off these samples (A43 and A44) compared with A14 (heteroscedastic t-tests assuming normal distribution and unequal variance gave $P<0.05$ indicating that the results was statistically significant) and the morphology of the cells had a more fibroblastic like appearance. On samples incorporating hydroxyapatite whiskers, the cells appeared to favour adhering to the sides of the whiskers as seen with materials A42 and A44, Plate 2.11. A42 (AMO:EEMA:MEMA:THFFMA:Hap W 25:25:25:25:10) was a similar material to A29 (AMO:EEMA:MEMA:THFFMA 25:25:25:25), however, A42 incorporated hydroxyapatite whiskers. The whiskers did not increase spreading

(statistically significant) and proliferation of the cells, although the appearance of the cells, closely resembled fibroblastic cell adherence patterns noted on a number of fibres such as those described by Wan *et al.*[31] When comparing a sample containing pores and channels such as the hydrogel A30 (AMO:EEMA:MEMA:THFFMA:Dex:Dextran 25:25:25:25) with the same hydrogel incorporating hydroxyapatite whiskers (A42) inplace of pores and channels no statistical differences were seen in cell adhesion or proliferation.

Plate 2.11 Scanning electron micrograph of 3T3 SME cells seeded on A44 (THFFMA:AMO:PU:Hap W 30:50:20:10) for 72 hours (magnification X88)

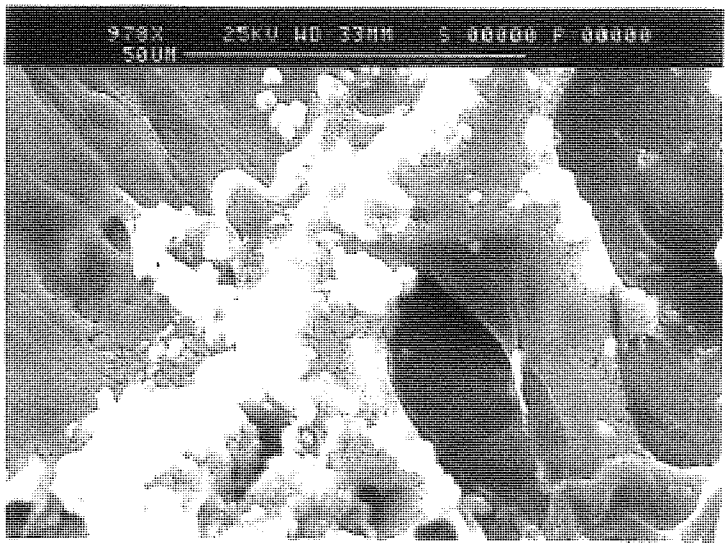

2.4.18 Calcium Sodium Alginate Fibres

Polymers were polymerised around Ca Na alginate by placing a sponge of Ca Na alginate within a molding cassette and pouring the molten polymer into the cassette. In all samples containing calcium sodium alginate the cell morphology of 3T3 Swiss Mouse Embryo cells appeared to resemble flattened spreading cells, with long filopodia extensions, Plate 2.12. There was greater fibroblastic like spreading on the fibres of calcium sodium alginate than on the smoother areas of the surrounding hydrogel. Incorporating calcium sodium alginate into A16 (THFFMA:AMO:PU polymerised around NaCa alginate 30:50:20), A20 (THFFMA:AMO:PU polymerised around NaCa alginate 25:60:15) and A21 (THFFMA:AMO:PU:DEX polymerised around NaCa alginate 21:25:51:12.75:15) gave no increase in cell numbers when compared to hydrogels which did not include calcium sodium alginate fibres. However, the calcium sodium alginate fibres did improve cell spreading on the hydrogel, Plate 2.13. In A17 (THFFMA:AMO:PU:DEX polymerised around NaCa alginate 24:40:16:20) the calcium/sodium alginate fibres appeared to have sunken into the underlying

hydrogel. A17 had fewer cells adhering to the material statistically (heteroscedastic t-tests assuming normal distribution and unequal variance $P<0.05$) than its counterpart A15 (THFFMA:AMO:PU:DEX 24:40:16:20) and the cell spreading was also markedly better than A15. The calcium alginate fibres of A17 incorporated a dextrin pore with a size of approximately 38μm diameter, however few pores were seen on the surface. Samples of A16 (THFFMA:AMO:PU polymerised around NaCa alginate 30:50:20) with no dextrin pores only gave a low increase in cell numbers.

Plate 2.12 Scanning electron micrograph of 3T3 SME cells seeded on A21 (THFFMA:AMO:PU:DEX polymerised around NaCa alginate) for 72 hours (magnification X58)

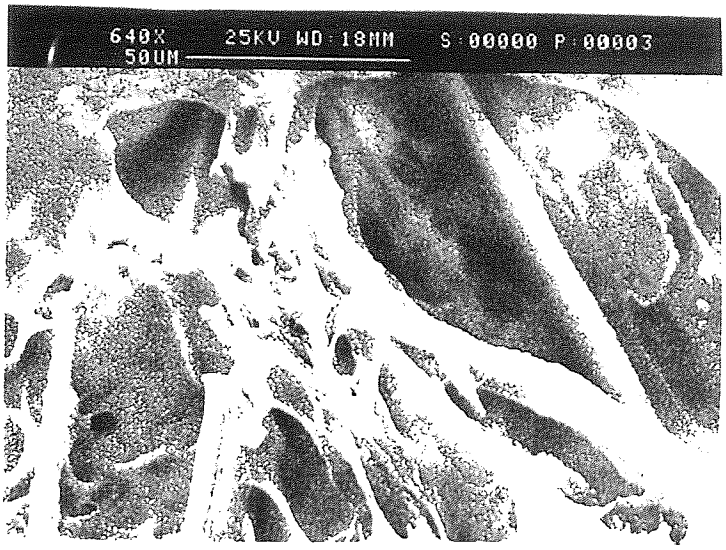

Plate 2.13 Scanning electron micrograph of 3T3 SME cells seeded on A17 (THFFMA:AMO:PU:DEX polymerised around NaCa alginate 24:40:16:20) for 72 hours (magnification X105)

2.5 Discussion

2.5.1 Cell Viability

The high mean cell viability measurements for samples indicate that the samples were sufficiently inert and did not release any cytotoxic materials in the short term. However, with such low cell counts stripped from the samples, caution should be used in the determination of cell viability and cell number. Even a small number of additional viable or non-viable cells would change the viability results by a significant amount. To have a reasonably statistically accurate measurement of the number of cells in a given volume using a haemocytometer, requires a cell count of at least $8x10^5$ cells/ml. Counts of less than $8x10^5$ cells/ml using a haemocytometer have a large margin of error. For a more accurate indication of the cell numbers on a sample Coulter counting techniques should be used. However, the Coulter counting technique does not determine the extent of viability of cells in a given cell suspension, so there would remain a need to incorporate some test for cytotoxicity within such an investigation. It was expected that leaching of monomers from the materials would not be a significant problem as all samples were thoroughly soaked for one week in distilled water prior to investigation to remove any unreacted monomers present from polymerization. Incomplete hydration of the materials may have been present. The SEM micrographs of polymers subject to limited hydration as reported by Downes *et al.* Appear similar to the 'mosaic' appearance seen with some hydrogels in this report.[30]

Stripping of cells from polymers required 10 minutes. Wan *et al.* stated that 30 minutes was required to strip fibroblastic cells from fibre samples, yet, no difference in the number of cells stripped from samples were found when stripping times were 10 and 30 minutes respectively.[31] If the cells are exposed to trypsin for too long then the cell membranes may become weakened and result in an increase in the apparent numbers of non viable cells as the cell membranes fracture.

2.5.2 Controls

The TCPS negative control produced the expected result of confluent growth of 3T3 cells over the surface when cultured overnight. TCPS is a gas plasma treated polystyrene designed for cell adhesion. Plasma polymerisation and gaseous plasma modification techniques effectively modify polymeric surfaces without altering their bulk properties. Introduction of functional groups (i.e. hydroxyl and amide groups) to the polymer surface possibly causes reorientation of alkyl groups leading to more favourable cell adhesion.

The positive control p(HEMA) produced the expected result that p(HEMA) was less conducive to cell adhesion and tissue integration compare to TCPS. Possibly p(HEMA) with a high negative surface energy charge (polar component) lead to a mutual electrostatic repulsion between the polymer surface and cells. It should be noted that blending of polyHEMA with more hydrophobic species can lead to greater cell adhesion.[13]

2.5.3 A1 as a Starting Material

A1 (NVP:MMA:CAB:DEX 45:23:12:20) was used as a foundation from which other materials could be investigated for their physical and biocompatible properties. Previously, this material had been utilised as a material designed for chondrocyte adherence allowing chondrocytes to produce replacement cartilage in sites of damaged cartilage (PU123).[32] For the production of cartilage, chondrocytes are required to exhibit a rounded morphology, when their morphology is fibroblastic the cells do not produce cartilage.[33] A1 was originally designed to support chondrocyte cells in a rounded morphology and to prevent them from spreading out. Although the 3T3 Swiss Mouse Embryo cells could adhere to the polymer, the cells did not spread and rounded cells were observed. The cells were not dead as dead cells do not adhere.

Although A1 is not suitable for producing a skirt in the keratoprosthesis this material did show that the materials used in the samples (MMA and NVP) were non-cytotoxic. This corresponded with similar results by Horbett *et al.* also using 3T3 Swiss Mouse Embryo cells.[34] Horbett *et al.* found no cell attachment to MMA copolymers. Poly(MMA) is fairly rigid and hydrophobic, cell adhesion to p(MMA) can be limited and the plastic and soft tissue interface may lead to the formation of gaps that may allow the down growth of the epithelial tissue and cells. As MAA is a strongly negatively charged monomer the negative charge on the surface acts as a repulsive force for cell adhesion. However, the inclusion in the polymer of materials such as NVP would provide "islands" of other charge, which would allow cellular adhesion to take place. By producing a material that is a combination of different hydrogels, non-cell adhesive materials can be converted to cell adhesive materials and still retain some of their original physical characteristics. The "islands" of charge would be localized concentrations of NVP that lowered the negative charge at that point. Any cells that were attracted to the polymer would have a greater possibility of attaching at such points. Although the cells are able to attach, the bulk of the hydrogel is made of MMA, so retaining its overall negative charge causes any cells that adhere to the surface of the material to remain rounded in morphology. A more positively charged surface would be required if the cells are to spread out. In addition, the anterior surface of the epithelium below the optical centre prevents diffusion of nutrients to the tissues below it. Thus with present designs p(HEMA) may have limitations in use.

2.5.4 THFFMA

A continuing theme noted with THFFMA was that THFFMA had a negative effect on cellular adhesion, increasing the concentration of THFFMA decreased the number and extent of cellular spreading. THFFMA does display hydrophilic properties and this polar hydrophilic material possesses a strong ability to adsorb water. Downes *et al.* states, that when the THFFMA concentration is increased it leads to less water being absorbed, this would reduce the wettability in a hydrogel which may have implications on the hydration shell around the polymer.[30] This would reduce the propensity for the surface to attract adhesive proteins such as fibronectin, this in turn, may cause less adhesion of cells on the surface of the

hydrogel. Downes *et al.* states that when using THFFMA in combination with other polymers the surface topography of the polymers varies according to the composition of the polymers.[30] This could explain why, in combination with other hydrogel monomers, THFFMA can have different cell adhesive properties. Although samples A8 (THFFMA:NVP:PU 41.6:41.6:16.8) and A9 (THFFMA:NVP:PU 36.6:41.6:21.8) incorporated PU and NVP, both have been noted for their bio-adhesive characteristics, the substantial amounts of THFFMA present resulted in an increased propensity for cells not to adhere and a reduced propensity for cells to proliferate.

2.5.5 THFFMA in Combination with AMO and PU

The surface of A18 (THFFMA:AMO:PU 25:60:15) was more rugose than A14 (THFFMA:AMO:PU 30:50:20) in appearance. The rugosity appeared to be more effective in favouring cell adhesion and this effect may mask any changes in cell adhesion caused by variation in THFFMA concentration. Although the surface energy of a sample is important to the adhesiveness of a polymer the topography of a material may be of more importance for cell adhesion.

2.5.6 EEMA and MEMA

EEMA and MEMA when incorporated into a hydrogel, such as A27 (EEMA) and A28 (MEMA), produced high cell numbers adhering to the polymer. This made the use of A27 or A28 unsuitable for the optical core of the keratoprosthesis. However, the high degree of cell adhesion would possibly make MEMA and EEMA containing materials suitable for inclusion into a hydrogel for fabrication of the Kpro skirt. MEMA appears to be a more cell adhesive material than EEMA if we observe the results of cell adhesion to A27 and A28 hydrogels. EEMA and MEMA are tough materials with high elasticity and low modulus. Such properties could be used to advantage in the manufacture of the skirt component which would then be flexible and move when stresses were placed on the surrounding tissue. When AMO was added to either EEMA or MEMA this resulted in the formation of a smooth hydrogel surface unsuitable for cell adhesion. This could possibly be caused by the hydroxyl group interaction between AMO and EEMA (or MEMA). By interacting with the functional hydroxyl groups of EEMA and MEMA the AMO shielded the hydroxyl groups being exposed on the surface and resulted in a decreased cell adhesion.

P(MMA) is marginally more polar than PEMA therefore we could expect MEMA to be marginally more polar than EEMA. It is generally agreed that covalently derived substrata that included NH_2 or hydroxyl surface groups are most likely to lead to adsorption of adhesion proteins such as fibronectin laid down by cells in order to attach extracellular matrix and cell membrane to surfaces.

Samples comprised of both EEMA and MEMA produced low cell integration and this was surprising considering the irregularity of their surface. However A23 (AMO:EEMA:MEMA 50:25:25) did contain concentrations of AMO that may possibly produce lower cell adhesion when in combination with EEMA and MEMA. The A26 (AMO:EEMA:MEMA 20:40:40) result may also be erroneous, perhaps arising from the result of the fixation procedure.

A29 (EEMA:MEMA combined with AMO and THFFMA) had an irregular "mosaic" surface. This allowed cells to integrate and proliferate to a greater extent over the surface. The "mosaic" surface may be a more suitable substrate for cell adhesion than smoother surfaces (as seen with crystalline poly-hydroxybutyrate) allowing cells to gain a foothold and then proliferate.

2.5.7 Poly(acrylamide)

A22 (Poly(acrylamide):HPA:PU:THFFMA:AMO 10:10:10:30:40) incorporated a poly(acrylamide) component into the hydrogel that is similar to the chosen optical core material used in other OOK's. The limited extent of cell adhesion and spreading over the surface of poly(acrylamide) may indicate that the material would be a good candidate for use as the optical core. The amount of AMO incorporated into the hydrogel was moderately high yet this was required to convey suitable physical parameters to the hydrogel but this did not appear to have produced the desired cell adhesion characteristics. With poly(acrylamide) and substituted poly(acrylamides) the competitive hydrogen bonding between water and the polymer chain and polymer chain to polymer chain interactions, can result in a non-wettable, hydrophobic material which would inhibit cell adhesion to poly(acrylamide).

2.5.8 CAB and PU

CAB is an interpenetrant, reinforcing a hydrogel material analogous to steel rods reinforcing concrete. Comparisons with other materials used to toughen the haptic segment (NVP and PU) showed that although CAB was more effective at cell adhesion than NVP, CAB did not support the same degree of cell adhesion as PU. Thus in aiming to reinforce a hydrogel, NVP should be chosen over CAB and PU when the optical core needs to be strengthened. When reinforcing the haptic periphery with PU, not only would PU provide the sufficient toughness desired, it would also allow increased cell adhesion. Increasing the NVP concentration decreases the cell numbers recovered from samples possibly because NVP changes the surface charge of the hydrogel leading to decreased wettability in the material. It should be noted that there were some differences in the composition between the hydrogels, so the comparison were not entirely valid.

Polyurethane (PU) has been extensively used in previous implantable devices.[17] PU is hydrophobic, inert and non-toxic, yet there is a lack of data on its long-term stability. In addition, the material does not allow diffusion of nutrients so it is unable to support a surface epithelial cell layer. However, in animal trials PU heart valves have not performed well with thrombosis and calcification prominent in failed valves. Calcium deposits on PU have been associated with surface defects and appear to accumulate in areas undergoing the greatest flexure.[35-39]

2.5.9 Pores

Dextrin was used in the manufacture of many of the hydrogels to investigate whether pores were generally more effective in promoting cellular adhesion and proliferation. The pores would be created by dextrin dissolving out of the hydrogel during soaking in water after the polymerisation procedure. The pores would be 'safe havens' for cells to attach and proliferate rather than allowing cells to adhere randomly over a smooth surface with low adhesive potential. After colonization of the pores, it was hoped that the cells would start to spread out over the material from the location of the pore. The pores would also allow the ingrowth of cells to integrate the material of the keratoprosthesis skirt with the adjacent tissue.

The pores would also act as protection for cells during the washing stages of the SEM fixation procedure, so that cells would remain attached and not be lost during handling and the washing steps during the SEM preparation. The pores did appear to achieve this goal, with several instances of cells found in pores, having a more fibroblast like appearance compared to the cells exposed on the surface of the hydrogel.

The incorporation of pores in a sample was complicated by the fact that the dextrin had a tendency to fall out of solution during manufacture. In addition, the initial attempts at using dextrin employed 10μm diameter particles. This pore diameter was found to be too small for cells to colonise. In later work larger sized dextrin particles were used in the range of 30-50μm. Dextrin falling out of solution may have produced a smoother surface which was less adhesive to cells than otherwise expected.

If the extent of pores on the surface of the hydrogel were too great such as seen with A2 (THFFMA:NVP:PU:DEX 35:35:10:20) and A3 (THFFMA:NVP:PU:DEX 30:35:15:20) (giving a honey combed appearance). The cells might have been able to spread but had difficulty in migrating over the surface, and showed a reduced rate of proliferation over the material and thus the cells would remain in isolated pockets. When the pockets of cells were full, contact inhibition would act to terminate further proliferation of the cells, preventing total coverage and integration of the material. A certain number of pores can therefore be an advantage for cell adhesion and spreading, however, too many pores results in a surface which is far too irregular for cell spreading and proliferation to occur.

It should be noted that if dextrin was not removed during the soaking procedure then the polysaccharides may be utilized by the cells as an additional energy source. This energy source could also be used by contaminating micro-organisms if the samples had not been sterilized before use.

2.5.10 Pores and Channels

It would be expected that cells would be able to adhere more readily to materials incorporating pores and channels. Pores and channels produce an irregular roughened surface suitable for cell attachment. However, in only one sample did the pores appear to actually improve cell adhesion A38

(THFFMA:AMO:PU:DEX:Dextran 30:50:20:10:4) and in the other samples the pores had a negative , A34 (THFFMA:AMO:PU:DEX:Dextran 37:42:21:10:4), A12 (THFFMA:AMO:PU 36.6:41.6:21.8), or neutral, A29 (AMO:EEMA:MEMA:THFFMA 25:25:25:25), A30 (AMO:EEMA:MEMA:THFFMA:DEX:Dextran 25:25:25:25), effect. This could have resulted from loss of dextrin. The dextrin dissolution initially produces a rugose surface favouring cell adhesion. However, as the dextrin was further eluted from the sample the rugosity of the sample surface increases to such an extent that the topography of the surface is inhibitory for cell adhesion. Indeed A30 (25 per cent dextrin) had more dextrin content than A38 (10 per cent dextrin) the additional dextrin loss from the surface could have changed surface topography. An alternative possibility may have been that the formation of a smoother surface than expected was produced and hence reduced the propensity for cells to adhere. However, the materials were actually quite rough, (A38 was smoother than A29/A30). In addition, A29 might have been removed from the glass plates during the moulding process and produced an irregular surface that increased cell adhesion.

One would have expected that more cells could have spread out in the presence of pores and channels, such as in sample A30, however, the same concentration of cell numbers was seen with A29 and A30. Pores and channels gave sample A30 an irregular topography but did not seem to improve cell adhesion when compared with A29. Yet, A29 did have a strange "mosaic" appearance on the surface of the hydrogel which possibly boosted cell adhesion. The "mosaic" appearance was possibly caused by removal of the hydrogel from the glass plate used in its manufacture whilst still hot or by the hydrogel being insufficiently hydrated.

The presence of pores and channels, enable cells to spread over the surface of the hydrogel but at the same time make migration difficult because the cells remain in isolated pockets. When the pockets are filled with cells, contact inhibition prevents the further proliferation of cells and stops both the coverage and integration of the material with cells.

2.5.11 Calcium Sodium Alginate Fibres

Calcium sodium alginate fibres are water soluble and absorb water to form a gel like material.[35] The alginate is a polymeric acid composed of 2 monomer units; α-L guluronic acid (G) and β-D-mannuronic acid (M). High M alginate (rich in MM blocks), swells readily because Na^+ ions are easily replaced. While high G alginate swells only slightly because the Ca^{2+} ions bind so strongly that ion exchange is slow and therefore a gel does not readily form. If some of the Ca^{2+} ions are replaced during manufacture in a high G alginate, this leads to a Ca^{2+}/Na^+ alginate that allows rapid swelling of the fibre.[20]

A16 (THFFMA:AMO:PU polymerised around NaCa alginate 30:50:20) and A17 (THFFMA:AMO:PU:DEX polymerised around NaCa alginate 24:40:16:20) were polymers which incorporated fibres of calcium alginate into their matrix. The fibres appeared to favour the growth of cells, possibly due to the tendency for the cells to clump together. The fibres may act akin to a tea strainer, catching the cells that were in the cell suspension that had been used to seed the hydrogels. It has been

widely noted that the growth of mammalian cells *in vivo* is density dependent, when cells are concentrated together the cells are able to proliferate more rapidly. Clumping of cells would be advantageous for regeneration of tissue structure, however, it has also to be remembered that cells need to be supplied with nutrients. If a vascular supply were not able to supply nutrients to the aggregations of cells that have grown into the implant then the cells may eventually become necrotic. Furthermore, when sufficient cell numbers occupy the same region contact inhibition will inhibit further growth of cells.

It was also surprising that the cell numbers stripped from the samples were so low. Perhaps the fibres aided in entrapment of the cells seeded onto the material. The cells tangled in the fibres would be more resistant to disaggregation by trypsin. An assay incorporating a colour dye in proportion to the extent of metabolic activity such as the MTT assay, would perhaps counter the problem of recovery of cells from a fibrous material. Individual cells would not need to be recovered and counted, the colourimetric assays reagents would be able to make contact with the cells and the resulting colour change detected by the optical system of the measuring spectrophotometer. However, as an initial screening procedure, counting the cells previously to the polymer and observing their morphology is a rapid technique to employ. When the screening has selected several key candidate polymers then a more sophisticated cytotoxicity test such as MTT assay can be employed.

The calcium alginate fibres in A17 incorporated a pore size of approximately 38μm diameter, this produced no increase in cell numbers compared to controls. Although with smooth materials were found to be less effective than materials containing pores, perhaps the pores created may have been too large to allow cells integrate with the material efficiently. It was hoped that the pores would allow cells to proliferate and spread out from the pores to cover the surface of the polymer.

The fibroblastic cells that adhered to the alginate fibres had a similar appearance to adherent fibroblastic cells observed by Wan *et al.*[31] Wan *et al.* discovered actively mobile fibroblastic cells traversing along fibres of polybutylene/polypropylene and reported that the results were favourable for cell adhesion. It appears that calcium/sodium alginate fibres may also be suitable materials to aid in the enhancement of cell adhesion in a hydrogel.

2.5.12 Hydroxyapatite

Hydroxyapatite particles of 250μm diameter provided protection for cells to adhere and allowed cells to spread out between the gaps between particles. Thus materials that contain hydroxyapatite should be considered for inclusion into the haptic periphery to improve cell adhesion.

2.5.13 Hydroxyapatite Whiskers

It was thought that the hydroxyapatite whiskers would increase the adherence of cells, in a similar manner to the calcium sodium alginate fibres. As the whiskers would provide a network where cells would be protected by destructive shear forces

which would tend to strip cells off the surface during handling. It was expected that the cells would attach to the roughened substrate and integrate between the whiskers. The rapid adherence would allow cells to rapidly enter a proliferative stage, however, the reverse was found. The whiskers within A30 did not contribute to increased cell numbers, although the appearance of the cells, Plate 2.90, closely resembled fibroblastic cell adherence on a number of fibres as reported by Wan *et al.*[31] This may be an indication that the whiskers improve cell-tissue-implant integration using a matrix of the hydroxyapatite whiskers, yet, there is a lag phase that proceeds cell proliferation. Perhaps the whiskers could be used as a biocompatible material to add strength to cell adhesive materials.

2.5.14 EWC

Although water content is an important factor in determining whether a material will be cell adhesive it is only one of many possible factors that can be involved in determining the adhesive properties of a hydrogel. Although Figure 2.10 appears to show a clear relationship of increasing EWC leads to decreasing cell adhesion. Because the hydrogels investigated are made of widely differing materials it is not possible to just plot polymers water content against cell adhesion potential. EWC is a bulk property of the material, surface bound water would be more directly relatable to the cell adhesive properties of the materials. Lydon *et al.* notes, "Hydrophilicity is neither necessary nor sufficient for cell adhesion", in order to explain that many nonpolar polymers are capable of supporting cell attachment and spreading even with EWC's very different from those expected cell adhesive EWC's seen with Minett's cell adhesion with EWC curve.[14] Although Minett states that hydrogels with over 30% EWC may inhibit cell adhesion, Thomas notes that there is a shift in the Minett curve depending on different materials thus the rule that 30% EWC may inhibit cell adhesion may not hold all the time.[40]

Figure 2.10 Cell adhesion versus Equilibrium Water Content

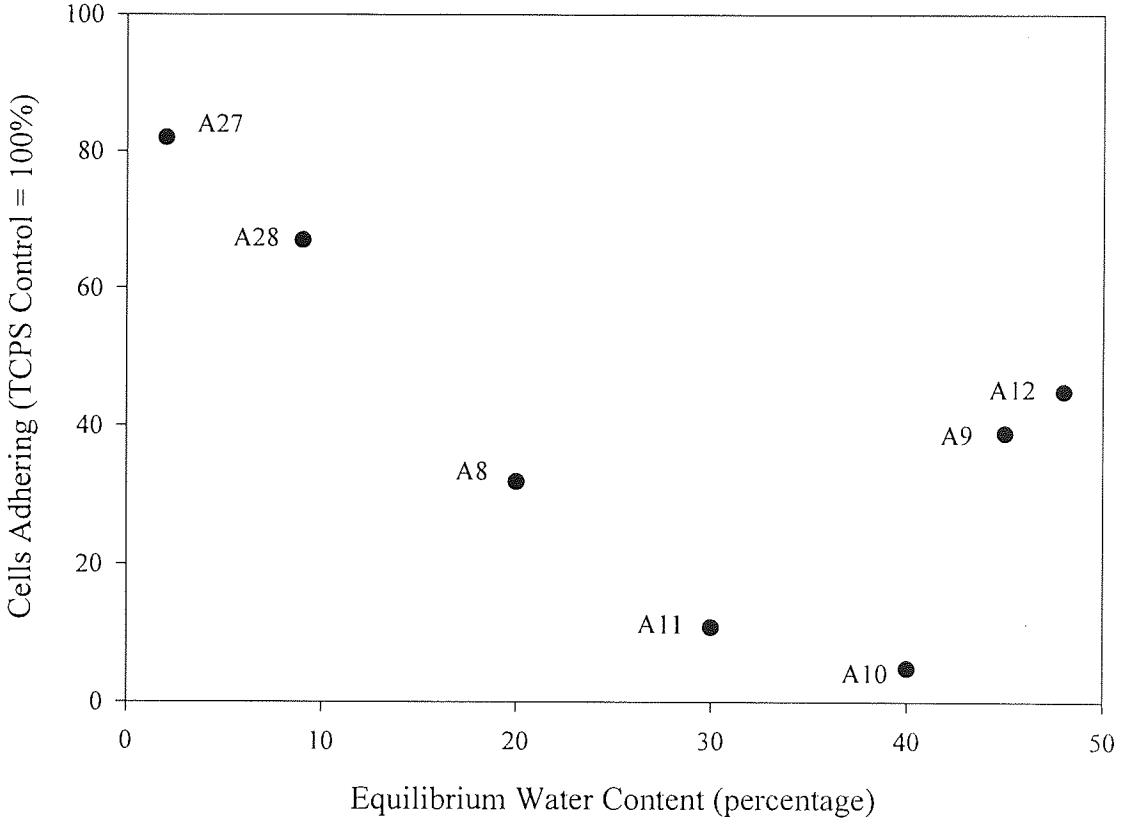

2.5.15 Surface Rugosity

Surface irregularities may allow cells to anchor to a greater extent when compared with materials with the same adhesive parameters but with a smoother surface. This theory is supported by the 'Wenzel effect' which states that "a more rugose surface of the nature of 50nm irregularities caused by plasma treatment, is more wettable than might be assumed from its chemical structure alone".[41]

An irregular surface, as seen in Plate 2.14, A12 (THFFMA:AMO:PU 36.6:41.6:21.8), shows a number of cells extending out filopodia. This may be an indication that the material not only allowed fibroblastic cells to adhere but also to spread extracellular matrix over the surface of the sample. This may indicate that the cells were able to enter a proliferative stage and the cells which divided were able to migrate over the surface of the material to reach areas where contact inhibition did not inhibit growth. The surface of A12 (THFFMA:AMO:PU 36.6:41.6:21.8), appears to be conducive to cell migration and would allow cells to

avoid reduced proliferation by cell contact inhibition if there was still space for cells to migrate to. It appears that a surface may inhibit cell spreading and proliferation over the surface, the surface is just too irregular for cells to migrate over. A surface with "hills" would be more effective at cell spreading than a surface with "mountains" or a surface that was "completely flat".

Plate 2.14 Scanning electron micrograph of 3T3 SME cells seeded on A12 (THFFMA:AMO:PU 36.6:41.6:21.8) for 72 hours (magnification X250)

Several of the hydrogels appeared to have surfaces more rugose than expected. The appearance of the surface, as seen with A27 (EEMA), could be explained by the hydrogel having been removed from the plate used to mould the hydrogel when still hot. This would artificially add a rough surface to the sample and the resulting modified surface would lead to more cells than expected adhering to a polymer.

The morphology of fibroblastic cells can give an indication to the extent of adhesion of the cells to the polymer. Rounded cells may indicate either poor surface adhesion ability or dead cells. Fibroblastic like morphology may indicate that the cells are able to spread over a material and probably will be able to multiply. Cell adhesion is an important prerequisite before cells are able to undergo cellular function such as multiplication and the synthesis of metabolities and proteins.[5]

Although a destructive technique SEM micrographs can indicate if there are significant differences in the degree of spreading of cells on materials and therefore the images can be used to assess the biocompatibility of a material.[42] The SEM micrographs mainly showed cells with a rounded morphology and little fibroblastic

cell spreading. On some samples, such as A27 (EEMA), although few cells were visible, there were substantial amounts of debris on the material which may have been extracellular matrix proteins from cells. This may be an indication that although no cells were seen, they had been present and had been stripped off the surface during processing for SEM observation. The extracellular matrix protein debris resulted from the remains of cells that had adhered more firmly to the hydrogel. This gives an indication that more cells were probably attached and spread out over the surface of the polymer prior to fixation and follows the commonly held view that cells will be lost in the fixation procedure for SEM observation. As an alternative to SEM, oil phase microscopy may have enabled cells to be seen, however, it is likely that the resolution would be insufficient to observe the fine surface details of the cells.[43-45]

2.5.16 Considerations on Fixation of Cells

The problem of retaining cells on a sample whilst it is prepared for SEM could be seen with optically clear samples such as A24 (AMO:EEMA 50:50). After exposure to 3T3 cells for three days the hydrogel appeared to have an almost confluent layer of cells over the surface. However, as the sample was washed and soaked in the various dehydration stages for fixation the cells systematically sloughed off. In addition, filopodia can be destroyed and cracks in the hydrogel produced as artifacts through dehydration through critical point drying.[46]

The most significant loss of cells appeared to occur when samples were initially rinsed with phosphate buffer to remove the medium that interferes with SEM images. When samples were dehydrated in a graded ethanol series often the samples became opaque and so the extent of cell loss was unable to be followed after this stage.

2.5.17 Sample Handling

A number of external factors associated with the structural composition and condition of the polymer may have contributed to the extent of cell adhesion upon the samples. Scratches on a polymer surface may have influenced the extent of cell adhesion, as the surface will be possibly be modified by ridges caused by the abrasive event. Depending on the size of the scratch, the marked surface may inhibit cell migration when cells migrate or spread out. Surface topography showing variations greater than 3μm are thought to be able to alter cellular migration, hence with scratches larger than 3μm the space between the two sides of the groove may not be able to be crossed during cell migration. However, cells may still be able to crawl into the groove and the daughter cells of the original cells migrate out of the groove and colonize the surface of the hydrogel. If the material has many depressions the full colonization of the material may take some time.

2.6 Future Considerations for Keratoprosthetic Material Investigation

The number of cells grown on samples overnight were probably at the lower end of a population that the surface could support before contact inhibition. Longer periods of incubation would allow cells to spread and proliferate to a greater extent, however, the study was designed to screen a large numbers of polymers and to investigate their initial response to cell adhesion. When a choice of which hydrogels were to be investigated further was made then longer incubation times could be used on the smaller set of samples.

An alternative positive control to using HEMA would be to use a solution of dissolved rubber. However this would produce only a cytotoxic response and would just leave dead cells. It would not show the effect of a polymer with a poor tendency to adhere cells.

The fixing procedure adopted for SEM did not adequately fix cells in large numbers and those cells that were fixed usually did not exhibit a fibroblastic like morphology. Perhaps an increase in the concentration of glutaraldehyde in the fixation solution may have enabled more cells to remain fixed to the samples.

Many of the polymer samples were also sensitive to the action of the critical point dryer. When the samples were removed from the critical point dryer the surface of several hydrogels were seen to have had blistered and some of these blisters had actually disrupted the surface considerably. This was particularly apparent with sample A25 (AMO:MEMA 50:50). The action of the critical point dryer may appear to lead to artifact creation on the surface and subsequent loss of cells from the surface of the polymer after blister disruption.

From SEM images, samples cultured with cells for three days instead of one day did allow cells to adhere and proliferate to a greater extent over the surface of the polymers. Therefore the low numbers of cells counted on the samples may be increased if the incubation time is extended to three days instead of one day. Furthermore, when a number of materials are selected for further study it would be recommended that the samples are seeded with cells and left for the cells to proliferate over the sample for periods of 1, 3 and 5 days. Thus, the lag phase of the cell proliferation may be found and allow the length of time before cells reach exponential growth to be determined. Materials can then have cells recovered from their surfaces before the cells reach confluency. However, extending the length of the trial to five days would require the periodic replacement of the spent medium.

Neutral Red and Kenacid Blue R methods as described by Atkins *et al.* should be used to determine cellular viability to materials under test.[47] The Neutral Red assay would replace the Trypan Blue Dye Exclusion method as a more accurate indicator of cell viability. Neutral Red enters cells by diffusion and accumulates in lysosomes and gives an accurate determination of viable cell numbers where the colouration is directly proportional to the Neutral Red concentration. The Kenacid Blue R method would determine the amount of protein and thus the extent of cell growth of the cells within the well. Cytotoxicity assays can oversimplify the events that they measure and therefore there is a need for cytotoxicity testing to be supplemented with tests of metabolic activity. The 3-(4,5-dimethylthiazol-2-yl)-2,5

diphenyl tetrazolium bromide (MTT) assay would give an indication of metabolic activity by measuring the efficiency of lactate dehydrogenase enzymes in cell mitochondria. This would give a better estimate of the cell viability of the cells exposed to the samples. However, compared with the rapid evaluation of cell viability as determined by the Trypan Blue Dye Exclusion method the experimental time involved in testing large numbers of samples using this MTT assay would have been prohibitive for an initial screening study unless the test was automated. The aim of the project was to initially screen a comparatively large number of materials so as to select a small number of materials for more comprehensive investigation.

2.7 Conclusions

This investigation suggests that a composite of different hydrogels is likely to give the desired core and skirt components for a keratoprosthetic device. A composite would allow the Kpro to have improved cell adhesion and proliferation on the base and lessen cell adhesion on the optical core, as well as retaining the desired physical characteristics to produce an efficient long term implant.

When polymer composites are tested with a wide range of properties it is often difficult to determine individual characteristics of the composite hydrogels. Different hydrogels can have different effects depending on their component monomers e.g. AMO with MEMA or EEMA. In addition, it is not guaranteed that the expected characteristics of a polymer will be replicated when it is incorporated with other hydrogels.

Surface topography is an important consideration, pores, channels and fibres exposed on the surface of the hydrogels tested have significant effects on the extent of cell adhesion and proliferation. Additionally, it should be noted that different cell types have different reactions to the same surface, although one cell type may adhere another may not. However, by using a fibroblast cell line the effect of the first cells to adhere to the hydrogels during the healing response in the corneal tissue should be measured, not the cells which form during the later stages of recolonization. *In vivo*, it is expected that in the short term the materials will behave as expected, this is all that can be predicted when using a simple cell culture model. Studies of long term behaviour of an implant do need to be undertaken *in vivo*, however, this investigation has hopefully reduced the time and expense of later developmental stages by reducing the number of candidates to be tested.

The importance of a consistent standard of manufacture cannot be overemphasised, batch to batch variation caused by deviations from standard operating procedure could have serious consequences on the efficiency of keratoprosthetic implant integration. Stringent laboratory procedure must be carried out to reduce possible misleading information.

It is recommended that the core component is fabricated out of one of the following:

Sample	Hydrogels	Composition (percentage)
A8	THFFMA:NVP:PU	41.6:41.6:16.8
A11	THFFMA:AMO:PU	41.6:41.6:16.8
A13	THFFMA:AMO:CAB	36.6:36.6:26.8
A22	Poly(acrylamide):HPA:PU:THFFMA:AMO	10:10:10:30:40
A23	AMO:EEMA:MEMA	50:25:25

All core candidates showed low rates of cell adhesion and proliferation. An important feature of the chosen selection is that they are all quite different in their hydrogel compositions. If one was found to be unsuitable in later stages of development then there exists alternatives with sufficient differences in composition to possibly overcome the undesired characteristic. For example, polyurethane valves in animal trials have been susceptible to calcification. If the keratoprosthetic core device is required to be free from biospoilation caused by polyurethane, there are alternative candidates of A13 and A23 that can be possibly employed.[30-34,46]

The haptic periphery is recommended to be fabricated out of one of the following:

Sample	Hydrogels	Composition (percentage)
A33	AMO:EEMA:MEMA:THFFMA:HA (250μm)	25:25:25:25
A37	THFFMA:AMO:PU:HA (250μm)	37:42:21:10
A38	THFFMA:AMO:PU:DEX:DEXTRAN	30:50:20:10:4
A42	AMO:EEMA:MEMA:THFFMA:Hap W	25:25:25:25
A43	THFFMA:AMO:PU:Hap W	37:42:21:10
A44	THFFMA:AMO:PU:Hap W	30:50:20:10

The skirt component candidates mostly include hydrogels containing hydroxyapatite components. This is because the cell numbers from components containing hydroxyapatite, (especially whiskers) were superior compared with alternatives. If alternative materials are required that do not contain any hydroxyapatite components, two alternatives are, A16 and A30:

Sample	Hydrogels	Composition (percentage)
A16	THFFMA:AMO:PU	30:50:20
A30	AMO:EEMA:MEMA: THFFMA:DEX:DEXTRAN	25:25:25:25

CHAPTER THREE
Cellular Adhesion to Biodegradable Materials

3.1 Aim

To determine the cell adhesiveness and cytotoxicity of blends of polyhydroxybutyrate-hydroxyvalerate (PHB-HV) polysaccharide containing blends after their degradation under physiological conditions. *In vitro* cell techniques may enable initial degradation of PHB-HV to be monitored with greater sensitivity as physical monitoring by water uptake and weight loss techniques of the initial degradation profile is difficult to monitor under physiological conditions.

3.2 Introduction

3.2.1 Polyhydroxybutyrate

Polyhydroxybutyrate (PHB) and polyhydroxyvalerate (PHV) are polyesters produced by bacteria such as Bacillus megatenium for the purpose of carbon and energy storage. The degradation product of PHB is 3-hydroxybutyric acid, which is found in man and is considered to be a non-toxic and biodegradable. Due to its ease of fabrication and slow hydrolysis PHB is ideal as a temporary implant in the body and as such is used for sutures. The degradation of PHB may also have an application in wound healing, when spun into fibres, the fibres can be used at the site of a wound to provide a wound scaffold until the dermal architecture has been replaced. The PHB is eventually assimilated into the host so there is no need to rely on invasive surgery to remove such artificial wound scaffolding.

3.2.2 Biodegradation

The term biodegradation refers to the hydrolytic, enzymatic or bacterial degradation of a polymer matrix.[48] Degradation of a polyhydroxybutyrate-polyhydroxyvalerate (PHB-HV) blend commences with the diffusion of aqueous buffer into the matrix of the copolymer as can be seen by an increase in wet weight of the polymers. Degradation continues with low molecular weight molecules dissolving into the buffer and eluting out from the matrix of the polymer resulting in a corresponding increase in surface energy and rugosity. As the polymer commences to fragment larger molecules are able to diffuse out and there is a marked decrease in weight and tensile strength.[48]

3.3 Materials

3.3.1 Cell Culture

The cell lines used were NCTC (L929) mouse areolar cells (ECACC 88102702) and BHK-21 (Clone 13) baby hamster kidney cells (ECACC 850111433). Both cell lines were routinely maintained in Dulbecco's Modified Eagles Medium (DMEM) (Life Technologies) supplemented with 10% foetal calf serum (Life Technologies), 2mM L-glutamine (Sigma), 250μg/ml Fungizone (Life Technologies) and 10mg/ml Gentamycin (Sigma). Sub confluent cells were used for testing to ensure maximum viability with cells typically subcultured at $1x10^4$ cells/ml after 3 days and 7 days for BHK-21 (growth rate $0.56h^{-1}$) and L929 (growth rate $0.24h^{-1}$) cells respectively, Figure 3.1 and 3.2. Passage numbers 2 to 6 were used for experimentation.

Figure 3.1 Growth Curve of BHK-21 Baby Hamster Kidney Cell Line

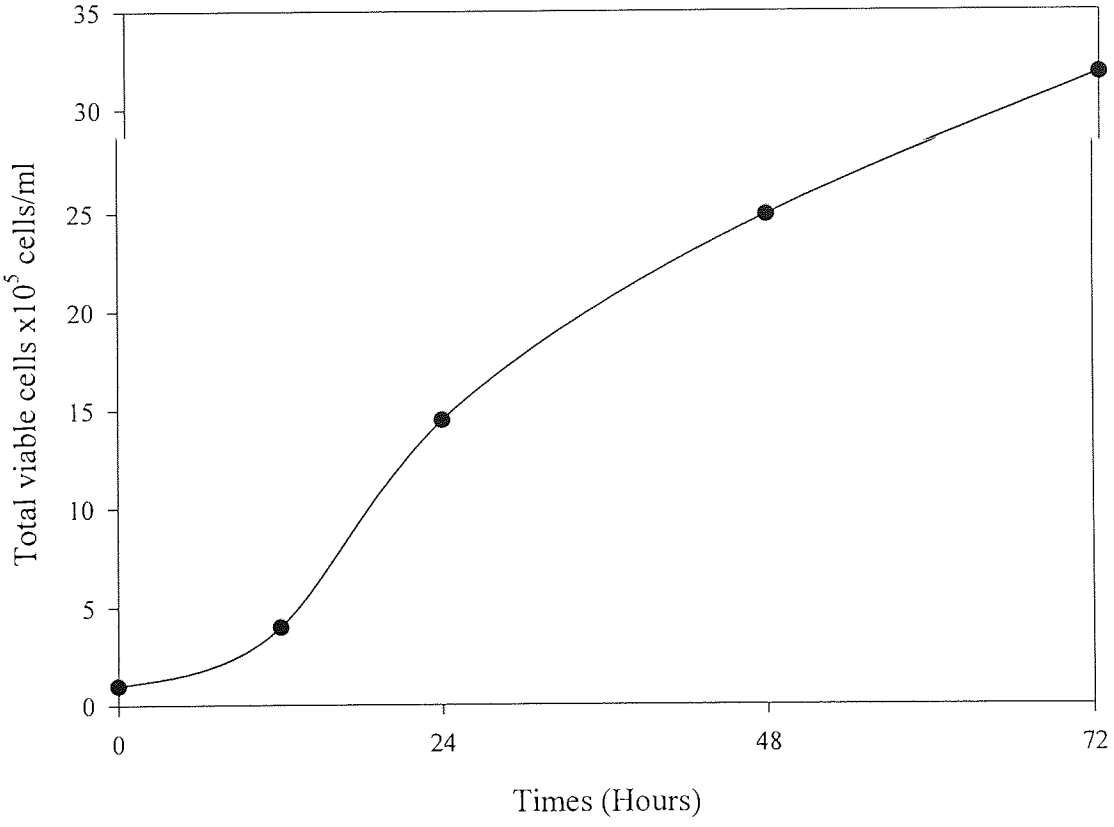

Figure 3.2 Growth Curve of NCTC (L929) Mouse Areolar Cell Line

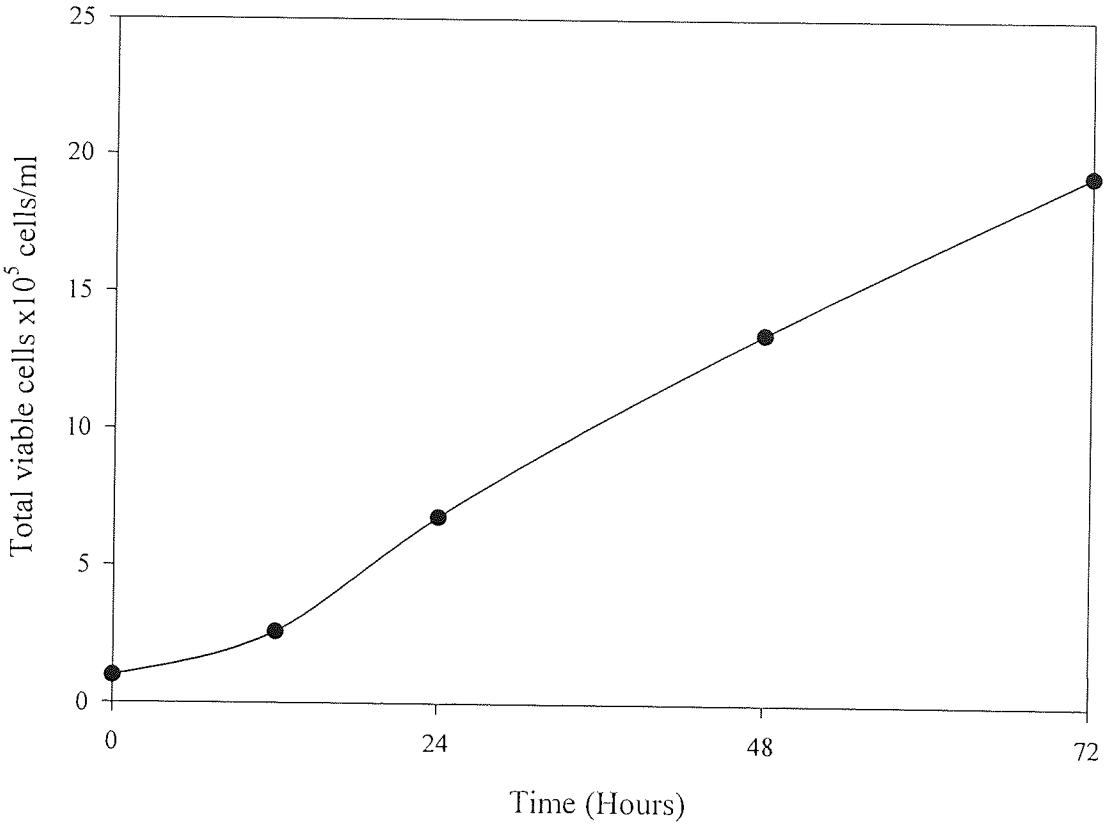

3.3.2 Polymer degradation

Blends of PHB-HV and HV polymers that contained amylose, dextrin and dextran were prepared using conventional melt blending techniques by Yasin according to the method described by Yasin *et al.*[49] Degradation of the PHB-HV copolymers was carried out in phosphate (KH_2PO_4/K_2HPO_4) buffer solution at pH7.4 at defined times as noted in the results. Yasin *et al.* had previously placed the samples in 50ml of the buffer solution and maintained at 37°C in a water bath.[49] The samples were periodically removed washed with distilled water and placed between filter paper to remove the surface water in preparation for dry weight measurement. Samples were dried *in vacuo* at 80°C.

3.3.3 Material Testing for Cell Numbers and Viability

Samples were sterilized by autoclaving (121°C/15 minutes/2 bar) and by washing in a 1% Tween 20 (Sigma) solution for one hour, followed by aseptic rinsing in sterile

water and then placed in individual wells of a 24 well plate (Corning). They were seeded with 1ml of cell suspension at a cell density of $1x10^5$ cells/ml. The plates were placed in a Gallenkamp CO_2 incubator for 18 hours at 37°C with a 95% air/5% CO_2 atmosphere. Post incubation, samples were rinsed in Phosphate Buffered Saline (without Ca^{2+} or Mg^{2+}) (Sigma) and placed in a fresh 24 well plate with 1ml of 2.5% trypsin/EDTA solution (Sigma), incubated at 37°C, to effect cell removal and then counted using a haemocytometer. Cell viability was determined by the Trypan Blue Exclusion test. 0.1ml of 0.4% Trypan Blue solution (Sigma) was added to 1ml of cell suspension, cell counts taken and the percentage of viable cell calculated. Samples for cell counts recorded were the mean values of five replicates.

3.3.4 Scanning Electron Microscopy

Samples were prepared for SEM by fixing in 2% glutaraldehyde (Sigma) in 0.1M sodium cacodylate buffer, dehydration of the samples was achieved through a graded alcohol series and final drying achieved under liquid Freon-113 (TAAB) in a Polaron E3100 II critical point dryer. Samples were mounted on aluminium SEM stubs (Biorad) and gold coated in a Polaron sputter coating unit at 1kV and 20mA. Following coating, samples were examined in a Cambridge Stereoscan electron microscope at accelerating voltages of 15-25kV.

3.4 Results

Blends of PHB-HV with different compositions of polysaccharide fillers and controls of TCPS and HEMA were cultured with BHK-21 (clone 13) and NCTC(L929) cell lines as described in 3.3.3 to determine cell adhesion. In addition, the polymer blends and controls underwent examination by SEM techniques as described in 3.3.4 to examine the cell adhesion and proliferation responses.

3.4.1 BHK-21 (clone13) and NCTC(L929) Cell Adhesion to Control Surfaces

Table 3.1 Cell adhesiveness and cytotoxicity of BHK-21 (clone 13) cells on Tissue Culture Polystrene (TCPS) and HEMA (controls)

Description	Mean Cell Value ($x10^5$ cells/ml) ± S.D	Viability (%)
TCPS (positive control)	3.34±0.6	99
HEMA (negative control)	1.09±0.2	100

The extent of cell adhesion and spreading on SEM samples was graded as follows:

Grade	Description
0	No cell attachment
*	Few cells exhibiting rounded morphology
**	Cells showing fibroblast morphology and clearly adhering to surface
***	Fibroblast cells proliferating over the sample
****	Confluent cell layer over sample with fibroblast morphology

Table 3.2 SEM observation of the extent of cell adhesion of BHK-21 (clone13) cells to TCPS and HEMA (controls) over three days

Sample	1 Day seeding with BHK cells	2 Day seeding with BHK cells	3 Day seeding with BHK cells
TCPS	***	****	****
PHEMA	*	*	*

BHK-21 cells exhibited classical fibroblast morphology and the cells rapidly spread across the TCPS material as a confluent cell layer. On HEMA the cells did not proliferate and those BHK-21 cells that had adhered remained rounded in morphology. SEM photographs showing BHK-21 cell adhesion to TCPS and HEMA can be seen in Plates 3.1-3.2 and 3.3 respectively.

Plate 3.1 BHK-21 cells seeded on TCPS 3 days (magnification X13)

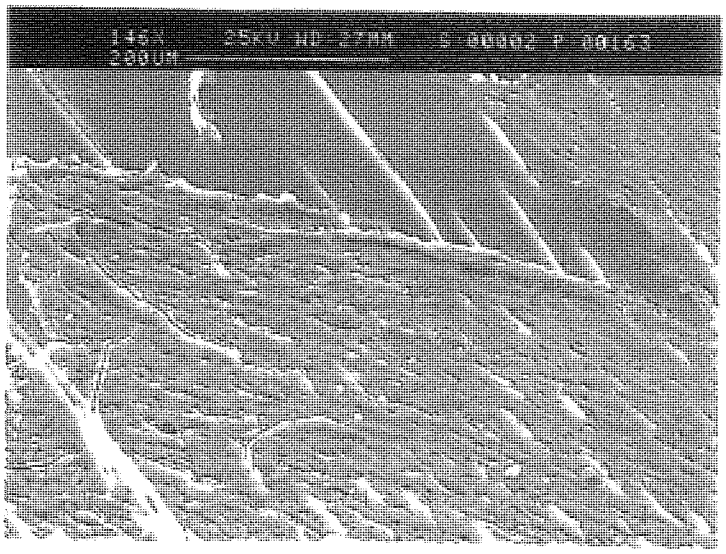

Plate 3.2 BHK-21 cells seeded on HEMA 3 days (magnification X145)

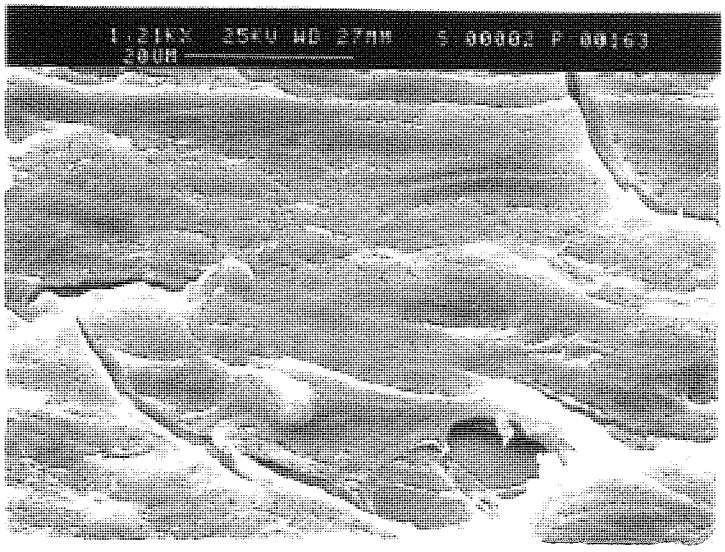

Plate 3.3 BHK-21cells seeded on HEMA 3 days (magnification X38)

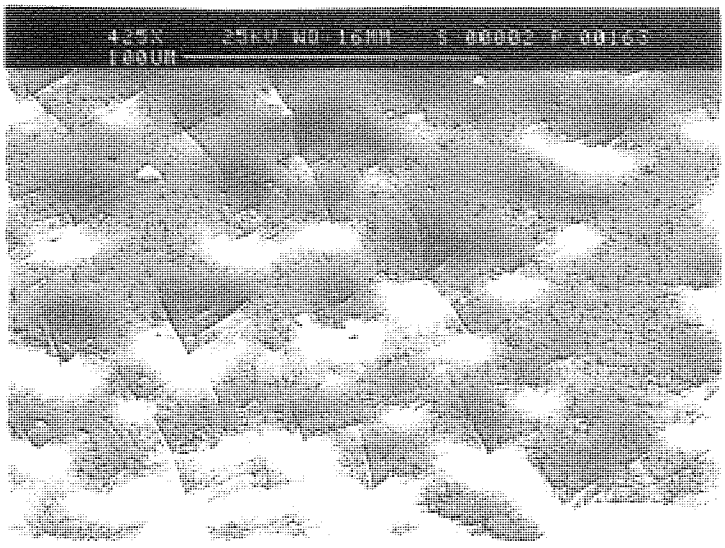

After 1 day NCTC (L929) cells on TCPS showed classical fibroblast morphology. However, cells seeded on HEMA samples exhibited a rounded morphology even after three days in contact with the sample. SEM photographs showing NCTC L929 cell adhesion to TCPS and HEMA can be seen in Plates 3.4-3.5 and 3.6 respectively.

Table 3.3 Cell adhesiveness and cytotoxicity of NCTC (L929) on TCPS and HEMA controls

Description	Mean Cell Value ($x10^5$ cells/ml) ± S.D	Viability (%)
TCPS (positive control)	2.47±0.6	99
HEMA (negative control)	0.58±0.1	98

Table 3.4 SEM observation of the extent of cell adhesion of NCTC (L929) cells to TCPS and HEMA controls over three days

Sample	1 Day seeding with NCTC cells	2 Day seeding with NCTC cells	3 Day seeding with NCTC cells
TCPS	***	***	***
PHEMA	*	*	*

Plate 3.4 NCTC (L929) cells seeded on TCPS 3 days (magnification X35)

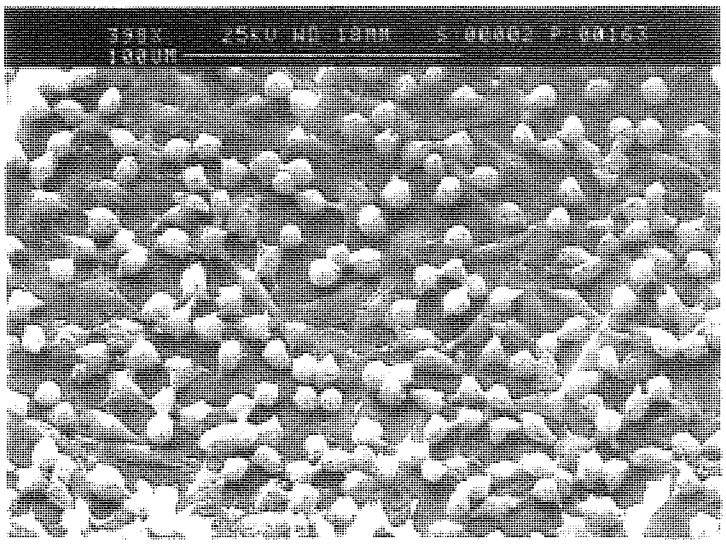

Plate 3.5 NCTC (L929) cells seeded on TCPS 3 days (magnification X145)

Plate 3.6 NCTC (L929) cells seeded on HEMA 3 days (magnification X16)

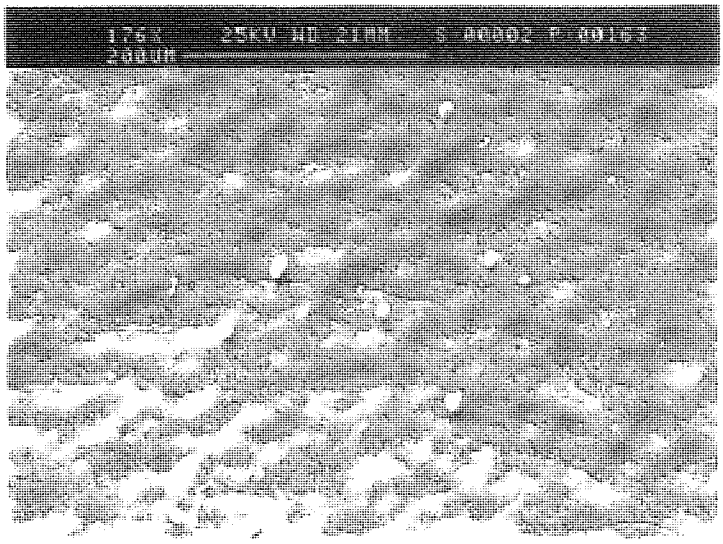

3.4.2 BHK-21 (clone13) and NCTC (L929) Cell Adhesion to Blends of PHB-HV /polysaccharides

Degradation of 12% PHB-HV blends containing polysaccharides generally increased cell numbers adhering to the material until a peak in cell adhesion was reached, Figures 3.3-3.4. After the peak in cell numbers the cell numbers gradually decreased with degradation time and eventually levelled out to a plateau. The PHB-HV sample that contained amylose showed only the later half of the peak, Figure 3.5. Individual results for BHK cell adhesion to 12% PHB-HV blends containing polysaccharides can be seen in Appendix I Tables 6.1-6.3.

Figure 3.3 Cell Adhesion of BHK-21 Cells Seeded 18h on 12% HV PHB-HV 10% Dextrin (n=5 +/-S.D)

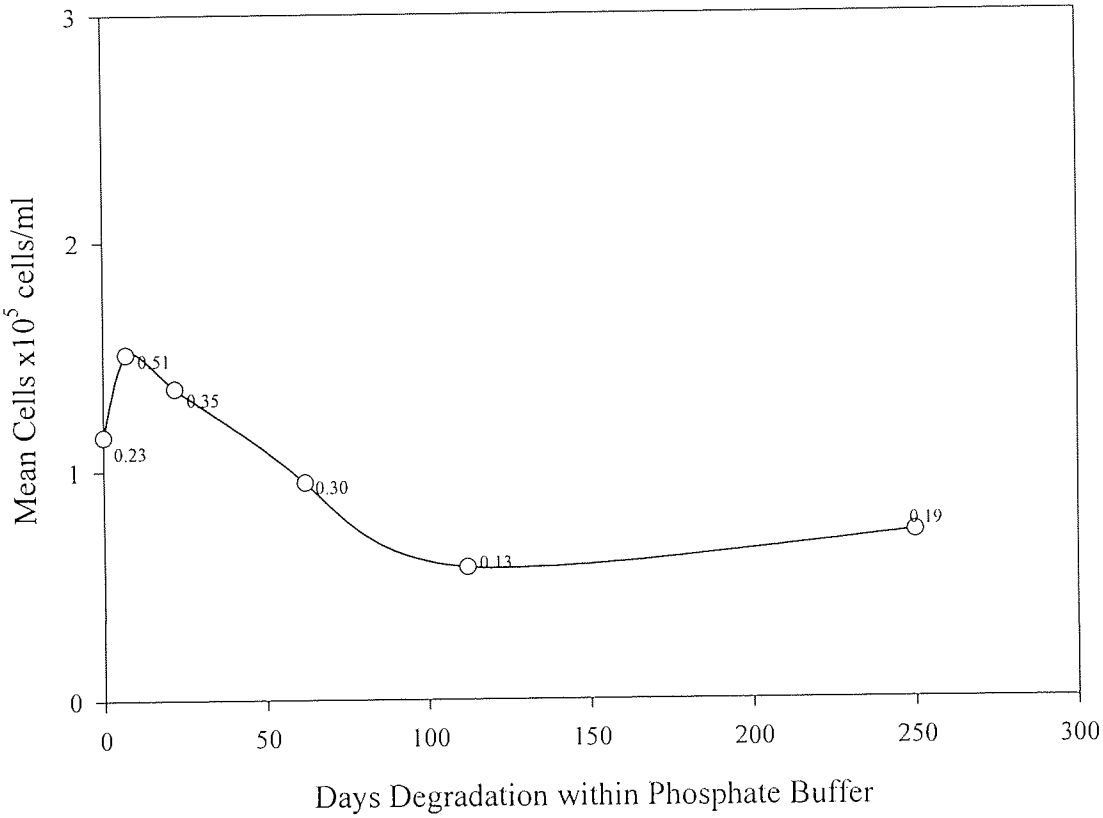

Note: S.D. Displayed next to plot points

Figure 3.4 Cell Adhesion of BHK-21 Cells Seeded 18h on 12% HV PHB-HV 10% Dextran (n=5 +/- S.D.)

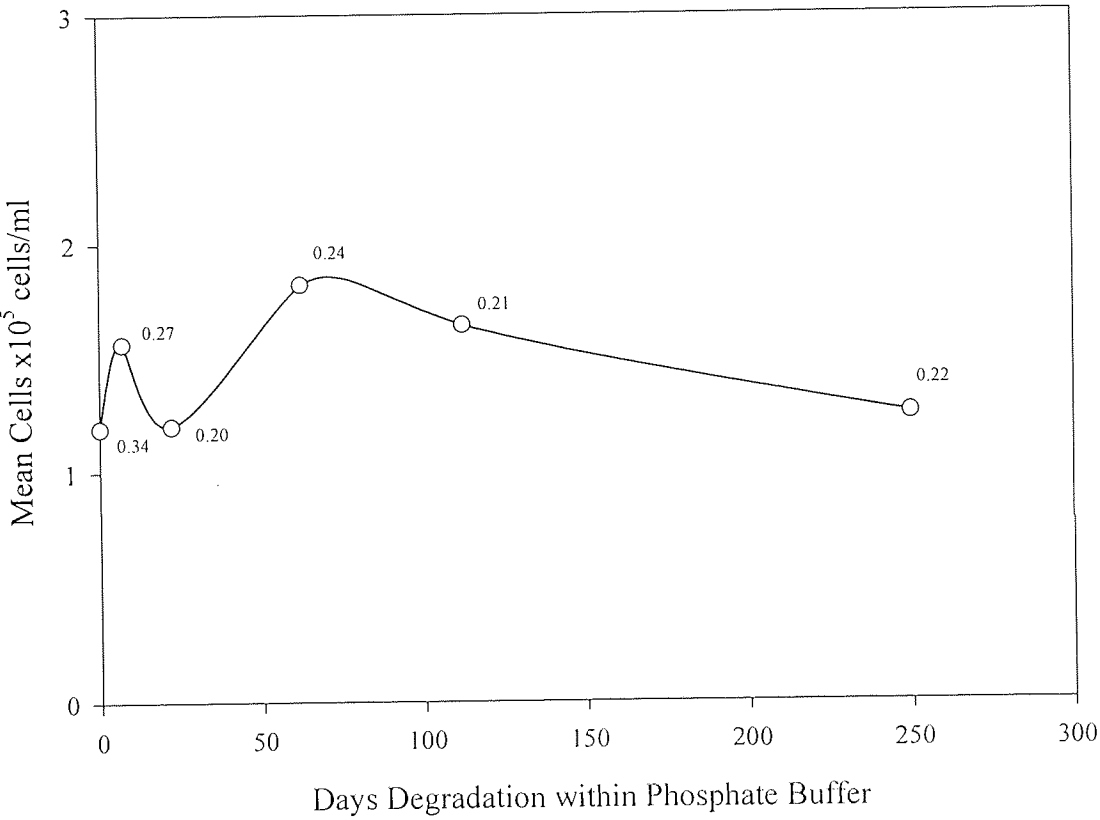

Note: S.D. Displayed next to plot points

Figure 3.5 Cell Adhesion of BHK-21 Cells Seeded 18h on 12% HV PHB-HV 10% Amylose (n=5 +/- S.D.)

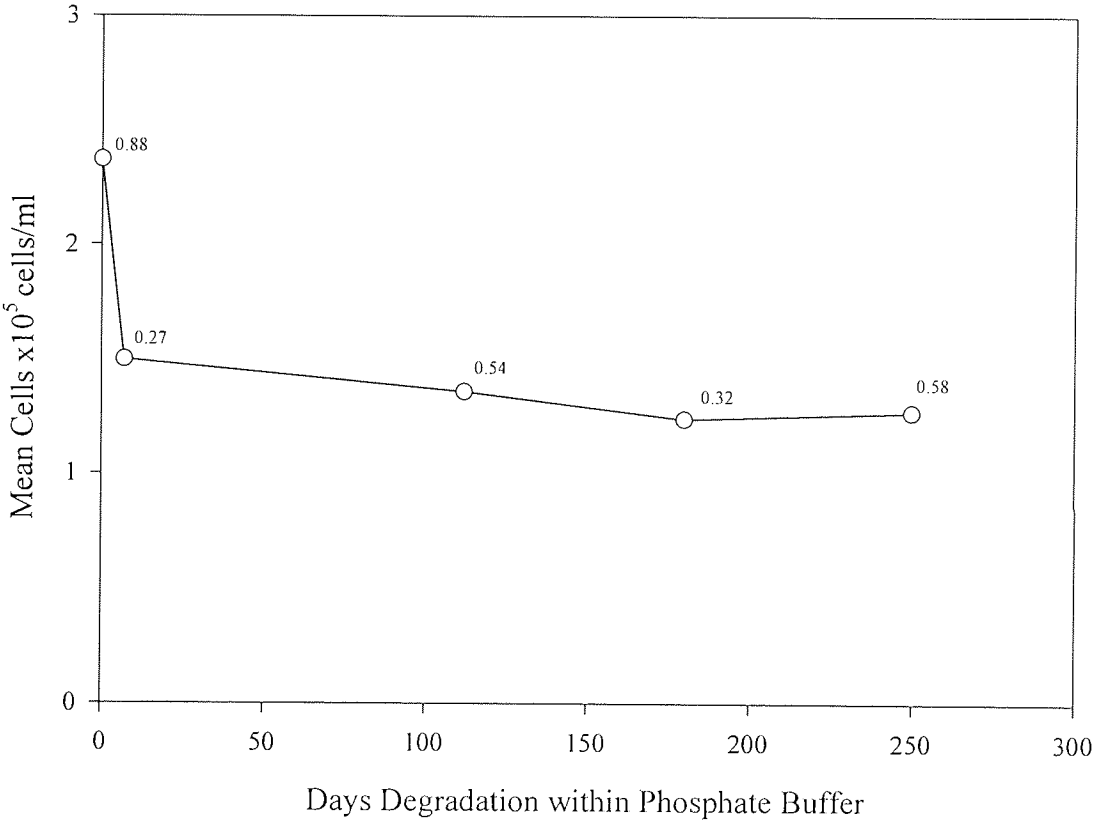

Note: S.D. Displayed next to plot points

12% HV PHB-HV samples seeded with NCTC (L929) cells duplicated the results seen with BHK-21 cells, Tables 3.6-3.8, as did those blends containing 20% HV seeded with both cell lines, Figure 3.6 and Tables 3.9-3.13. However, with 20% HV PHB-HV the initial decline of the slope of cell numbers appeared to be steeper with those samples that contained dextrin, Figure 3.6.

Table 3.5 Cell adhesiveness and cytotoxicity of NCTC (L929) cells seeded onto 12% HV PHB-HV 10% Dextrin blend (5 replicates)

Description	Mean cell value ($x10^5$ cells/ml± SD	Viability (%)
Undegraded	0.73±0.15	100
Undegraded	0.94±0.16	100
7 days	1.02±0.19	100
7 days	0.88±0.27	100
22 days	0.88±0.22	96
112 days	0.90±0.18	96
250 days	0.67±0.25	95

Table 3.6 Cell adhesiveness and cytotoxicity of NCTC (L929) cells seeded onto 12% HV PHB-HV 10% Dextran blend (5 replicates)

Description	Mean Cell Value ($x10^5$ cells/ml) ± SD	Viability (%)
Undegraded	1.02±0.18	98
7 days	0.42±0.20	94
7 days	0.66±0.21	98
22 days	1.12±0.28	96
22 days	0.17±0.10	90
62 days	0.77±0.17	97
112 days	0.48±0.14	94
180 days	0.22±0.09	100

Table 3.7 Cell adhesiveness and cytotoxicity of NCTC (L929) cells seeded onto 12% HV PHB-HV 10% Amylose blend (5 replicates)

Description	Mean Cell Value ($x10^5$ cells/ml) ± SD	Viability (%)
0 days	1.90±0.62	96
7days	1.18±0.36	100
112 days	0.64±0.13	89
180 days	0.91±0.27	98
250 days	0.95±0.39	94

Figure 3.6 Cell Adhesion of BHK-21 Cells Seeded 18h on 20% HV PHB-HV 10% Dextrin (n=5 +/- S.D.)

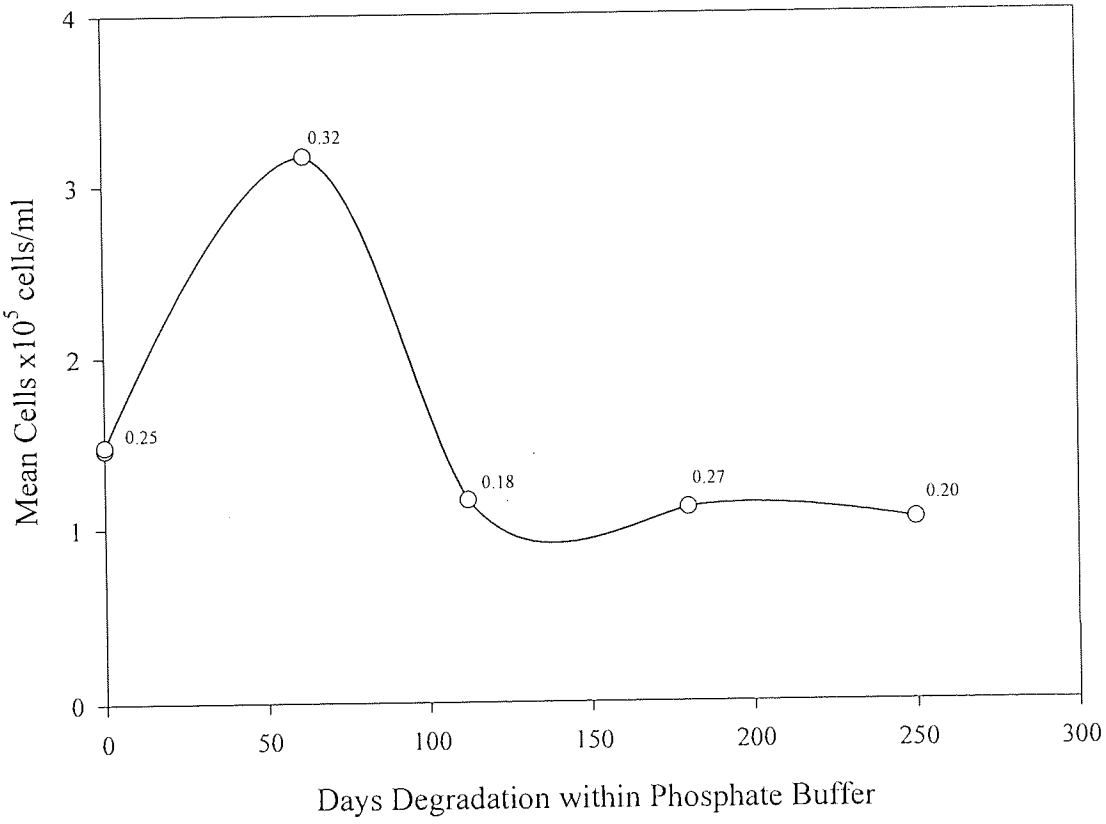

Note: S.D. Displayed next to plot points

Table 3.8 Cell adhesiveness and cytotoxicity of BHK-21 cells seeded onto 20% HV PHB-HV 10% Dextran blend (5 replicates)

Description	Mean Cell Value ($x10^5$ cells/ml) ± SD	Viability (%)	SEM
Undegraded	1.15±0.25	94	****
Undegraded	1.15±0.13	98	
7 days	1.68±0.33	99	****
7 days	1.79±0.21	97	
22 days	1.84±0.19	98	
112 days	1.48±0.29	98	****
180 days	1.57±0.21	100	****
250 days	1.54±0.24	99	****

Table 3.9 Cell adhesiveness and cytotoxicity of BHK-21 cells seeded onto 20% HV PHB-HV 10% Amylose blend (5 replicates)

Description	Mean Cell Value ($x10^5$ cells/ml) ± SD	Viability (%)	SEM
0 days	0.77±0.20	99	
7 days	1.43±0.77	96	*
62 days	1.23±0.32	94	**
112 days	1.07±0.30	97	**
180 days	1.81±0.76	96	**
250 days	1.82±0.85	95	*

Table 3.10 Cell adhesiveness and cytotoxicity of NCTC (L929) cells seeded onto 20% HV PHB-HV 10% Dextrin blend (5 replicates)

Description	Mean Cell Value ($x10^5$ cells/ml) ± SD	Viability (%)
Undegraded	0.94±0.17	96
7 days	0.70±0.15	96
112 days	0.71±0.17	96
250 days	0.73±0.21	98

Table 3.11 Cell adhesiveness and cytotoxicity of NCTC (L929) cells seeded onto 20% HV PHB-HV 10% Dextran blend (5 replicates)

Description	Mean Cell Value ($x10^5$ cells/ml) ± SD	Viability (%)
Undegraded	1.01±0.15	100
7 days	1.17±0.25	100
22 days	0.87±0.25	100
22 days	0.59±0.15	100
62 days	0.93±0.22	97
112 days	0.72±0.19	99
180 days	0.43±0.16	91

Table 3.12 Cell adhesiveness and cytotoxicity of NCTC (L929) cells seeded onto 20% HV PHB-HV 10% Amylose blend (5 replicates)

Description	Mean Cell Value ($x10^5$ cells/ml) ± SD	Viability (%)	SEM
0 days	0.56±0.20	95	*
7 days	0.34±0.11	86	*
62 days	1.54±0.43	93	*
112 days	0.56±0.26	95	*
112 days	0.50±0.25	86	
180 days	0.42±0.24	94	*
250 days	0.78±0.23	97	

It was found that 12% HV and 20% HV PHB-HV blends that contained dextran were less cell adhesive than blends that contained dextrin. Although the result was not statistically significant with 12% HV (assuming normal distribution and unequal variance heteroscedastic t-tests) comparing dextran to 7 and 22 days dextrin. In the later stages of the measured degradation, e.g. 250 days degradation, blends that contained dextran and amylose were found to be very similar in cell adhesion and were not statistically significant in differences in cell adhesion numbers, Figures 3.7 and 3.8.

Figure 3.7 Cell Adhesion of BHK-21 Cells Seeded 18h on 12% HV PHB-HV Blends Degraded for 250 Days (n=5 +/- S.D.)

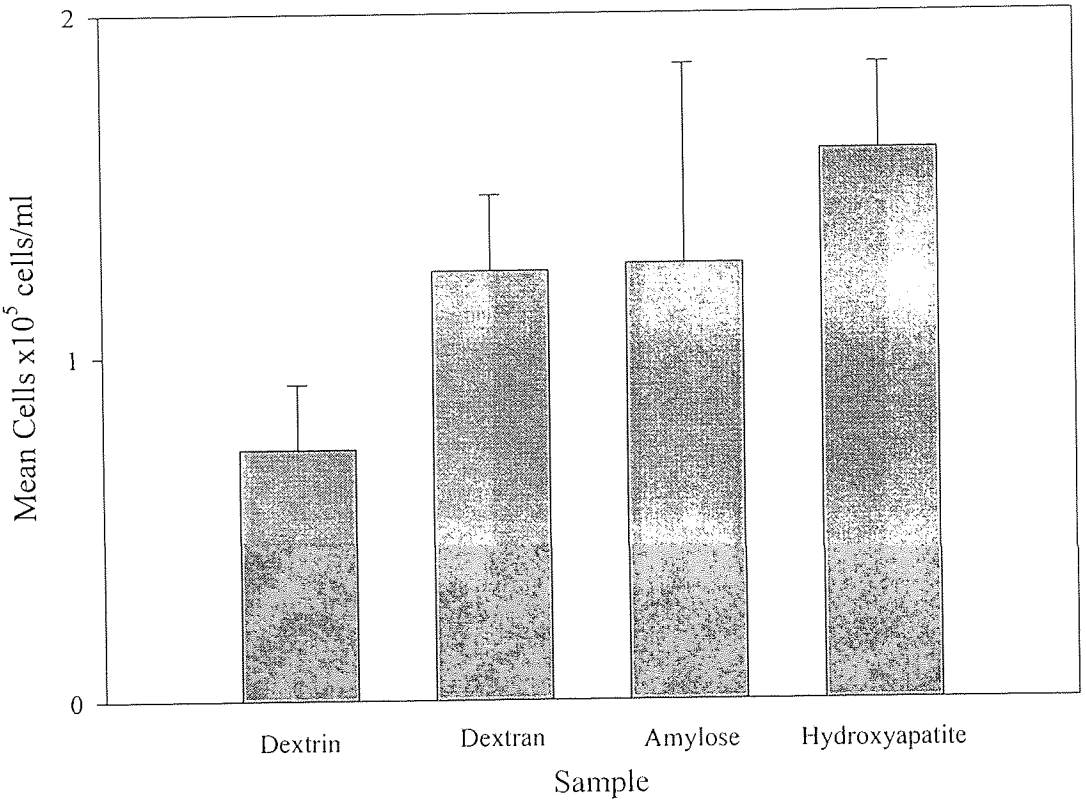

Figure 3.8 Cell Adhesion of BHK-21 Cells Seeded 18h on 20% HV PHB-HV Blends Degraded for 250 Days (n=5 +/- S.D.)

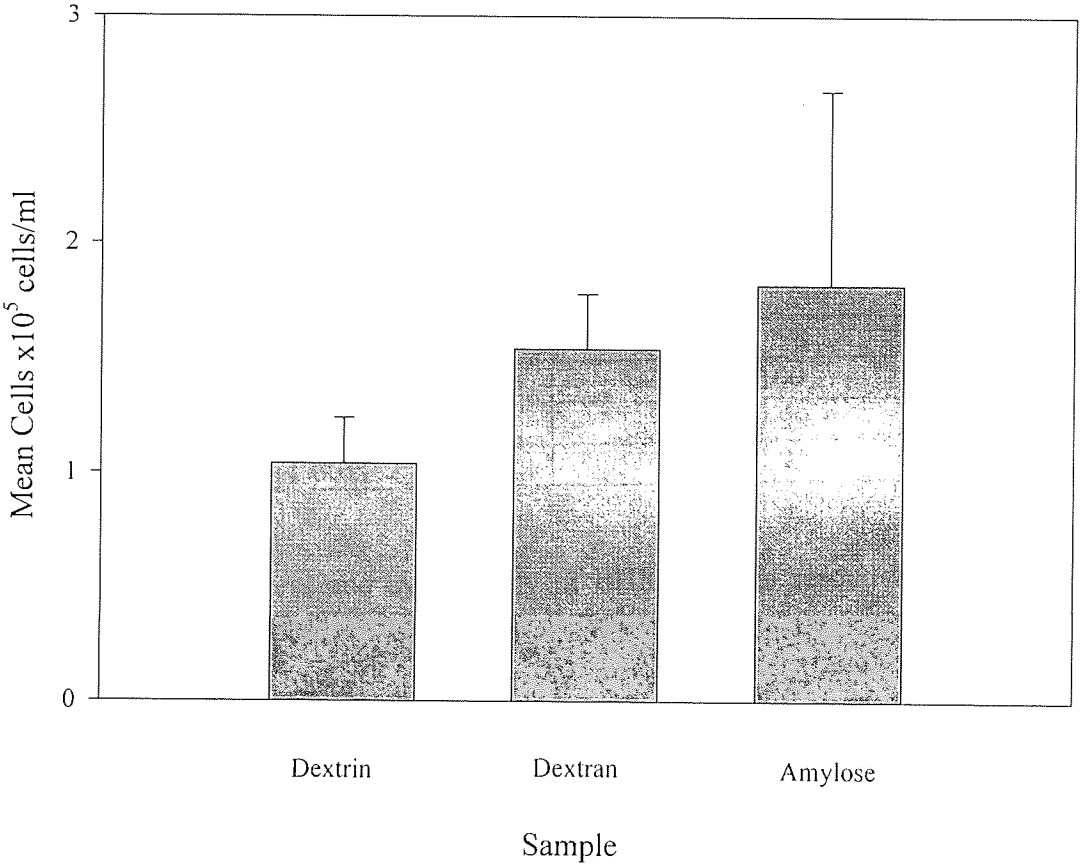

The samples that contained hydroxyapatite as a nucleating agent produced the highest cell adhesion numbers, when compared to samples that contained polysaccharides, Tables 3.13-3.16. Comparing hydroxyapatite 12% and 20% HV seeded with BHK-21 cells (assuming normal distribution and unequal variance) heteroscedastic t-tests indicated that the results were statistically significant only with dextran $P<0.001$. With NCTC (L929) cells hydroxyapatite 12% HV reflected the same results seen with BHK-21 cells as did the undegraded and 7 days degradation samples of 20% HV. Cell adhesion on progressively more degraded samples followed the same trend as seen with blends containing polysaccharides with an initial peak in cell adhesion followed by a decline in cell numbers.

Table 3.13 Cell adhesiveness and cytotoxicity of BHK-21 cells seeded onto 12% HV PHB-HV blend containing Hydroxyapatite (5 replicates)

Description	Mean Cell Value ($x10^5$ cells/ml) ± SD	Viability (%)
0 days	2.26±0.67	98
7 days	4.01±0.44	100
112 days	2.61±0.81	99
250 days	1.60±0.25	95

Table 3.14 Cell adhesiveness and cytotoxicity of BHK-21 cells seeded onto 20% HV PHB-HV blend containing Hydroxyapatite (5 replicates)

Description	Mean Cell Value ($x10^5$ cells/ml) ± SD	Viability (%)
0 days	1.68±0.41	90
7 days	3.70±0.45	97
62 days	3.02±1.22	94
180 days	1.37±1.13	100
250 days	0.28±0.13	100

Table 3.15 Cell adhesiveness and cytotoxicity of NCTC (L929) cells seeded onto 12% HV PHB-HV blend containing Hydroxyapatite (5 replicates)

Description	Mean Cell Value ($x10^5$ cells/ml) ± SD	Viability (%)
0 days	2.24±0.77	98
7 days	3.92±1.80	99
180 days	1.37±0.37	100

Table 3.16 Cell adhesiveness and cytotoxicity of NCTC (L929) cells seeded onto 20% HV PHB-HV blend containing Hydroxyapatite (5 replicates)

Description	Mean Cell Value ($x10^5$ cells/ml) ± SD	Viability (%)
0 days	8.96±3.20	99
7 days	2.77±0.34	99
7 days	7.96±0.82	98
62 days	1.63±0.26	100

Undegraded blends with a 12% HV content gave very similar cell adhesion trends to those observed with long term degradation samples. However, blends that contained amylose were more cell adhesive with BHK-21 cells than those blends with hydroxyapatite, Figure 3.9. It should be noted that the results were not statistically significant. Using 20% HV content hydroxyapatite again gave the highest cell adhesion particularly with NCTC (L929) cells, Figure 3.10. After 7 days degradation the extent of cell adhesion on 12% HV blends containing polysaccharides was very similar with BHK-21 cells, the cell adhesion, appearing indifferent to the polysaccharide used whilst PHB-HV containing hydroxyapatite still adhered the highest number of cells, Figure 3.11.

Figure 3.9 Cell Adhesion of BHK-21 Cells Seeded 18h on 12% HV PHB-HV Undegraded Samples (n=5 +/- S.D.)

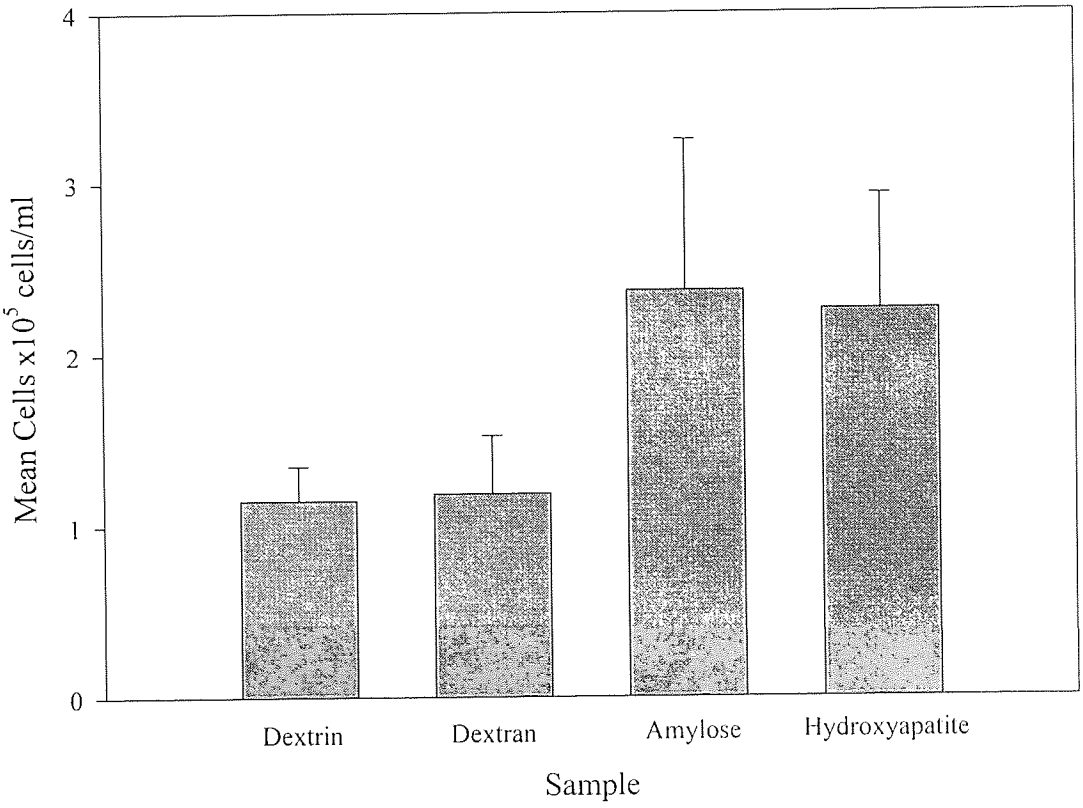

Figure 3.10 Cell Adhesion of NCTC L929 Cells Seeded 18h on 20% HV PHB-HV Undegraded Samples (n=5 +/- S.D.)

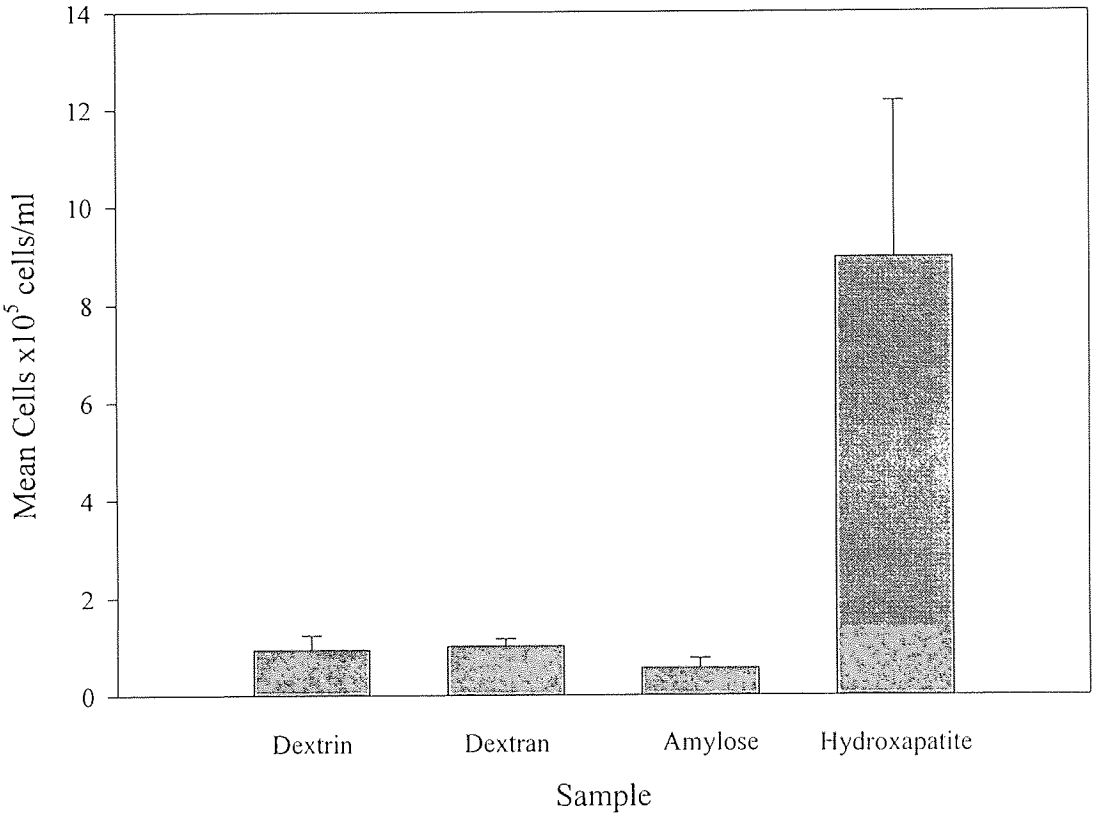

Figure 3.11 Cell Adhesion of BHK-21 Cells Seeded 18h on 12% HV PHB-HV Samples 7 days Degradation (n=5 +/- S.D.)

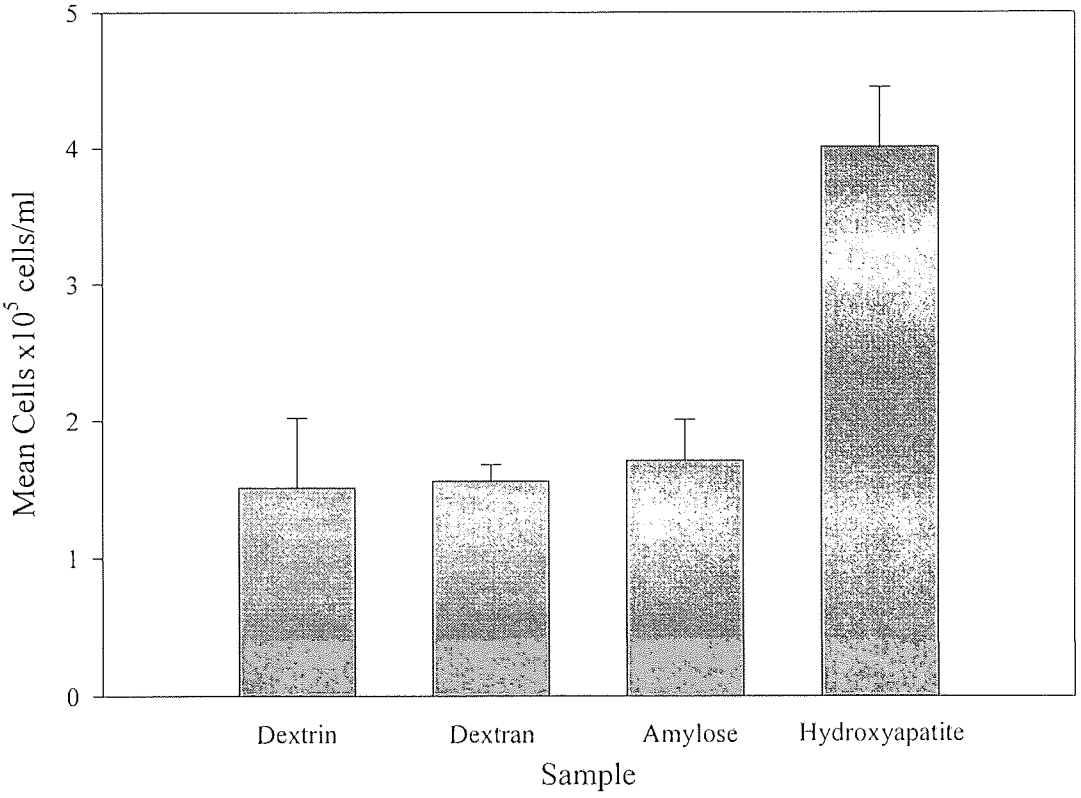

3.4.3 Scanning Electron Microscope Images

BHK-21 cells cultured on PHB-HV blends for 1 day were rounded and many cells may have been stripped off the surface of samples as indicated by the amount of cellular debris that had remained. After three days in culture with BHK-21 cells the small number of cells that had attached to samples had spread out and in many cases appeared to have been able to colonize and proliferate over the materials.

The SEM micrographs of BHK-21 cells cultured on 12% HV PHB-HV/10% dextrin blends showed that the cell proliferation progressed as the duration of degradation was extended, Plates 3.7 to 3.11. Compared with 12% HV PHB-HV/10% dextran blends fewer cells were observed on the samples containing dextrin. After 62 days degradation blends that contained dextrin, the samples were covered with a confluent cell layer, however, there were clearly defined spaces between the cells and the cell layer also appeared to have begun to flake off the sample. Despite the apparent poor preservation, the cells exhibited fibroblastic morphology with rounded cells only seen on undegraded samples. Plate 3.12.

Plate 3.7 BHK-21 cells seeded on 12% HV PHB-HV 10% Dextrin blend undegraded (magnification X26)

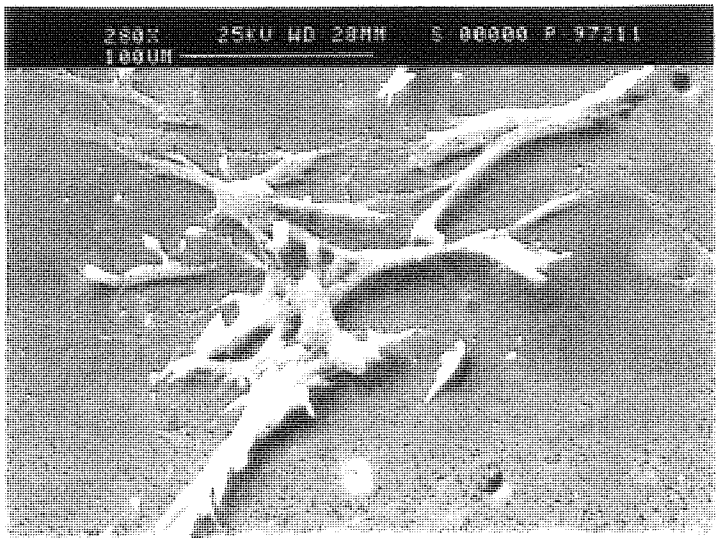

Plate 3.8 BHK-21 cells seeded on 12% HV PHB-HV 10% Dextrin blend 7 days degradation (magnification X32)

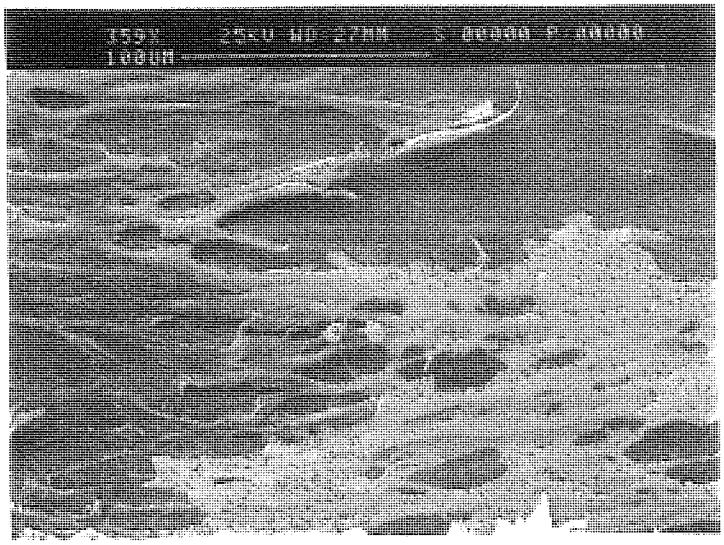

Plate 3.9 BHK-21 cells seeded on 12% HV PHB-HV 10% Dextrin blend 22 days degradation (magnification X31)

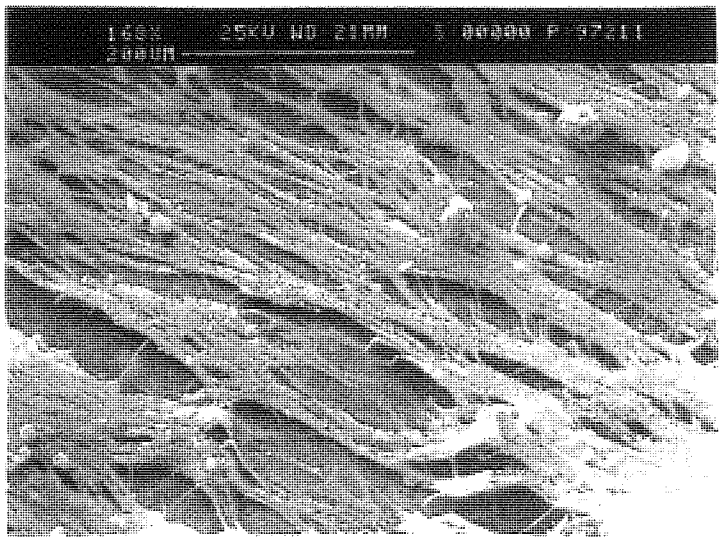

Plate 3.10 BHK-21 cells seeded on 12% HV PHB-HV 10% Dextrin blend 112 days degradation (magnification X36)

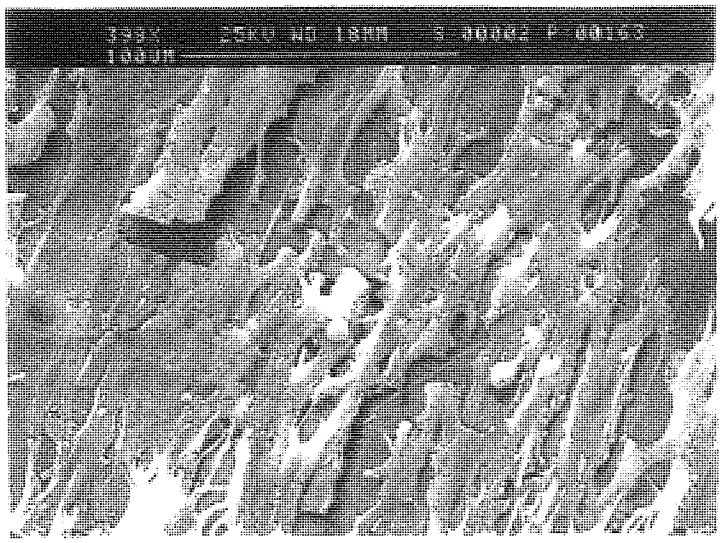

Plate 3.11 BHK-21 cells seeded on 12% HV PHB-HV 10% Dextrin blend 250 days degradation (magnification X25)

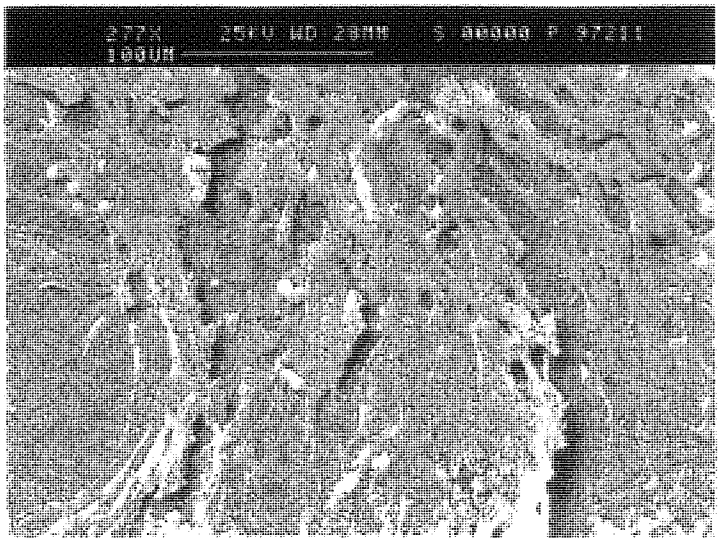

Plate 3.12 BHK-21 cells seeded on 12% HV PHB-HV 10% Dextran blend 62 days degradation (magnification X24)

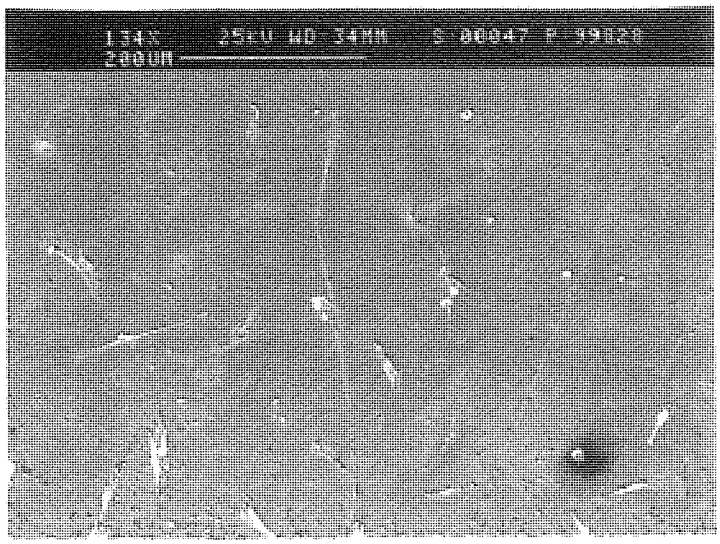

Those cells cultured on 20% HV PHB-HV/10% dextrin blends showed classical fibroblastic morphology with a progressively greater colonization of cells on the more degraded blends, Plates 3.13 and 3.14. At earlier degradation stages, e.g. 0 and 7 days degradation, BHK-21 cells, were found to be more extended in morphology than predicted with typical BHK-21 fibroblast type cells, Plate 3.15. When compared with 20% HV PHB-HV/10% dextran blends the 20% PHB-HV/10% dextrin blends adhered fewer cells.

The cells cultured on 12% HV PHB-HV/10% dextran samples that were undegraded or at early stage of degradation showed a high degree of colonization and the cells exhibited fibroblastic like morphology, as degradation progressed, fewer cells appeared to adhere. All samples of 20% HV PHB-HV/10% dextran blends appeared equally confluent with a cell layer of BHK cells covering the sample, at some points, however, the cell layer did appear to be flaking off.

The 12% HV PHB-HV/10% amylose blend sample was only available for testing after 7 days of degradation. The SEM micrographs showed a layer of BHK-21 cells that exhibited fibroblastic morphology covering the material. The 20% PHB-HV 10% amylose blend samples were cultured with BHK-21 cells at $1x10^4$ for 1 day and although the cells adhered to the samples, the cells exhibited a rounded morphology. However, there were some signs of the cells converting to a fibroblastic like appearance on samples that had been subject to degradation for a longer duration.

Cell seeding of NCTC (L929) cells used $1x10^4$ cells/ml onto 12% HV PHB-HV 10% amylose blends and 20% HV PHB-HV 10% amylose blends and were fixed after one day. It was found that there were lower rates of cell adhesion after 3 days than that found with the PHB-HV samples seeded with BHK-21 cells.

Plate 3.13 BHK-21 cells seeded on 20% HV PHB-HV 10% Dextrin blend undegraded (magnification X44)

Plate 3.14 BHK-21 cells seeded on 20% HV PHB-HV 10% Dextrin blend 180 days degradation (magnification X25)

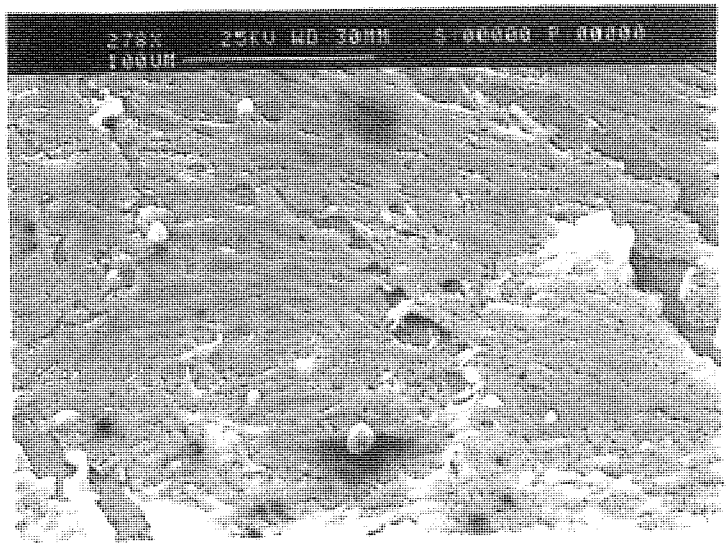

Plate 3.15 BHK-21 cells seeded on 20% HV PHB-HV 10% Dextrin blend 7 days degradation (magnification X90)

3.5 Discussion

The low cytotoxicity recorded by the Trypan Blue Dye Exclusion tests indicated that the majority of the cells recovered from the PHB-HV blend surfaces still retained an intact cell membrane. No measurable cytotoxic materials appear to have been released by the samples, however, it should be noted that the viability of the cells measured by this method is probably an overestimate. In the longer term it might be expected that the viability would be lower, as the Trypan Blue dye will not differentiate between viable and non viable cells where the cell membrane is still intact.

TCPS gave high levels of cell growth and support for the cell lines used and this was to be expected, as the polystyrene was gas plasma treated. Gas plasma treatment incorporates random functional groups such as hydroxyl groups to facilitate and improve cell adhesion. HEMA is not a substrate that supports high levels of cell growth, the polymer will allow cells to adhere, however, cell spreading and proliferation is not as abundant as on a polymer that has hydroxyl groups on its surface. The results of the TCPS and HEMA controls indicated that the cell lines showed typical cell adhesion behaviour and the growth rate of NCTC (L929) cells was lower than that of BHK-21 cells as a result of the longer cell cycle of the NCTC (L929) cells.

The characteristic peak of cell adhesion followed by a decrease in cell adhesion seen with many of the blends tested may be explained by the presence of polysaccharides in the polymers creating a more rugose surface as they degraded. Initial degradation increases the surface energy of the material increasing the polar component of surface energy. Although cells also have a slight net negative charge the polarity of the samples was initially cell attractive. However, as the degradation proceeded, so did the rugosity of the material and the polarity of the material increased and eventually become repulsive to cell adhesion. Yasin *et al.* agrees with this hypothesis providing evidence of PHB-HV blends increasing their cell attachment up to 7 days before decreasing their cell attachment.[49] Weight loss measurements may offer an alternative means of measurement of the rate of degradation of a PHB-HV blend. The assessment of the negative gradient slope of cell adhesion after the initial rise in cell numbers, could confirm the extent of polymer degradation. In addition, measurement of the wettability using the sessile drop method may confirm the changes in surface energy of the material.

It would be expected that the slope of cell adhesion would be steeper with dextrin as the polymer degrades faster in the conditions used. This degradation results from the dissolution of dextrin, which is incorporated into the blend as fine particles and is quite soluble because of its branched structure. Dextran is also soluble but its additional fibrous properties and the strength of its stable α 1-4 glycosidic bonds retard its elution from the blends compared to dextrin. In initial stages of degradation the hydroxyl and carboxyl groups in the backbone of dextran would help in cell adhesion. Comparison of 0 and 7 days degradation of samples within the physiological conditions, do indeed, show that cell adhesion had increased. The physical size of amylose contibutes more to weight loss than the hydrolytic stability

of its α1-4 glycosidic bonds which appear to have an intermediate effect on degradation compared with dextrin and dextran.[50]

Amylose has hydroxyl groups in its backbone that can convey a hydrophilic polarity, these hydroxyl groups would initially aid cell adhesion leading to the attraction of cells. When a level of polarity was reached that had a tendency to repel cells there would be a decrease in cell adhesion. In addition, hydrolysis or swelling of amylose granules would lead to the surface becoming increasingly more rugose and thus the peak and slope pattern would be expected in samples containing amylose. The higher levels of cell adhesion to the hydroxyapatite containing PHB-HV blends corresponds to the increased crystallinity of the sample, a characteristic of hydroxyapatite. The crystalline hydroxyapatite is not subject to rapid degradation although it should be noted that the amorphous components of the sample are eluted during degradation.[13] Cell adhesion appears to converge at later degradation times, possibly because the majority of the polysaccharides have eluted from the sample and hence in the end, cell adhesion may be solely dependent upon the PHB-HV as a substrate.

Degradation of 12% HV PHB-HV 10% dextrin blends appeared not to effect NCTC (L929) cell adherence as much as degradation of 12% HV PHB-HV 10% dextran blends. However, the lower cell growth rate with NCTC (L929) cells may have masked the observation of the negative slope. The increase in negative gradients of the adhesion slope with 20% HV PHB-HV dextrin blends may indicate that the dextrin had dissolved out of the sample at a greater rate than the other polysaccharides. As a result the sample became more rugose with a greater polar energy component than the other materials so lessening the number of adherent cells.

Holland *et al.* found that the polar surface energy of blends of PHB-HV containing amylose increased to approximately 30mN/m after 180 days degradation under physiological conditions. This was significantly greater than the polar surface energy encountered with PHB-HV copolymers that contained dextrin and dextran with polar surface energy of 17mN/m and 12mN/m respectively.[51] This may be an indication that blends containing amylose have a dramatic increase in cell adhesion potential followed by a gradual decline in cell adhesion potential. As the rate of degradation of amylose blends is greater than dextran and dextrin it would be expected that this would lead to more rapid increases and decreases in cell adhesion. As the polar surface energy would increase to such an extent that the polar surface energy became repulsive to cell adhesion.

Yasin *et al.* confirm that dextrin was subject to greatest degradation followed by, amylose and dextran in PHB-HV blends in the short term (10 days) and longer term (100 days) using weight loss studies.[50] Yasin *et al.* also found that the extent of degradation with amylose and dextrin was very similar.[50] In addition, Yasin *et al.* confirms that degradation increases marginally with an increase in percentage of PHV.[52] Increased concentrations of valerate would tend to enhance the degradation rate probably due to the fall in the crystallinity levels and the increase in the amorphous structure of the polymer rendering it more readily subject to degradation.[15]

It should be noted that the degradation of polysaccharides is dependent on conditions of temperature and pH as temperature and pH can affect the solubility of polysaccharides. In using physiological buffer to simulate physiological conditions it was hoped that a model of degradation closer to those conditions found *in vivo* would be achieved.[51]

It was not possible to discern accurately whether or not the cell density differed due to the SEM techniques employed. This was possibly the result of the cells becoming compressed together upon formation of a confluent layer, after which contact inhibition stopped further proliferation. BHK-21 cells have a shorter cell cycle and when compounded with 3 days of culture instead of 1 day this would give greater colonization compared with copolymers incubated with NCTC L929 cells.

The flaking off of cells from the samples was probably caused by the dehydration procedure used in the SEM. Although care was taken in handling the copolymers, the cells on the blends were very fragile and therefore some loss of cells from the copolymers was expected. Although some cells were lost, the majority of cells were retained and observed in SEM studies.

3.6 Conclusions

All materials were non toxic to cells as measured by Trypan Blue Dye Exclusion giving high cell viability results with all polymers assessed. Comparison of the polysaccharides and nucleating agents indicated that the most cell adhesive PHB-HV blends were those that contained hydroxyapatite, followed by PHB-HV blends that contained dextran, amylose and dextrin. The trend of cell adhesion may follow a pattern in that the more susceptible the blend is to degradation, then the more cells adhere to its surface in initial stages of degradation and fewer adhere after periods of extended degradation. The initial slight increase in cell adhesion could be due to the increased rugosity of the material that may have aided in focal attachment of cells to the blends when degradation was initiated. Ester hydrolysis at the polymer water interface leads to hydroxyl group exposure which increases the polar component of surface energy. As the degradation continued the number of cells that adhered to samples decreased possibly due to an excessive increase in polarity.

CHAPTER FOUR
Vitronectin Mediated Cell Adhesion to Contact Lenses

4.1 Aim

To develop and calibrate a cell based assay for vitronectin. To investigate the influence of contact lens material and wear regime on the adsorbance of vitronectin onto a contact lens surface and the location of vitronectin deposition in a contact lens system.[49,50,51]

4.2 Introduction

4.2.1 Vitronectin

Vitronectin is a adhesive plasma glycoprotein isolated as 2 monomers with molecular weights of 65KDa and 75KDa and primarily derived from hepatocytes in the liver. Although the liver is the only site to contain vitronectin mRNA, vitronectin is widely distributed in loose connective tissue and can be found in the cornea. However, vitronectin is not found in corneal basement membrane structures.[52,53,54]

It has been difficult to detect vitronectin by electrophoresis in tear fluid due to the fact that several proteins (albumin, lactoferrin and transferrin) in higher concentrations mask vitronectin due to similar molecular weights (65KDa, 74KDa and 75KDa respectively). In the reflex tear fluid, vitronectin is practically absent as it is excluded from the fluid by the blood tear barrier. However, vitronectin is found in the unstimulated tear pool open eye environment and its concentration has been found to vary from 0.58 to 0.75μg/ml. Vitronectin in the closed eye environment is found at a higher concentration of 3.65 to 6.62μg/ml.[55] The raised levels of vitronectin in tears is thought to be due to an increased vascular permeability when the eye is closed (this is also mirrored in levels of albumin with a similar molecular weight) and the build up of leakage products due to an decreased rate of fluid turnover.[56,57] Vitronectin is found at its highest concentration *in vivo* in mammalian plasma where it is found at a concentration of 200-400μg/ml.[58]

Vitronectin appears to improve the effectiveness of cell adhesion if the surface of a polymer is hydrophilic, commonly such polymers are found as components of contact lenses.[57,58,59] However, vitronectin when isolated from other proteins, binds equally well on both hydrophobic and hydrophilic surfaces. Cell adhesion to synthetic polymer implants *in vivo* as well as *in vitro* cell culture surfaces may be dependent to a large extent upon surface adsorbed vitronectin. In cell adhesion, vitronectin appears to be concentrated at the focal adhesion points of cells as demonstrated by immunofluorescence techniques.[52,54]

Changes in the conformation of vitronectin are thought to be important in the effectiveness of vitronectin in aiding cells to bind to a substrate and the energy driving vitronectin adsorption is thought to be primarily a result of the molecular structure of the protein rather than in the characteristics of the water/polymer interface.[58] A greater degree of change in conformation in vitronectin is observed upon binding to hydrophobic surfaces compared with other surfaces.[60]

Vitronectin can adhere to cells via cell surface receptors of the integrin family through the RGD sequence of its cell binding domain.[52] The RGD sequence represents three amino acids that are found near the amino terminal end of the molecule and is a repeated peptide sequence of arg-gly-asp. Although the sequence has a similar homology to fibronectin the flanking sequences that surround the RGD sequence are quite different and it appears that these differences in flanking sequence appear to convey specificity for cellular receptors.[60] The RGD sequence is also used to bind to cells when vitronectin is associated with the VnC5b complex.[57] Divalent cations may modify vitronectin properties in cell adhesion e.g. vitronectin binding can be significantly reduced when in association with Ca^{2+} as Ca^{2+} appears to block the cell receptor for vitronectin binding.[52,58]

Like fibronectin, vitronectin has been found to accelerate epithelial wound healing. When in plasma, vitronectin is nearly always bound to thrombin and so vitronectin is localized in tissues where there is injury and inflammation.[57] Sack *et al.* hypothesised that vitronectin was part of the external ocular host defence system acting with secretory IgA and polymorphonuclear (PMN) cells to enhance the efficiency by which PMN cells and monocytes can process microorganisms.[56] Vitronectin binds to the complement protein complex C5b7-9 to prevent the formation of a terminal cell lysis complex.[57,61] Although Vitronectin prevents bystander damage by complement and PMN cells, vitronectin still allows the phagocytic processing of pathogenic microrganisms.[55] Vitronectin thus appears to act as a fine control, to assist in controlling damage mediated by complement and PMN cell recruitment. This is especially important in the closed eye environment, where there is the induction of a state of sub-clinical inflammation, where complement is converted from C3 to C3b and there is activation of plasmin.[62-65] Vitronectin still allows phagocytic processing of microorganisms, possibly enhancing secretory IgA and complement C3b so that PMN cells and macrophages can still phagocytose microorganisms.[66,67] The changes in the ocular environment are important in the protection against the proliferation of microorganisms but there is also a need to protect against damage due to chronic exposure to the inflammatory environment.[56]

Sack *et al.* suggested that vitronectin may reduce the risk of autolytic damage caused by plasmin and complement activation. Vitronectin may stabilise plasminogen activator inhibitor-1 (PAI-1) and minimize inappropriate plasmin activation), Figure 4.1.[50,55,61] The plasminogen plasmin activation process is kept in equilibrium by plasmin activator (PA) and the plasminogen activator inhibitor (PAI) system, of which the most significant PAI is PAI-1. Vitronectin stabilizes PAI-1 on binding and the vitronectin-PAI-1 complex inhibits plasmin activator. However, if the complex is cleaved by plasmin the inhibition of plasmin activator is terminated.[50] If vitronectin is localized on a surface adjacent to a wound site it removes PAI from the reaction by fixing it and creates an imbalance in favour of PA and produces active plasmin.[69] Vitronectin is thus a key factor in the localized up regulation of the immunological inflammatory response.[50]

Figure 4.1 Action of vitronectin in immune responses (Sack, R.A., Underwood, A., Tan, K.O. and Morris, C., 1994, Vitronectin in human tears – protection against closed eye induced inflammatory damage. Sulivan, D.A. (Ed), Lacrimal gland, Tear film and dry eye syndromes (Plenum Press New York)

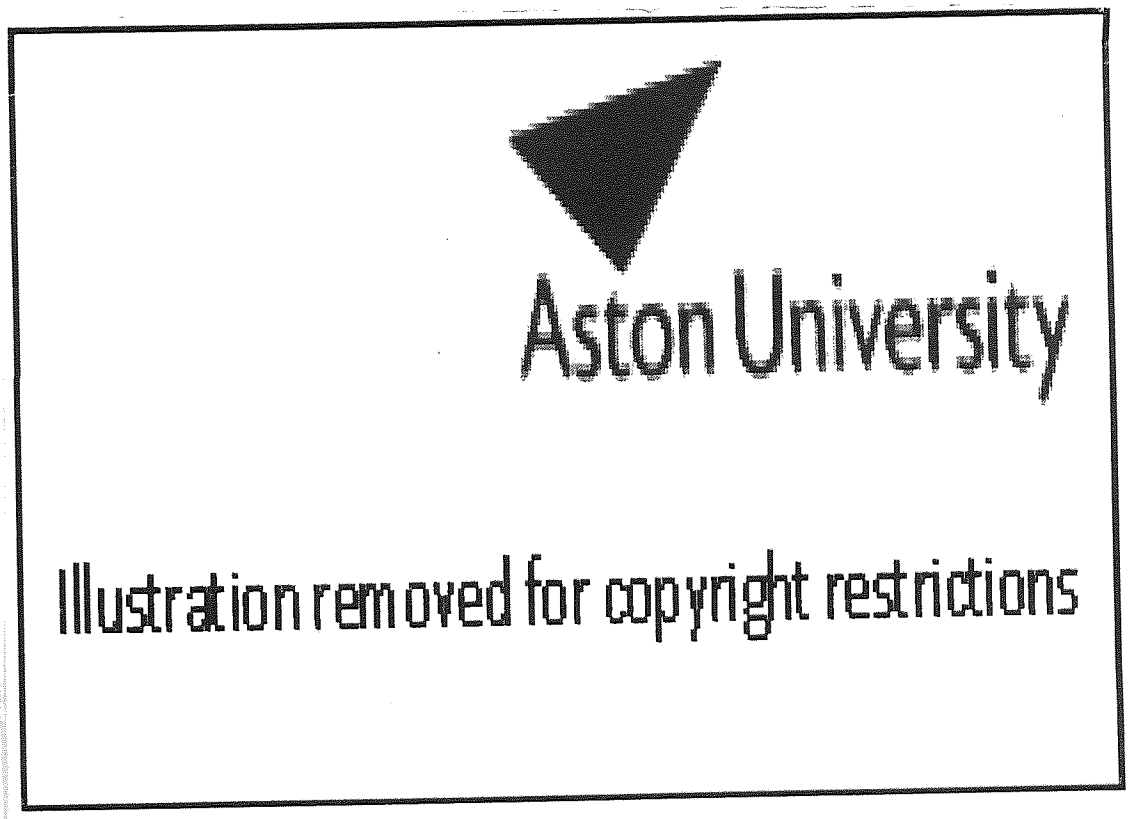

4.2.2 Food and Drug Administration (FDA) Classification for Contact Lenses

The FDA classification of contact lenses is a systematic methodology which involves placing contact lenses into groups with similar characteristics. Low water content is classified as less than 50% water content and high water content are those polymers that contain more than 50% water content. Ionic monomers are defined as those that contain greater than 0.5% ionisable monomer groups.

Table 4.1 Food and Drug Administration Classification for Contact Lenses

Group	Properties	Example
I	Low water content, Non ionic matrix	Vistagel (VP/MMA)
II	High water content, Non ionic matrix	Precision UV (NVP/MMA)
IV	High water content, Ionic matrix	Surevue (HEMA/MMA)

4.2.3 Vitronectin Mediated Cell Adhesion

Tighe *et al.* had previously used 20μg/ml bovine vitronectin to spoil polymacon (low water content, non-ionic Group I contact lenses) and Acuvue contact lenses with a daily wear regime.[51] Tighe *et al.* found that the use of human anti-fibronectin and human anti-vitronectin antibodies reduced cell adhesion to the lenses, Table 4.2 and Table 4.3. Cell adhesion with anti-fibronectin treated contact lenses was lower compared with contact lens treatment with IgG, however, use of anti-vitronectin was found to be most inhibitory to cell adhesion.[51]

Table 4.2 The effect of human anti-fibronectin and human anti-vitronectin antibody on polymacon lenses doped with 20μg/ml bovine vitronectin

Antibody	Mean cells per count ± S.D.
Control (No antibody)	59±9
IgG (Non specific)	54±10
Anti-Fn	36±7
Anti-Vn	4±0.5

Table 4.3 The effect of human anti-fibronectin and human anti-vitronectin antibody on Acuvue (daily wear regime) contact lenses doped with 20μg/ml bovine vitronectin

Antibody	Mean cells per count ± S.D.
Control (No antibody)	270±50
IgG (Non specific)	260±45
Anti-Fn	50±10
Anti-Vn	5±1

To investigate contact lens wear modality, Tighe *et al.* subjected Acuvue contact lenses to a daily wear and extended wear modality.[51] The daily wear modality was aimed at replication of a planned replacement lens regime (2 weeks daily wear for 196h) and the seven day extended wear modality (1 week extended wear for 168h) was aimed at replication of a disposable extended wear modality. Tighe *et al.* found that Acuvue contact lenses subject to a one day daily wear modality adhered fewer cells than Acuvue contact lenses subject to an extended wear modality, Figure 4.2.[51] This investigation was expanded to include a study of Group II and IV contact lens materials in a comparison of daily versus extended wear. Worn in a daily wear mode and extended wear mode modality model such contact lenses when subject to the vitronectin assay were found to have higher cell numbers on the posterior surface compared to the anterior surface ($P<0.001$), Figure 4.3. Greater cell adhesion was observed in extended wear versus daily wear (posterior surface). In addition, Tighe *et al.* found that cell counts were different when centre area counts were compared to periphery area counts, with higher cell numbers in the peripheral of the contact lenses compared to the centre of the lens on both anterior and posterior sides, Figure 4.4. and Figure 4.5.[50]

Figure 4.2 The Effect of Anti-Fibronectin and Anti-Vitronectin Antibodies on the Cell Adhesion of Acuvue Contact Lenses with a Daily Wear and Extended Wear Modality
(Mean Values +/- S.D. n=6) Tighe *et al.*[51]

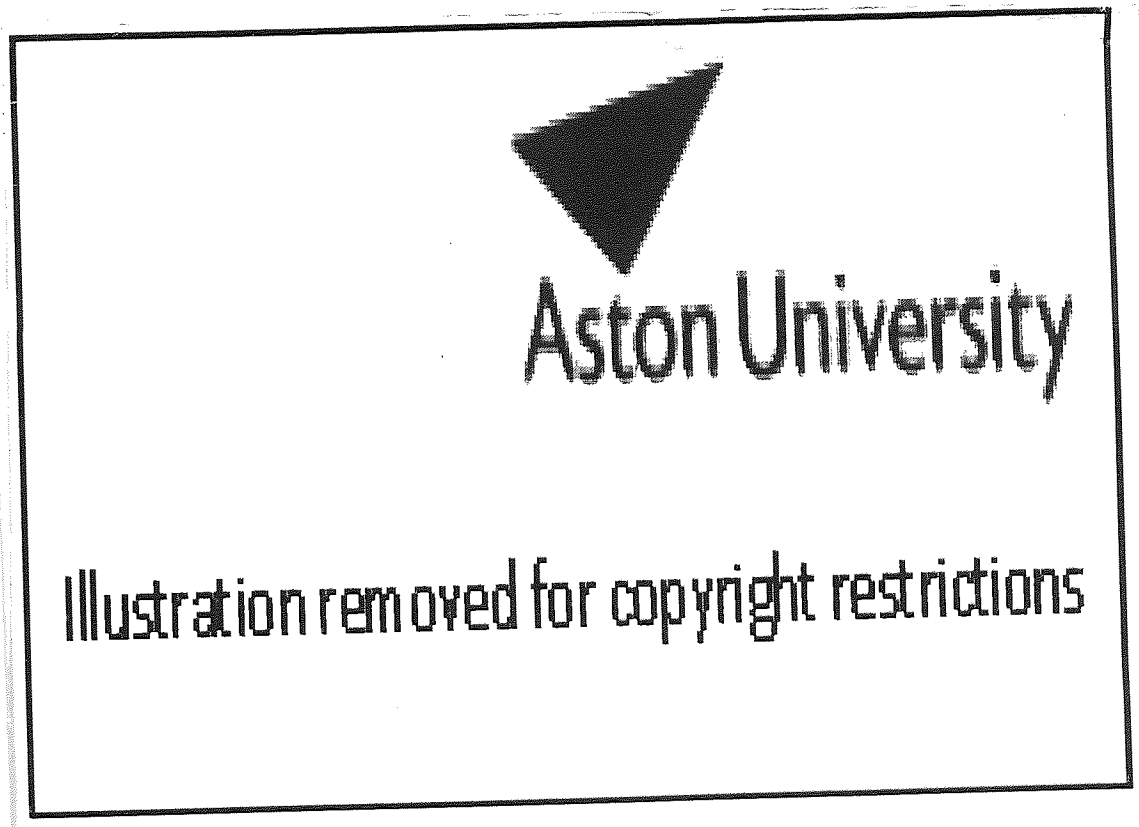

Figure 4.3 Cell Adhesion to Anterior and Posterior Surface of Acuvue Contact Lenses Peripheral Region (Mean Value +/- S.D. n=6) Tighe *et al.*[51]

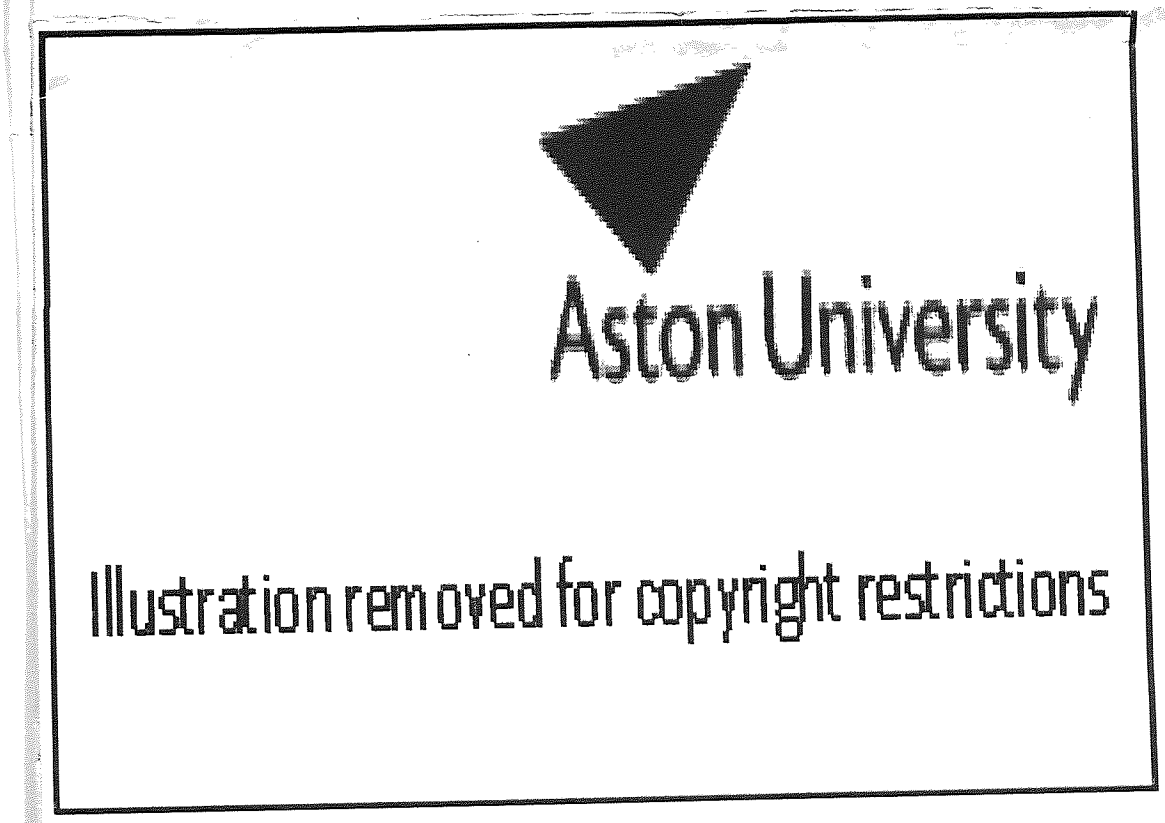

Figure 4.4 Cell Adhesion to Centre and Peripheral Regions of Posterior Contact Lens Surface (Mean Values +/- S.D. n=6) Tighe *et al.*[50]

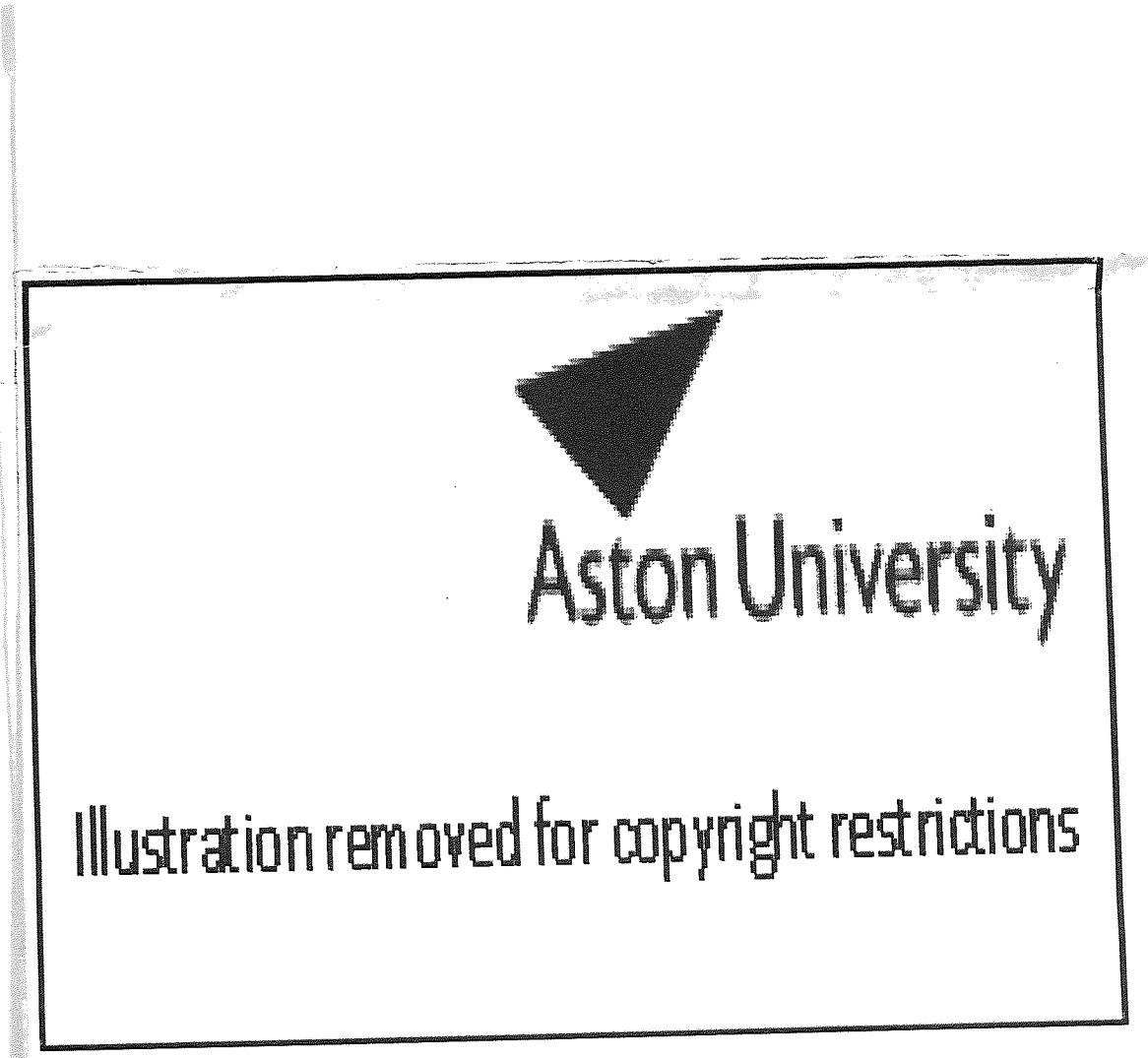

Figure 4.5 Cell Adhesion to Centre and Peripheral Regions of Anterior Contact Lens Surface (Mean Values +/- S.D. n=6) Tighe *et al.*[51]

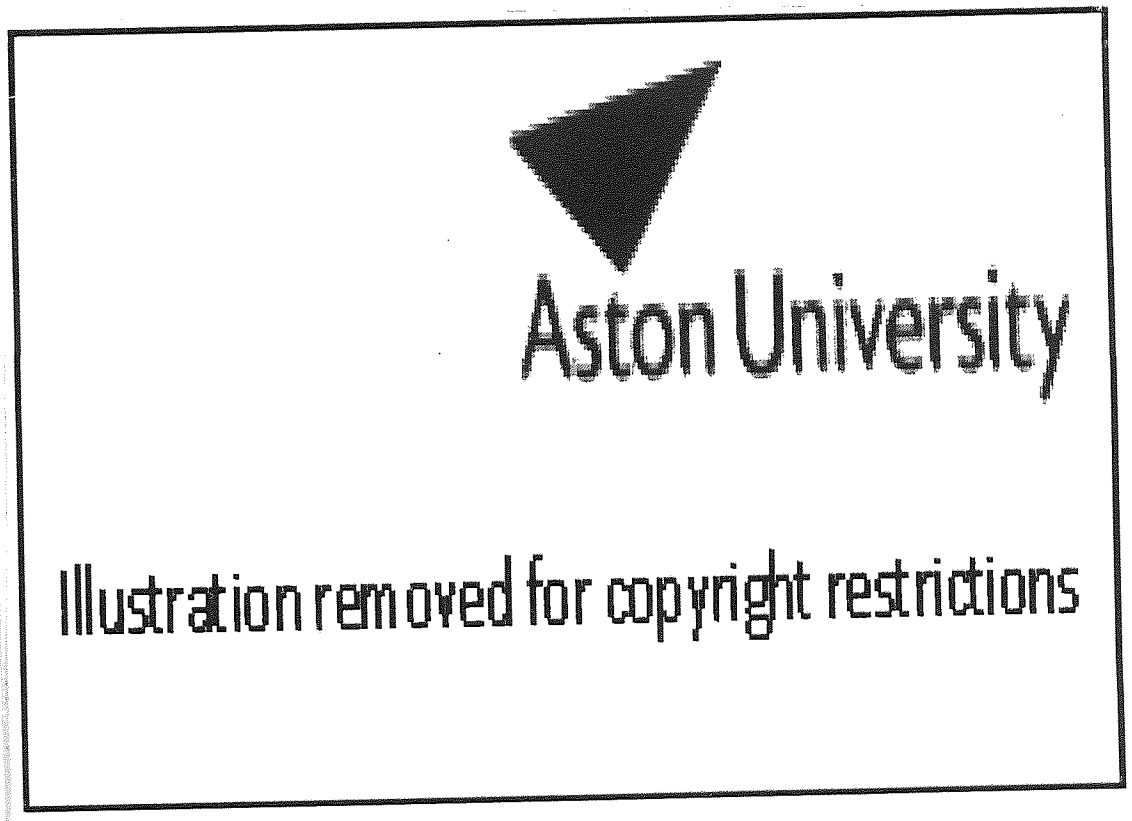

Further work by Tighe *et al.* repeated the above daily and extended modality studies and also used an additional seven day daily wear modality, (aimed at replication of a planned replacement daily wear modality, where the lenses were removed every night and disinfected with Softtab™, without prior use of a surfactant cleaner or digital rubbing). [50] Tighe *et al.* found that cell adhesion to the contact lens was greatest with a 7 day extended wear modality compared to a 7 day daily wear regime. The 1 day daily wear modality was found to adhere the fewest cells, using a mean of six lenses, Figure 4.6.[50]

Figure 4.6 The Effect of Wear Moduality on Cell Adhesion to Acuvue Contact Lenses (Mean Values +/- S/D. n=6) Tighe *et al.*[50]

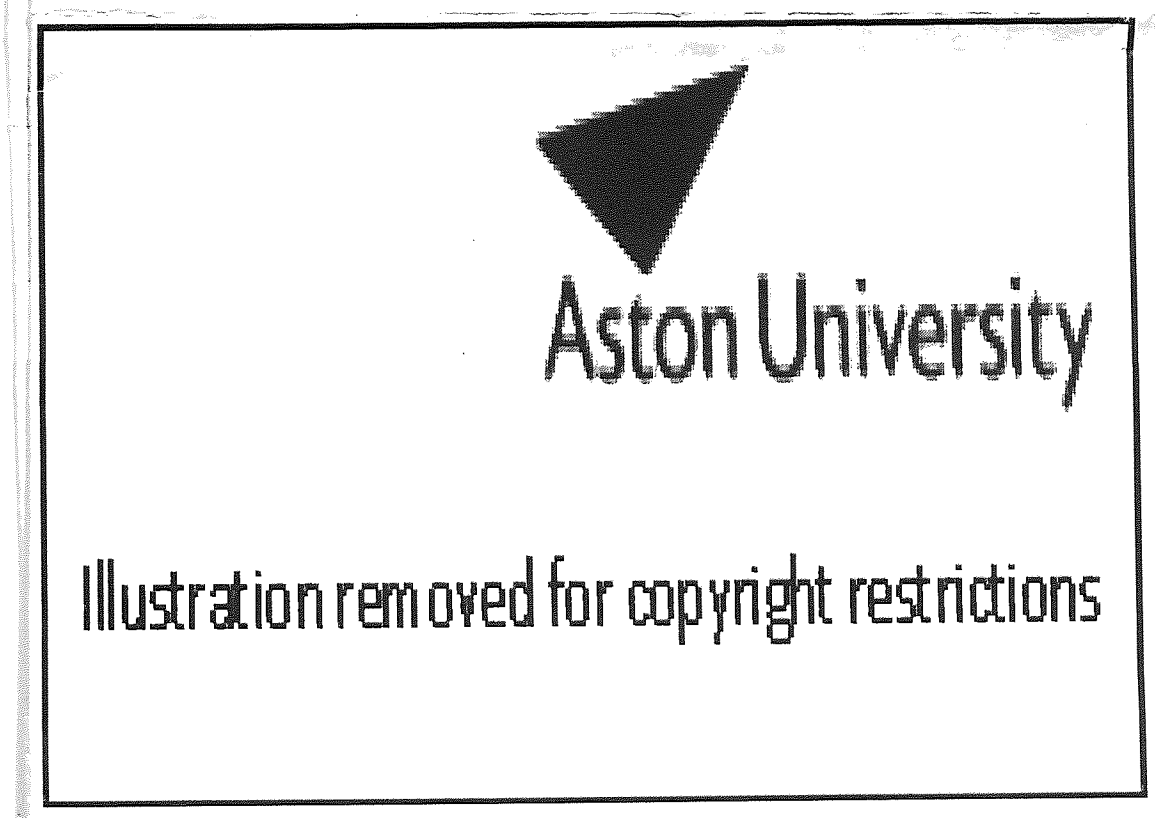

4.3 Methods

4.3.1 Cell Culture

The cell line used was 3T3 Swiss Mouse Embryo (SME) cells (ECACC 88031146). The cell line was maintained in Dulbecco's modified Eagle medium (Life Technologies), with 10% foetal bovine serum (Life Technologies) and 400mM/L L-glutamine (Sigma) to supplement growth and incubated in a Gallenkamp CO_2 incubator at 37°C and 5% CO_2/95% air atmosphere. Cells were sub-cultured at $1x10^4$ cells/ml when confluent with a growth rate of $0.23h^{-1}$, Figure 4.7 displays the growth curve for the 3T3 Swiss Mouse Embryo (SME) cells. Cells used in experimentation were from passage numbers 2 to 6.

Figure 4.7 Growth Curve of 3T3 SME Cell Line

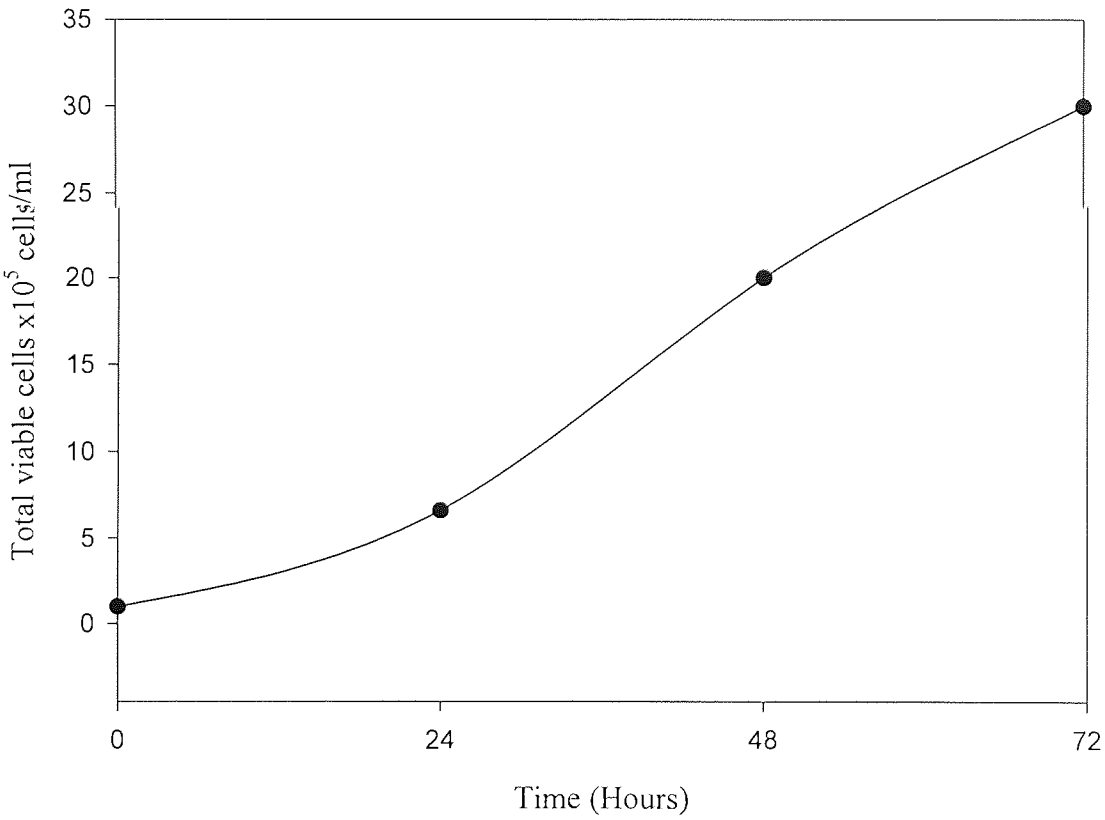

4.3.2 Doping of Contact Lenses with Vitronectin

Contact lenses were rinsed in PBS and placed aseptically in polystyrene bijoux bottles containing 2ml of a solution of vitronectin in phosphate buffer. The individual bijoux bottles were placed on an orbital shaker for 48h at 25°C.

4.3.3 Vitronectin Assay Procedure

Contact lenses were aspirated (by pipetting) whilst within bijoux bottles and rinsed with 1ml of 20mM HEPES buffer (Sigma). After rinsing each contact lens was placed aseptically into a well of a 24-wellplate cell culture (Corning) and 900µl of 20mM HEPES buffer was added to each well. 100µl of antibody (dependent on the assay) was added to antibody designated contact lenses, otherwise, an additional 100µl of 20mM HEPES buffer was added to the contact lens untreated with antibodies. The wellplates were placed in a Gallenkamp CO_2 incubator at 37°C and 5% CO_2/95% air atmosphere for 1h. Every ten minutes, the wellplate was agitated to ensure distribution of antibody over contact lenses and contact lenses were also checked to ensure that they had been submerged within the buffer solution.

After 40 minutes incubation of the contact lenses, confluent 3T3 SME cells were trypsinised with trypsin/EDTA 0.25% solution (Sigma). After 5 minutes, trypsin was neutralised with Dulbecco's modified Eagle medium (DMEM) and the cells were centrifuged ($2x10^3$rpm) for 5 minutes. The supernatant was aspirated with the pellet of cells re-suspended in 20mM HEPES buffer. The Trypan Blue Dye Exclusion method (section 4.3.5) was used to determine the number of viable 3T3 SME cells in the buffer suspension and the cell volume of the cell suspension was adjusted to provide a stock of $1x10^5$ cells/ml of viable 3T3 SME cells. Depending on the assay to be conducted the assay incubated cells on either posterior or anterior side of the contact assay. After 1h of incubation the contact lenses were rinsed twice with 1ml of 20mM HEPES buffer and placed aseptically in separate wells of a new wellplate. 1ml of the 3T3 SME cell suspension and 100µl of 50mM magnesium chloride solution was added to each contact lens and the contact lenses were incubated in the Gallenkamp CO_2 incubator for a further 60 minutes with the wellplate agitated every ten minutes. Controls of unworn contact lenses (unless mentioned) were treated as above. After 60 minutes incubation, each contact lens was removed to a new well containing 1ml of 20mM HEPES buffer. The buffer was aspirated and 1ml of 1% v/v glutaraldehyde (TAAB laboratories) added.

4.3.4 Determination of Cell Numbers

To determine the number of cells in contact with the contact lens 16 fields of view at different locations on the contact lens were taken at x100 magnification, with views of the peripheral and middle parts of the contact lens areas taken in equal numbers. Care was taken that the correct side of the contact lens was in focus by adjustment of the focus to determine where the base of the well plate, anterior and posterior surface of the contact lens were located. When anterior and posterior surfaces of contact lenses were investigated for cell adhesion, the contact lens was

cut aseptically into two pieces to make direct comparisons of the two sides of each subject.

4.3.5 Determination of Cell Viability with Trypan Blue Dye Exclusion

To determine cell viability, 250μl of cell suspension was added to 100μl of trypan blue in a bijoux bottle. Both sides of a standard haemocytometer were loaded with the cell/trypan blue suspension and ten counts on different haemocytometer squares were taken to determine number and viability of the cells.

4.4 Results

4.4.1 Evaluation of the Vitronectin Assay

Vistagel contact lenses (FDA Group I) were doped with either human plasma vitronectin (Life Technologies), human plasma fibronectin (Life Technologies) or chicken egg white lysozyme (Sigma) as described in 4.3.2. The mean values from six contact lenses were used to produce the results shown in Table 6.5 (Appendix II) and Figure 4.8.

This work was expanded to investigate the effect of anti-human fibronectin (Life Technologies) and anti-human vitronectin (Life Technologies) on 5μg/ml human plasma vitronectin and human fibronectin, Figure 4.9 and Figure 4.10 and Table 6.6 (Appendix II). The results shown followed the doping procedure outlined in 4.3.2 and anti-human fibronectin and anti-human vitronectin were used in the vitronectin assay as described in 4.3.3.

Figure 4.8 Cell Adhesion to FDA Group I Contact Lenses Doped with Vitronectin, Fibronectin or Lysozyme (Mean values n=6)

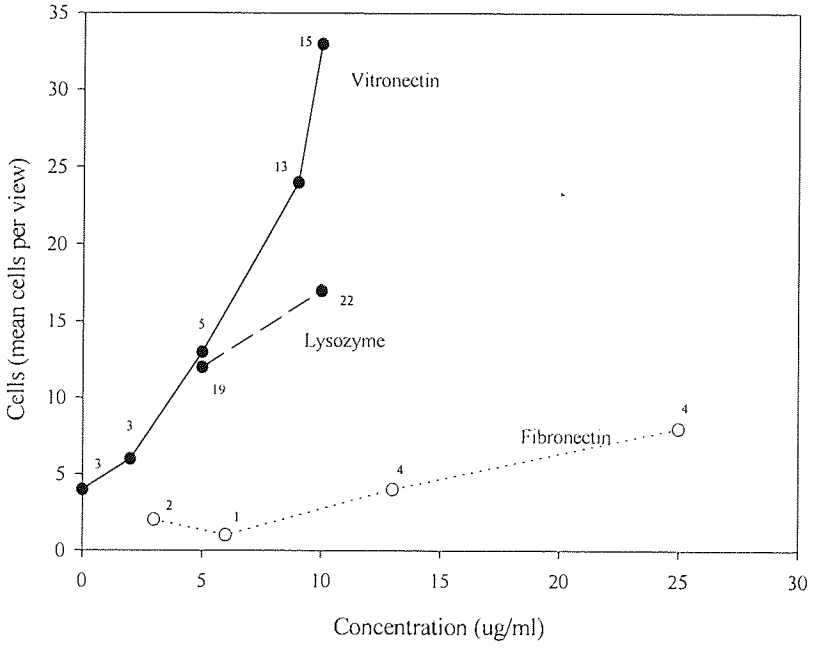

Note: S.D. Displayed next to plot points

Figure 4.9 The Effect of Antibody on Cell Adhesion to Acuvue (Daily Wear Modality) Contact Lenses (Mean values +/- S.D. n=6)

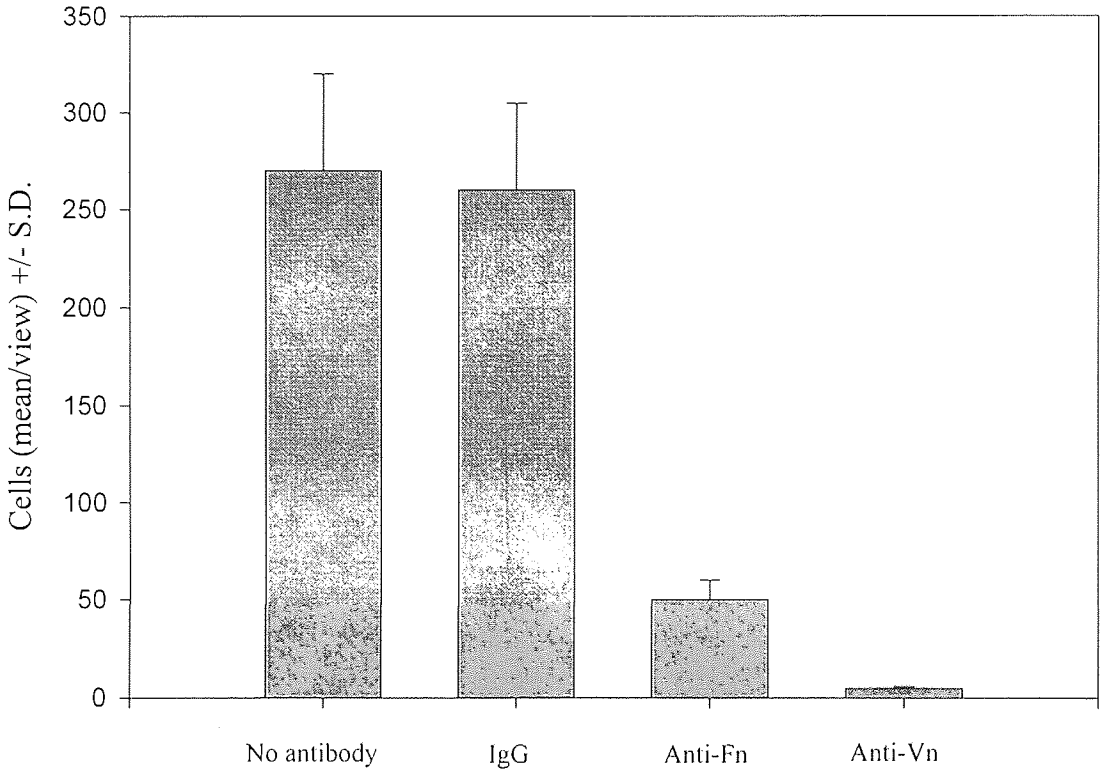

Human plasma vitronectin cell adhesion was effectively blocked by the use of anti-vitronectin (heteroscedastic t-test assuming normal distribution and unequal variance $P<0.001$) on Acuvue contact lenses, mean results of six lenses, while anti-fibronectin reduced cell adhesion to vitronectin doped contact lenses, however, the effect was not statistically significant ($P=0.456$). The results with vitronectin were also duplicated with the use of human plasma fibronectin. The effect of fibronectin

mediated cell adhesion was blocked by anti-fibronectin antibodies (heteroscedastic t-test assuming normal distribution and unequal variance $P<0.001$) and the use of anti-vitronectin antibodies reduced cell adhesion by fibronectin, however, the result was not statistically significant ($P=0.065$).

Figure 4.10 The Effect of Anti-Vitronectin and Anti-Fibronectin Polyclonal Antibodies on Vitronectin and Fibronectin Doped Group II+IV Contact Lenses
(Mean values +/- S.D. n=6)

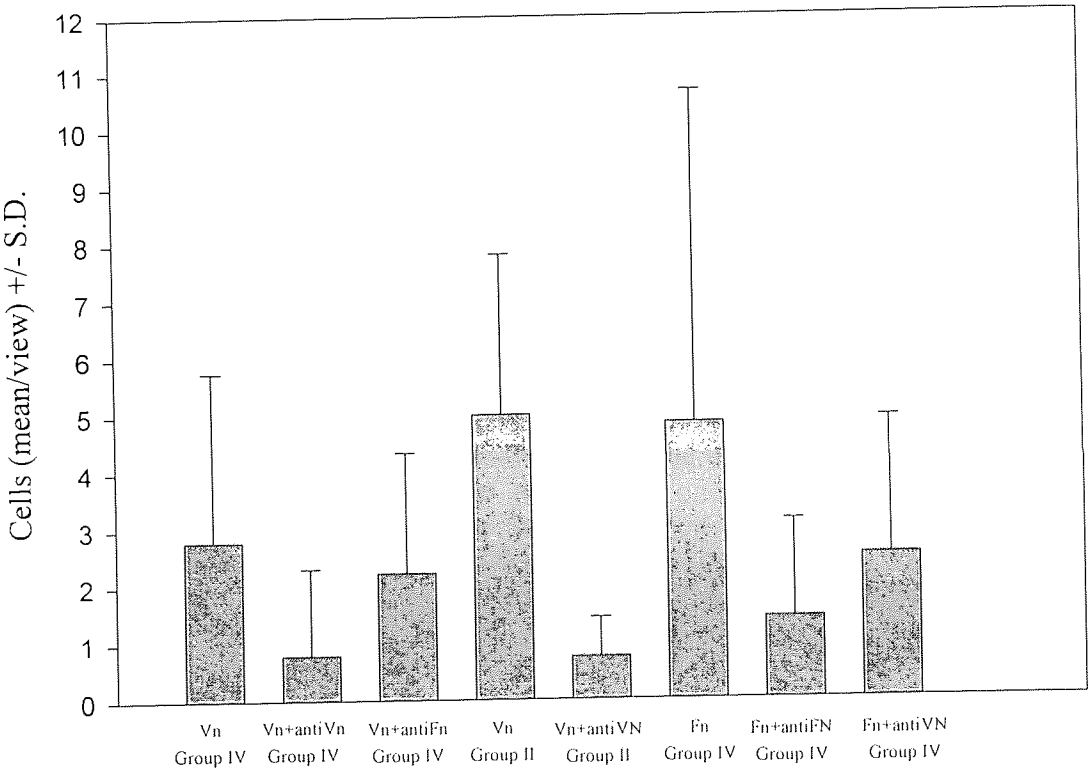

The effect of anti-vitronectin was also investigated with FDA Group II Rythmic and Lunelle contact lenses using contact lenses doped with 5μg/ml human plasma vitronectin as described in 4.3.2. The results showed that vitronectin also increased cell adhesion in Group II contact lenses when compared with undoped controls, Table 4.4, and with the addition of anti-vitronectin antibodies led to a reduction in cell adhesion.

Table 4.4 The effect of anti-vitronectin antibodies on Rythmic and Lunelle (Group II) contact lenses doped with vitronectin

Contact Lens	Vitronectin	Antibody	Mean cells per view ± S.D.	Statistical Significance
Rythmic	N	None	3±2	N/A
Rythmic	Y	None	5±3	P=0.02
Rythmic	Y	Anti-Vn	1±1	P=0.002
Lunelle	Y	N	5±5	N/A
Lunelle	Y	Anti-Vn	1±1	P<0.001

4.4.2 The Effect of Vitronectin Mediated Cell Adhesion to Anterior and Posterior Surfaces of Worn Group II and Group IV Contact Lenses

Six Precison UV (FDA Group II) and Surevue (FDA Group IV) contact lenses, worn daily for four weeks, were investigated by using the vitronectin assay as described in 4.3.3. Greater cell adhesion was seen with the posterior surface of Precision UV contact lenses when they were compared to the anterior surface (heteroscedastic t-test assuming normal distribution and unequal variance $P<0.01$), Table 6.7 (Appendix II) and Figure 4.11. However, the anterior surface of the Precision UV appeared to have fewer cell numbers than the unworn control contact lens surface. Greater cell adherence was also found on the posterior surface compared to the anterior surface of the Surevue lenses ($P<0.05$), Table 6.8 (Appendix II) and Figure 4.12.

Figure 4.11 Cell Adhesion to Precision UV (Group II) Contact Lenses (Mean values +/- S.D. n=6)

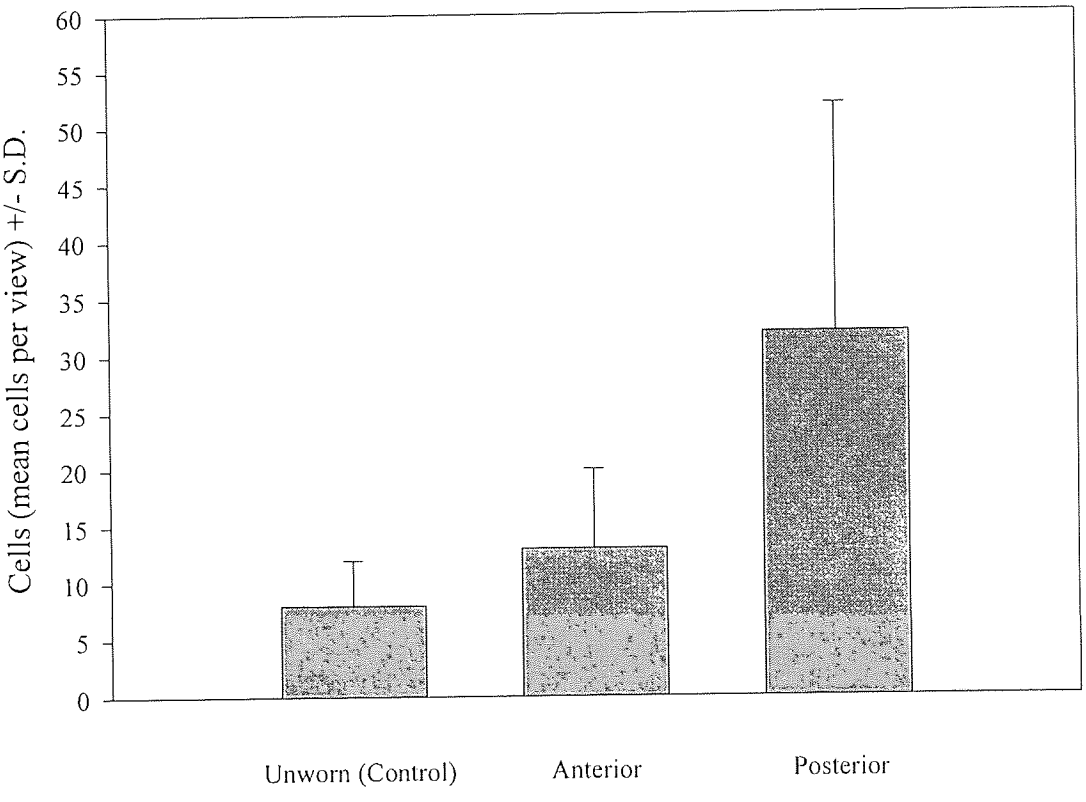

Figure 4.12 Cell Adhesion to Surevue
(Group IV) Contact Lenses
(Mean Values +/- S.D. n=6)

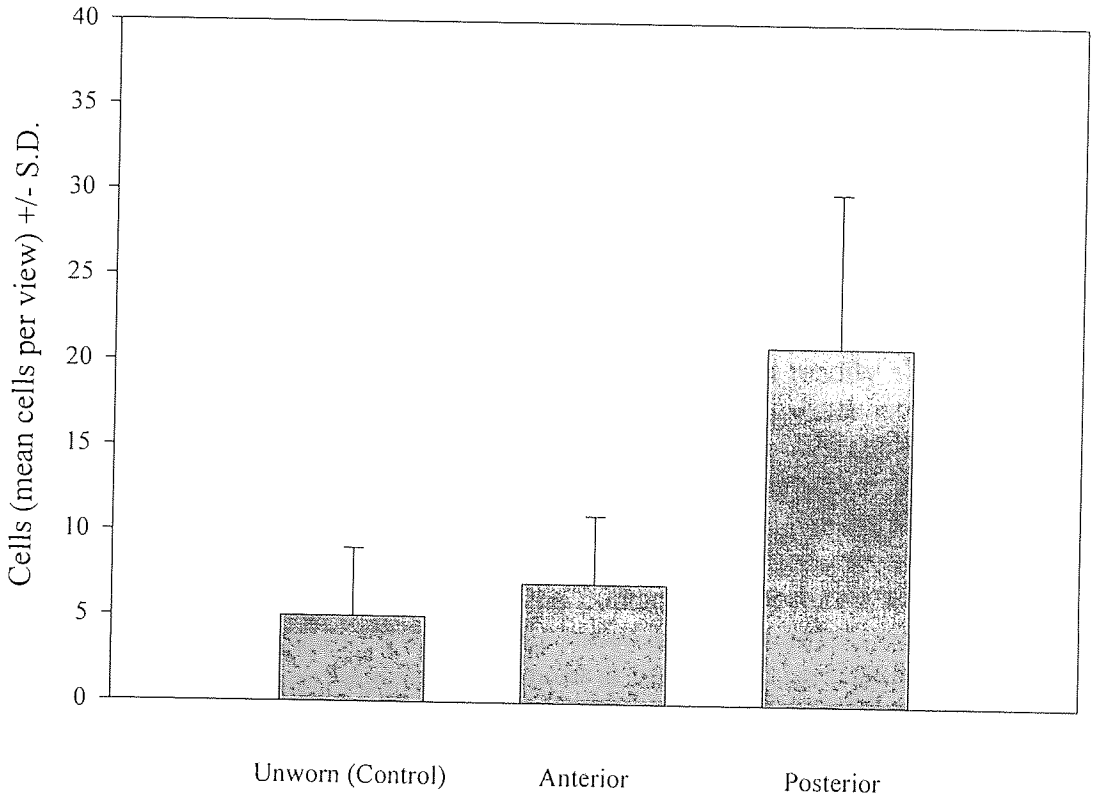

4.5 Discussion

It was to be assumed that vitronectin and fibronectin would have the effect of increasing cell adhesion on polymeric materials. As both proteins are present in focal contact sites of cells and appear to be involved in adhering cells to substrates. Evidence to support vitronectin adhesion comes from antibody assays, when a contact lens doped with vitronectin is treated with anti-vitronectin antibodies, there is a reduction in cell adherence (the same mechanism explains anti-fibronectin antibodies blocking fibronectin mediated cell adhesion).

Greater concentrations of vitronectin were found on Group IV lenses than Group II lenses and greater concentrations of vitronectin were found on Group II lenses than Group I lenses. This may indicate that Group IV contact lenses are able to absorb relatively high amounts of protein because of the high water content of the lenses. Once the protein has permeated into the hydrogel matrix the absorbance and retention of protein is enhanced by the ionic character of the lens matrix. The ionic polymer matrix may retain protein by the formation of polar interactions with the absorbed protein. In contrast, Group I contact lenses with a low water content and non-ionic matrix, characteristics opposite to Group IV lenses, do not readily absorb significant amounts of protein.[46] This would imply that high water content hydrogels with an ionic polymer matrix would be most subject to protein spoilation and hydrogels of a low water content with a non-ionic matrix the most resistant to spoilation.[69,70-73]

Vitronectin appears to attach predominately to the contact lens posterior surface rather than to the anterior surface in worn contact lenses and the numbers of cells adhering at *in vitro* concentrations equivalent to those in tears, are much lower than those found *in vivo* on worn contact lenses and has been reported by Tighe *et al.*[73] This is possibly due to ocular tissue and contact lens interaction, with the posterior microclimate favouring vitronectin attachment.[49,50] The volume of the tear exchange at the front of the contact lens is also much greater than that at the back suggesting that it is the closed post lens environment where tear exchange is low that helps vitronectin adhesion to the contact lens surface.[49]

The anterior tear film appears to contact the periphery of the contact lens first, this may lead to lower amounts of available vitronectin in the tear film attaching to the centre of the contact lens.[50] Whereas on the posterior surface of the contact lens, the periphery of the lens may be in direct contact with the ocular tissue, yet, has less direct contact with the ocular tissue at the centre of the contact lens. However, both the centre and pheriphery of the posterior surface of the contact lens are exposed to greater concentrations of vitronectin present in the ocular tissue than that of the anterior surface of the contact lens which is only exposed to vitronectin in the tear film.

If vitronectin enhances an immunological response then the accumulation of vitronectin at specific ocular sites may increase the production of plasmin which may possibly lead to an increased incidence in the formation of non-culturable ulcers.[50] If vitronectin was able to desorb or remain active on the surface of worn contact lenses that have significant quantities of vitronectin adsorbed to the contact lens, a possible deleterious immunological response may occur at corneal wound

sites. The additional vitronectin present may be able to bind to plasminogen activator inhibitor (PAI) present at the wound site and if plasmin was also at the wound site, PAI-vitronectin complex cleavage by plasmin may result. This could lead to a runaway plasmin reaction, where plasmin activator (PA) is not regulated by PAI which has been inactivated by plasmin cleavage. PA would upregulate plasmin activity which may lead to excessive cytolytic damage and the eventual formation of an ulcer. Possibly ulcer formation may have an increased incidence at the locations of the highest vitronectin concentration which would be at the site where the ocular tissue is in contact with the periphery of the contact lens.

Antibodies are highly specific for a particular antigen, yet, anti-fibronectin antibodies appeared to also have some cross reactivity in blocking vitronectin mediated cell adhesion, as do, anti-vitronectin antibodies upon fibronectin mediated cell adhesion. However, the antibody cross reactivity is only present with closely related protein species as unrelated antibodies such as IgG show no propensity to affect cell adhesion significantly.[51] It is also possible that fibronectin may be co-operative in vitronectin mediated cell adhesion to polymers. Indeed fibronectin and vitronectin share some common features such as the amino acid sequence, RGD, which is a binding site for specific integrins.[74] In addition, vitronectin and fibronectin have similar molecular binding activity that includes affinity for heparin and collagens.[75]

Although no experimentation was undertaken, it is likely that if a control (undoped) contact lens were treated with anti-vitronectin or anti-fibronectin antibodies, there may be a slight decrease in cell adhesion when cells are incubated with contact lenses because the cells used in the vitronectin assay produce small amounts of vitronectin and fibronectin *in vitro* as part of the requirement to adhere to the TCPS cell culture flask. Thus the cells ability to adhere because of cellular synthesized vitronectin is blocked due to anti-vitronectin antibodies present on the surface of the contact lens. As vitronectin appears to have better cell adhesive potential than fibronectin it is possible that the cell counts would be greater with undoped contact lenses treated with anti-vitronectin antibodies. If a contact lens doped with both proteins was treated with either anti-vitronectin or anti-fibronectin, the non-antibody blocked protein may compensate for the other blocked protein and still show some cell adhesion. Use of anti-fibronectin on a vitronectin and fibronectin doped contact lens may reduce cell adhesion to a lesser extent than treatment with anti-vitronectin possibly because of the improved cell adhesion with vitronectin.

It was found that lysozyme had a more adhesive effect than fibronectin at the concentrations studied. However, it should be noted that the standard deviations of lysozyme results were far greater than those with results of standard deviation relating to fibronectin and vitronectin.

4.6 Conclusion

The vitronectin assay has been proven to be a viable method of detecting vitronectin and cell adhesion to worn contact lenses. Vitronectin (and fibronectin to a lesser extent) can contribute to cell adhesion, this cell adhesive potential can be reduced by antibodies specific to vitronectin and to a lesser extent by antibodies specific to fibronectin.

Group IV contact lenses are able to absorb relatively high amounts of protein because of their high water content and ionic matrix. Once the protein has permeated into the hydrogel matrix the absorbance and retention of protein is enhanced by the ionic character of the lens matrix. In contrast, Group I contact lenses with a low water content and non-ionic matrix, characteristics opposite to Group IV lenses, do not readily absorb significant amounts of protein.

Vitronectin appears to attach predominately to the contact lens posterior surface rather than the anterior surface in worn contact lenses and the numbers of cells adhering at *in vitro* concentrations equivalent to that in tears, are much lower than those found *in vivo* on worn contact lenses. This is possibly due to ocular tissue and contact lens interaction, with the posterior microclimate favouring vitronectin attachment. In addition, the volume of the tear exchange at the front of the contact lens is also much greater than that at the posterior suggesting that it is the closed post lens environment where tear exchange is low that helps vitronectin adhesion to the contact lens surface.

Both the centre and pheriphery of the posterior surface of the contact lens are exposed to greater concentrations of vitronectin present in the ocular tissue than that of the anterior surface of the contact lens which is only exposed to vitronectin in the tear film.

If vitronectin enhances an immunological response then the accumulation of vitronectin at specific ocular sites may increase the production of plasmin which may possibly lead to an increased incidence and formation of non-culturable ulcers.

CHAPTER FIVE
Cytotoxicity of Artificial Lung Surfactant

5.1 Aim

The aim of this chapter was to undertake a preliminary analysis of cell adhesion to Poly(lysine ethyl ester adipamide) (PLETESA) and its cytotoxicity to mouse alveolar cells. Comparing PLETESA with other synthetic surfactant protein analogues.

5.2 Introduction

5.2.1 Physiology of Lung Surfactant

The lungs are made of a number of branching tubes which progressively divide and terminate into a number of tiny fluid filled sacks called alveoli. The function of these sacks is to increase the surface area of the lungs. The alveoli surface is the primary is the primary site for gaseous exchange.[76] To avoid the pressure difference tending to force air from smaller alveoli sacks to the larger alveoli of the lungs, the body produces surfactant which lowers the surface tension of the alveoli surfaces. The lung surfactant is secreted from osmophilic secretory bodies within cells lining the alveoli. In mammals a distinct cell (type II alveolar epithelial cells) is responsible for surfactant production, while the alveolar lining where gas exchange occurs is comprised of type I (squamous) epithelial cells. The surfactant controls the actions of the lungs through reducing surface tension in direct proportion to the reduction in surface area (caused by increased concentration of the surfactant per unit area of the surface). The surfactant also allows the lungs to inflate and deflate uniformly avoiding unequal forces.

Lung surfactant is largely composed of a mixture of phospholipids which become orientated at the air/fluid interface. Endogenous surfactant consists of 90% lipid in combination with 10% protein. The lipoidal fraction is 90% phospholipid of which 80% is phosphatidylcholine (PC) some 40-45% in the form of dipalmitoyl ester (Dipalmitoyl phosphatidyl choline or DPPC) and the reminder in the form of monoenoic PC. The lipid also contains 10-15% phosphatidylglycerol (PG) and 7-8% cholesterol.[77-79]

These are two components of pulmonary surfactant, an extracellular and intracellular compartment. The extracellular compartment is a mixture of distinct structures such as newly created lamellar bodies and tubular myelin derived from lamellar bodies, surfactant film is formed in the extracellular compartment from tubular myelin. The intracellular compartment comprises of lamellar bodies contained within the alveolar type II cells. These inclusion bodies are generally believed to store the surfactant before secretion into the alveolar saces.[80]

Neonatal lungs, under two months of age, lack surfactant which prevent lungs from inflating properly, the deficiencies of phospholipids, particularly DPPC in the alveolar surfactant fluid leads to a condition known as neonatal respiratory distress syndrome (RDS).[79]

5.2.2 Surfactant Secretion

Surfactant is synthesized by alveolar type II cells and then secreted into the alveolar hypophase (aqueous lining layer of the alveolar air space) and subsequently reorganized to form a surface active monolayer. The metabolism of the surface active material is very complex and secretion is only one part of the system.. The secretion and re-utilization cycle of surface active material involves a number of complex regulation processes that include:

1) Synthesis
2) Intracellular transport
3) Sorting and packaging into lamellar bodies
4) Movement of lamellar bodies to the apical plasma membrane of the type II cell
5) Exocytosis
6) Adsorption to the air-liquid interface
7) Physical separation of some of the surfactant components during compression at the air-liquid interface
8) Uptake of extracellular surfactant
9) Intracellular processing
10) Secretion of recycled material[76]

Surfactant proteins are extensively modified as they move through the biosynthetic pathway such that the fully processed proteins that interact with surfactant phospholipids are significantly different from the primary translation products. Synthesis of surfactant lipids and apoproteins occurs in the rough endoplasmic reticulum (apoproteins) and Golgi apparatus (lipid). When lamellar bodies are released from the cell by exocytosis the phospholipid is reorganized into a lattice like form, tubular myelin. This material is theorized to release phospholipid spontaneously into the air-liquid interface.[81-83] The apoprotein SP-B precursor is found in the membranes and organelles of type II bronchial and broncholar epithelial cells and travels along secretory pathways to be eventually translocated into the rough endoplasmic reticulum where the precursor protein is glycosylated. The N-linked carbohydrate is further processed in the Golgi apparatus and is also subject to proteolytic processing in the secretory pathway. The SP-B precursor protein is finally processed into the active protein and is then stored in the lamellar bodies.

Human SP-C protein is also processed into the active form from a precursor. This protein is produced by proteolytic processing of a 22KDa precursor, pro-SP-C, that enters the membrane secretory pathway during its biosynthesis, ProSp-C is also palmitoylated before cleavage and partial insertion of ProSp-C into the membranes of the endoplasmic reticulum.[84]

5.2.3 Apoproteins

There are four separate apoprotein surfactant proteins (SP), SP-A to SP-D, important for the efficiency of the lipoidal fraction in lung surfactant. Theses SP's modify the assembly of phospholipids so that the lipid monolayer/bilayer is formed at the

interface and are able to increase the speed of expansion and compression of films made up of phospholipids.[85]

SP-B is a small extremely hydrophobic proteolipid that aids in adsorption of phospholipids at the air/fluid interface. SP-B forms an amphipathic helical structure where the hydrophobic residues are arranged on one face perpendicular to the axis of the coil and the hydrophilic residues are arranged on the opposite sides. The molecule may be inserted into the phospholipid bilayer membrane so that the hydrophobic faces adjoin the acyl chains of the lipodial groups.[79] SP-C is a membrane bound protein with a central hydrophobic region which allows SP-C to span the lipid bilayer. The 'active' SP-C peptide in alveolar washings is comprised of approximately 35 amino acids. SP-C acts to increase the elasticity of the bilayer and may possibly play a role in spreading of phospholipids, like SP-B it is smaller than SP-A. Biodegradable synthetic polymers like PLETESA may mimic SP-C acting to solubilise lipids and lipophilic compounds.[79] Figure 5.1 shows a hypothetical model of the conformation of SP-B and SP-C in the membrane bilayer.

Figure 5.1 Hypothetical model of possible conformations of SP-B and SP-C in the membrane bilayer. For simplification monomeric forms of the proteins are shown.[86]

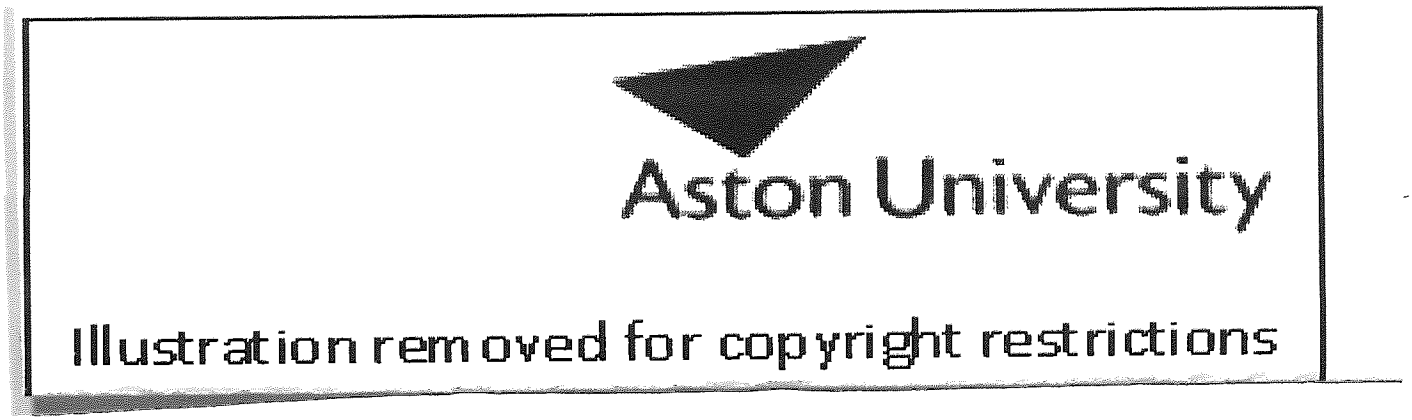

5.2.4 Artificial Lung Surfactant

Artificial lung surfactants have been proposed as changing from a liquid to a 'solid' state acting like an archway of bricks to 'splint' the alveoli open.[87] The main component of artificial surfactants is dipalmitoyl phosphatidyl choline (DPPC) and this makes up approximately 50% of the phospholipid in the natural surfactant. DPPC appears to be the component that stabilizes the film when compressed on expiration. Pure DPPC cannot function alone as it is a solid below 41°C and is therefore unlikely to spread. Synthetic lung surfactant is less effective than natural lung surfactant, because without a number of apoproteins the added phospholipids fail to completely adsorb and spread at the alveoli/air interface.

Several groups have studied artificial surfactant mixtures, these include the artificial lung surfactant known as ALEC, artificial surfactant made from DPPC and high density lipoprotein and Exosurf produced by Burroughs Wellcome.[88] Semi-synthetic lipoproteins have been successful in treating RDS, however, the cost is prohibitively expensive for use in places other than in the developed countries. The cost of treating one neonate with artificial surfactant is approximately 600 pounds sterling (1994

prices).[89] When the synthetic analogues to SP-B and P-C are combined in a polymer/phospholipid recombinant the surface tension recorded approximates to that of the best commercially available artificial surfactants yet it is estimated that costs will be significantly less to produce.

5.2.5 Biodegradable Polymers

To produce a polymer with a biodegradable backbone, ester or amide groups can be used, the resulting backbone can then be cleaved by esterases or proteases. Polymers such as PLETESA have the potential for use in drug delivery systems and are able to selectively release drugs in a manner dependent upon the environment they encounter.

5.2.6 PLETESA Poly(lysine ethyl ester adipamide)

Poly(lysine ethyl ester adipamide) (PLETESA) is a hydrophobically substituted polyamide that dissolves readily in polar solvents such as water and methanol. The amide backbone makes the polymer biodegradable. Partial de-esterisation of PLETESA can form a polymer that contains both pendant ester and carboxylate groups that are a mixture of hydrophobic and charged groups where the functional side chains give hypercoiling properties on the polymer.[79] Figure 5.2 shows a repeat unit segment of PLETESA-base polymer.

When dried, PLETESA can be deposited as a thin resinous layer. If left in aqueous solution, over time, strands of resinous material can become deposited presumably due to the hydrolysis of hydrophobic ester side chains and the formation of carboxyl groups.[79] Perhaps PLETESA initially forms micelles as charge is lost as hydrophobic groups become associated within the core of the micelles.[78]

Figure 5.2 A segment of PLETESA-base polymer, showing the through space associations and the likely conformation adopted. Dashed lines indicate a strong association and dotted lines indicate weak associations.

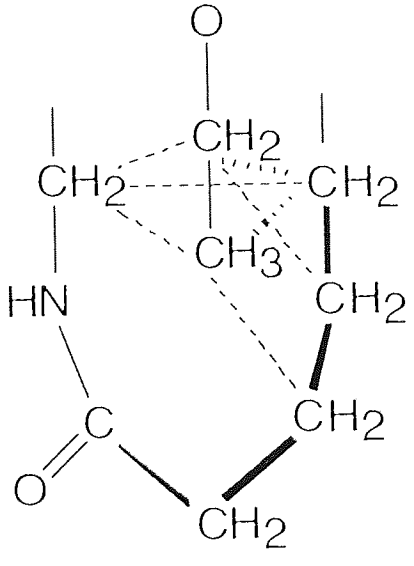

5.2.7 Copolymers of Maleic Anhydride

When hydrolysed copolymers of maleic anhydride with hydrophobic groups are converted to maleic acid and exhibit hypercoiling behaviour in aqueous solutions similar to SP-B, such copolymers are non-degradable. Figure 5.3 shows the chemical structure of Poly(styrene maleic anhydride).

Figure 5.3 Poly(styrene maleic anhydride)

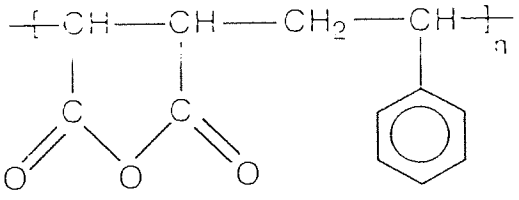

5.3 Methods

5.3.1 Cell Culture

The cell line used in the following experiments was CMT64/61 Mouse alveolar cells (ECACC 86082105) between passage numbers 2 and 6. The cell line was maintained in Waymouth MB752/1 Medium (Life Technologies), with 10% foetal bovine serum (Life Technologies) to supplement growth. Cells were sub-cultured at $1x10^4$ cells/ml when confluent and were found to have a growth rate of $0.57h^{-1}$, Figure 5.4.

Figure 5.4 Growth Curve of CMT64/61 Cell Line

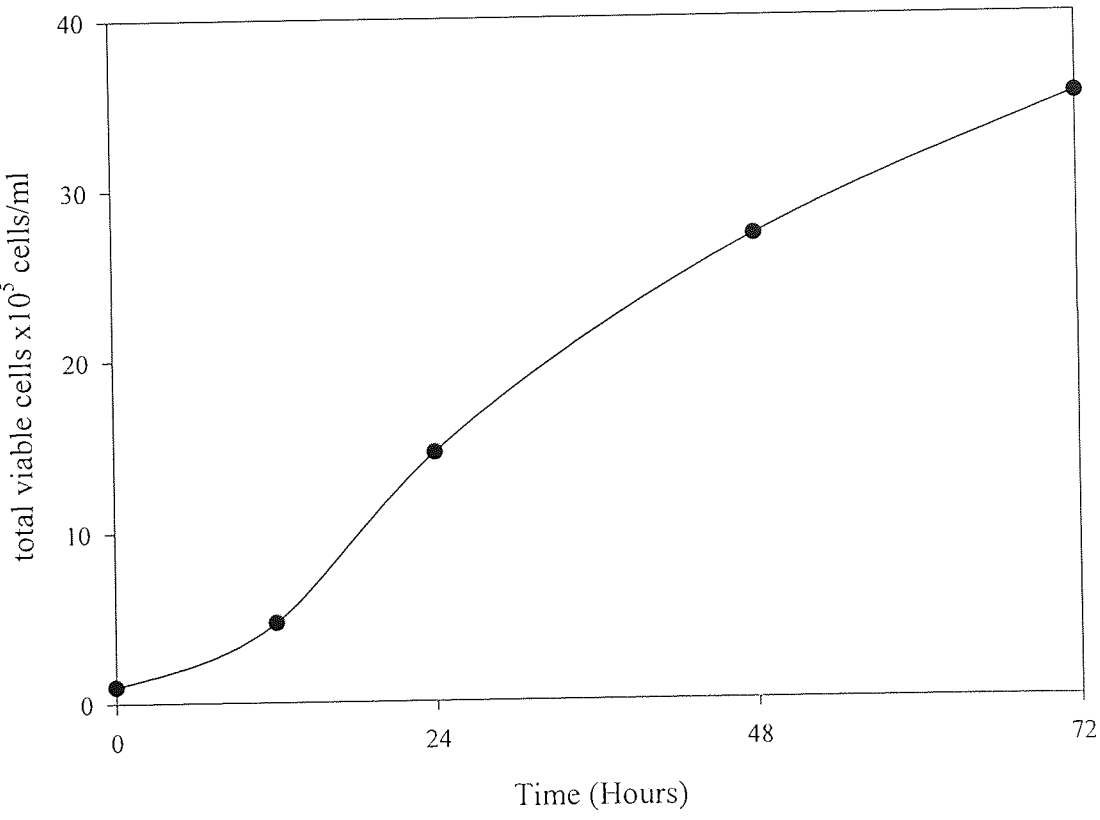

5.3.2 Determination of Cell Viability after Exposure to Artificial Surfactant

CMT64/61 cells were grown to 80% confluence within 25ml TCPS tissue culture flasks (Corning). Spent medium was taken off the cells, 20ml of new medium and 5ml of test solution added to the cells. The test solution was either Poly(lysine ethyl

ester adipamide) (PLETESA), Styrene maleic anhydride made in house (pMA/STY) or Styrene maleic anhydride from a commercial source (pMA/STY sp^2). The artificial surfactants were in a 0.4% NaCl saline solution (Sigma) ranging between 0.001 to 1 per cent wt/vol solution. The flasks of cells were photographed immediately before addition of the test solution, immediately after addition, 1h after addition, 6h after addition and after overnight culture (18h). Cells were then stripped from the flasks and the cell viability was counted using the Trypan Blue Exclusion Dye method.

5.3.3 Layering of TCPS Well Plates with PLETESA

A solution of PLETESA in HPLC methanol was added to 4 individual cell culture wells (Corning). The PLETESA ranging in concentration from 0.1% to 1%. The solutions were left overnight in a lamina flow hood to evaporate the methanol leaving a layer of PLETESA coating the bottom of the well. Mouse alveolar cells were then seeded onto the wells at a concentration of $1x10^5$ cells/ml. The well plate was left overnight in a Gallenkamp CO_2 incubator at 37°C and 5% CO_2/95% air atmosphere. In addition, untreated control wells, used to determine the background response of the Mouse alveolar cells, were seeded with the same concentration of cells.

5.3.4 Trypan Blue Exclusion Test for Viability

1ml of 0.25% trypsin/EDTA solution (Sigma) was added to the well and left to incubate with the samples for ten minutes within the Gallenkamp CO_2 incubator at 37°C and 5% CO_2/95% air atmosphere. Trypsin was neutralized by the addition of 1ml of Waymouth MB752/1 medium. Cell number and viability was determined by Trypan Blue (Sigma) prior to loading the haemocytometer and counting non viable (blue) and viable (translucent) cells.

5.4 Results

CMT/64/61 cells were exposed to solutions ranging from 0.001% to 1% wt/vol of PLETESA, pMA/STY and pMA/STY sp^2 in a NaCl saline solution were used to determine the cytotoxicity of the lung surfactant analogues as described in 5.3.2.

5.4.1 Exposure of CMT64/61 Mouse Alveolar Cells to Surfactants

Saline gave recovered cell numbers similar to the control (Waymouth medium), when seeded at 80% confluence the cells reached 100% confluence after 1 day both saline and medium, Figure 5.5. With surfactant there was a statistically significant trend showing that increasing the concentration of surfactant decreased the number of cell counts recovered from the sample with PLETESA concentrations above 0.1% and concentration's of pMA/STY and pMA/STY sp2 above 0.001% (assuming normal distribution heteroscedastic t-test assuming unequal variance), Figures 5.6 – 5.8. When the three surfactant cell counts were compared it was found that higher numbers of cells were seen with PLETESA containing samples, Figure 5.5. Samples with pMA/STY sp^2 gave the lowest degree of cell numbers recovered from wells (Figure 5.8) exposed to the surfactant and the surfactant pMA/STY (Figure 5.7) gave an intermediate result between the two other materials. Addition of pMA/STY sp^2 had no immediate effect on the alveolar cells although there was an indication of cells shrinking in size after 1h when 1% pMA/STY sp^2 was used. This effect was also seen to a lesser effect with 0.1% pMA/STY sp^2 after 1h.

After 24h, cells exposed to pMA/STY sp^2 at concentrations above 0.1% indicated that the cells appeared more spindly compared to controls, Plates 5.1 and 5.2. The layer of alveolar cells over the surface of the TCPS was not confluent and there was less proliferation of cells compared to cells exposed to similar concentrations of PLETESA. Lower concentrations of pMA/STY (0.001% and 0.01%) had no effect on cells until after 24h exposure. It was then observed that although the cells were intact they exhibited more of a fibroblastic like morphology as opposed to the expected epithelial morphology seen in controls and with cells exposed to PLETESA.

Exposure of alveolar cells to PLETESA appeared to produce no adverse cytotoxicity. Cells exhibited a confluent rounded epithelial morphology. At the 0.1% PLETESA concentration after 24h exposure, the cells started to exhibit fibroblastic like morphology and become more spindly. The appearance of the cells with 1% PLETESA was approximately the same as cells exposed to 0.1% pMA/STY sp^2, plates.

Figure 5.5 The Number of CMT64/61 Mouse Alveolar Cells Removed After Exposure to Lung Surfactant Protein Analogues Overnight (Mean Value n=4)

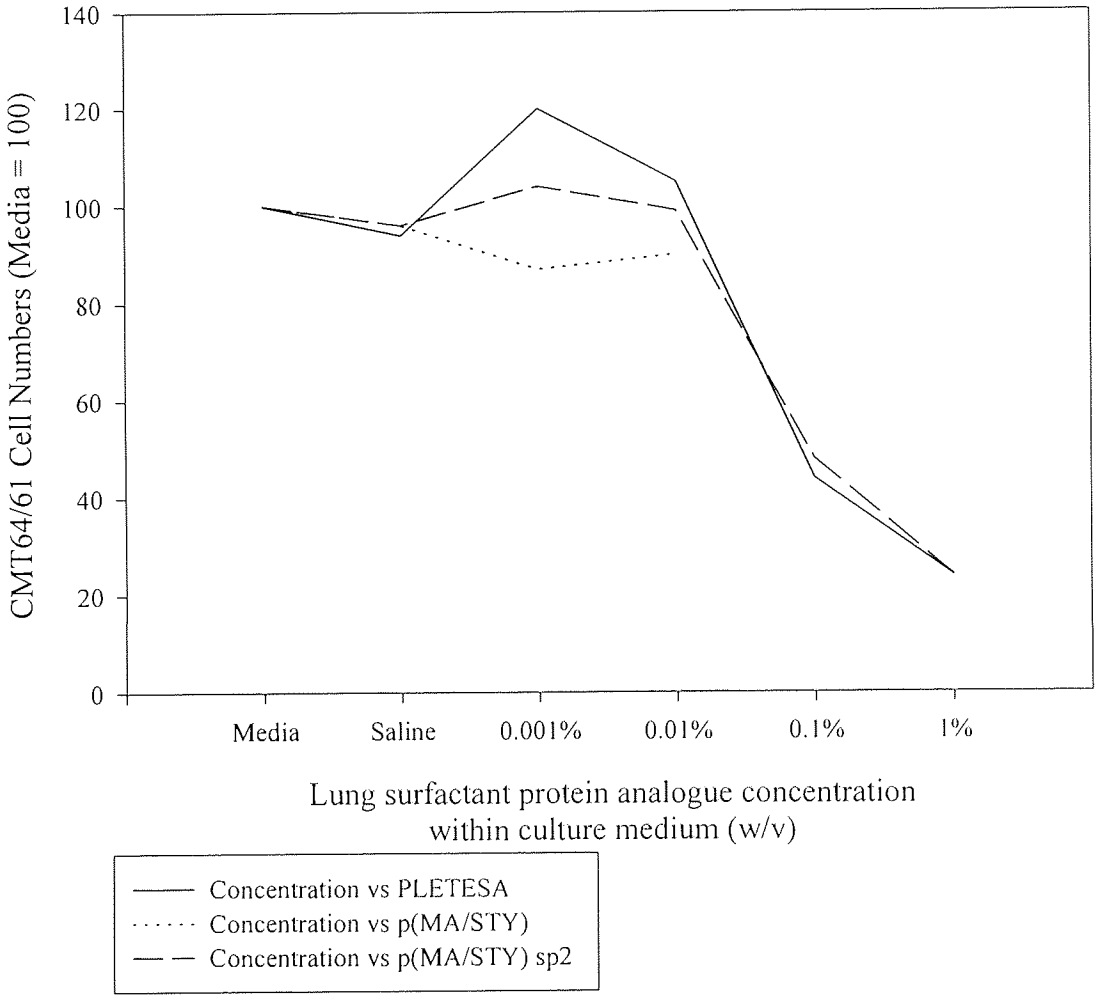

Figure 5.6 The Number of CMT64/61 Mouse Alveolar Cells Recovered After Exposure to PLETESA Overnight (Mean Value +/- S.D. n=4)

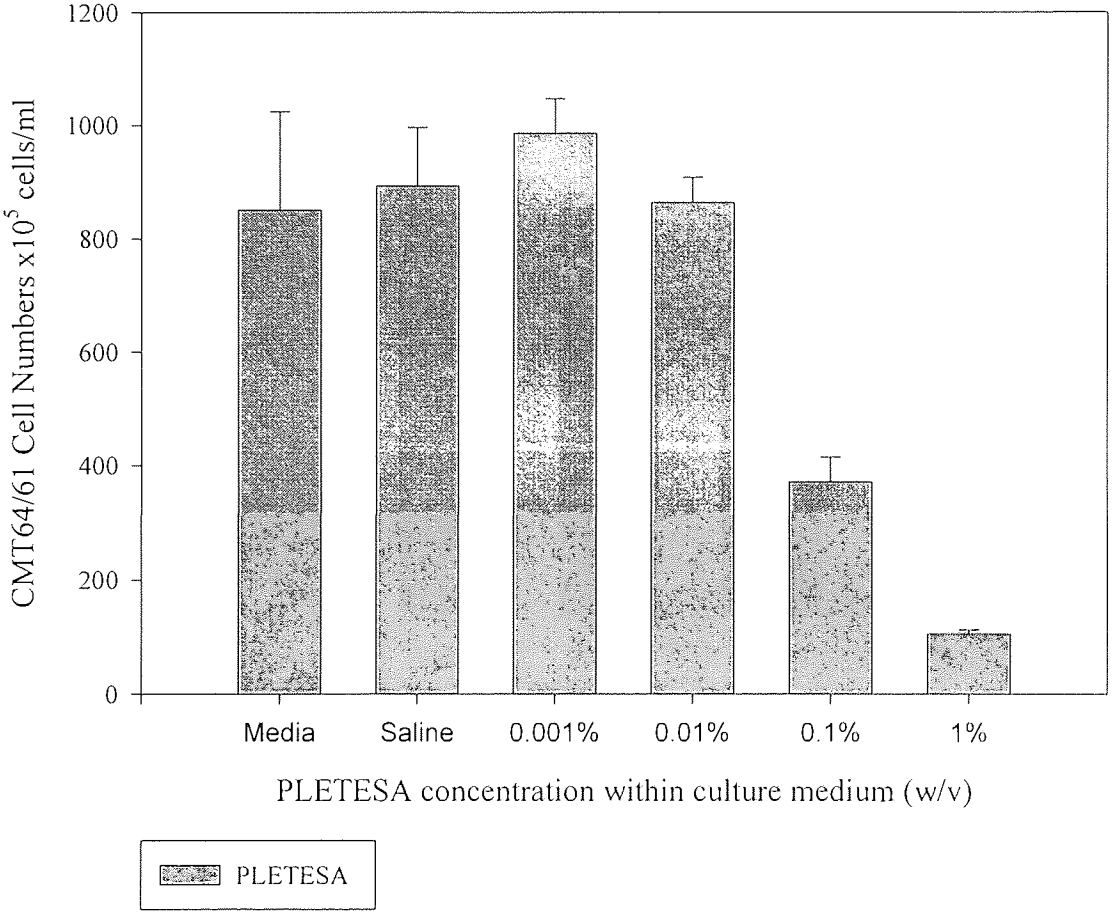

Figure 5.7 The Number of CMT64/61 Mouse Alveolar Cells Recovered After Exposure to pMA/STY Overnight (Mean Value +/- S.D. n=4)

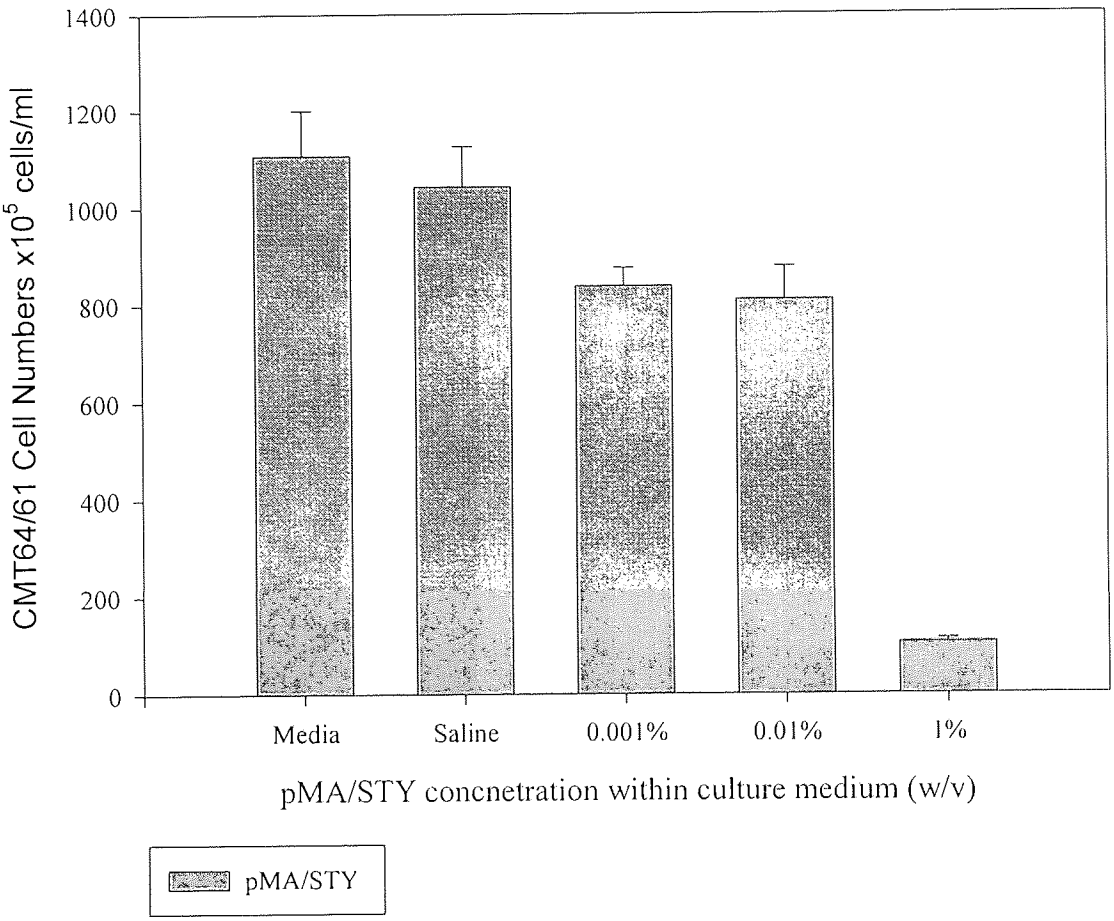

Figure 5.8 The Number of CMT64/61 Mouse Alveolar Cells Recovered After Exposure to pMA/STY sp^2 Overnight (Mean Value +/- S.D. n=4)

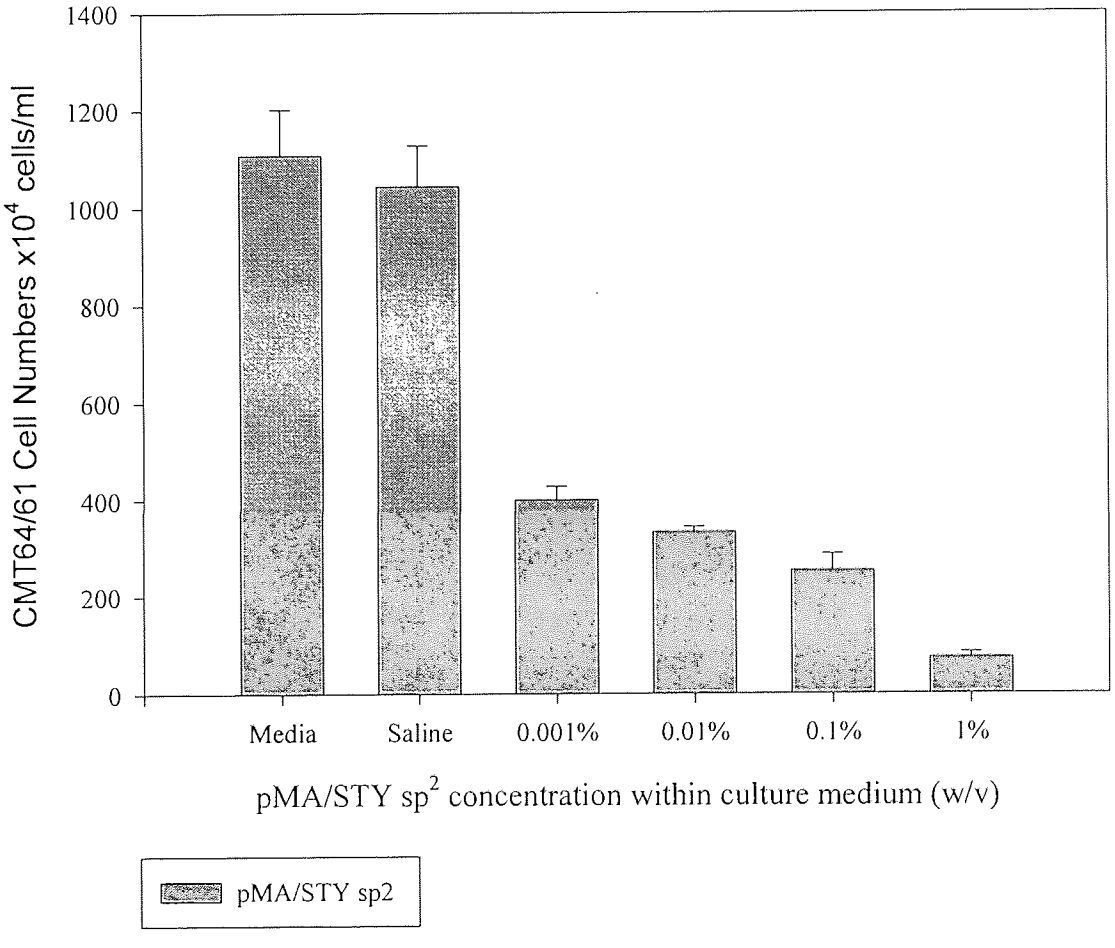

Plate 5.1 CMT64/61 cells 18h after addition of 1% pMA/STY sp^2
(magnification X200)

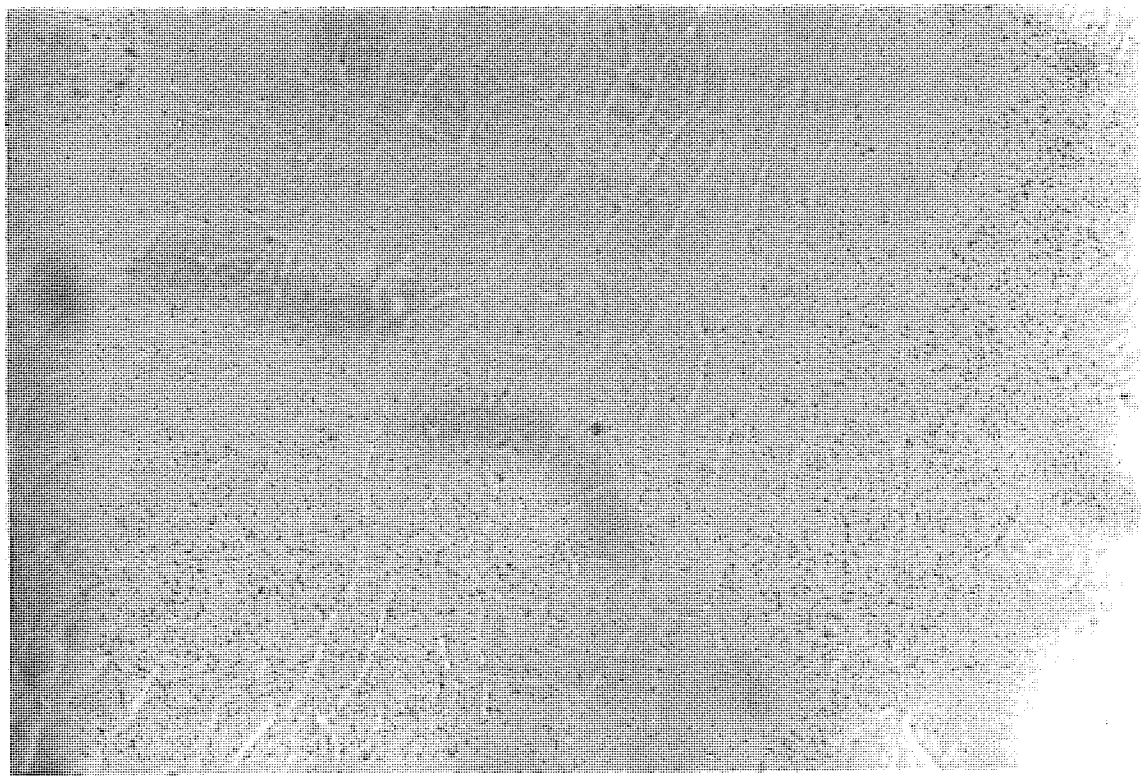

Plate 5.2 CMT64/61 cells control flask 18h after addition of new medium (magnification X200)

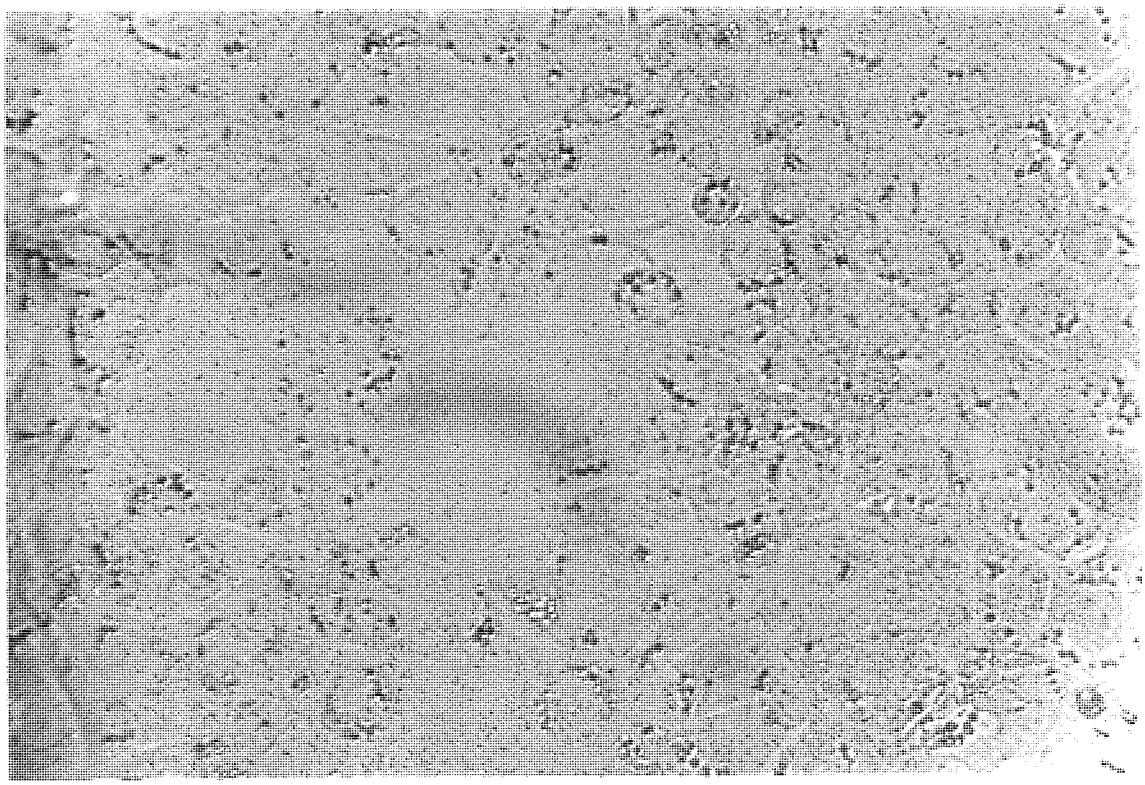

The viability of the samples exposed to surfactant all exhibited high levels of viability. With 1% pMA/STY sp^2 showing the lowest viability with 88% of total cells viable, Table 5.1.

Table 5.1 Viability of cells recovered from exposure of surfactant.

Sample	0%	Saline	0.001%	0.01%	0.1%	1%
PMA/STY	100	99	99	99	N/A	99
PMA/STY sp^2	99	99	99	100	99	88
PLETESA	100	100	99	99	99	100

PH

The pH of the medium did not change significantly when 1% pMA/STY was added.

Waymouth Medium (stock) pH	7.96
pH of medium removed from flask of CMT64/61 cells prior to addition of 1% pMA/STY	7.19
pH of medium removed from flask of CMT64/61 cells after 24h with 1% pMA/STY	7.09
pH of medium removed from control flask of CMT64/61 cells after 24h	7.08
pH of medium removed from flask of CMT64/61 cells after 24h with saline solution added	7.11

5.4.2 Layering of PLETESA on Tissue Culture Plastic

PLETESA was used at a concentration of 0.1% to 1% wt/v to layer TCPS well plate wells as described in 5.3.3.

The appearance of the cells in air dried methanol wells was identical to the untreated control wells. After 1h, the cells were rounded, however the cells were found to adhere to the surface of the tissue culture polystyrene (TCPS). After six hours there was clear evidence that the cells were spreading over the surface of the well plate, Plate 5.3. After 24h the bottom of the well plate was approximately 80% confluent. When 0.1% PLETESA was used to coat the surface of the well plate, cells still exhibited a rounded morphology after 6h. There was no indication of cell spreading over the well plate until after 22h of culture. At 22h, the extent of cell spreading was significantly less than that found with the control wells. With lower concentrations of PLETESA (below 0.3%) 60% confluence was reached, however, at concentrations above 0.3% at least 80% confluence was obtained.

Plate 5.3 CMT64/61 cells 6h after addition of new medium to well plate (control) (magnification X200)

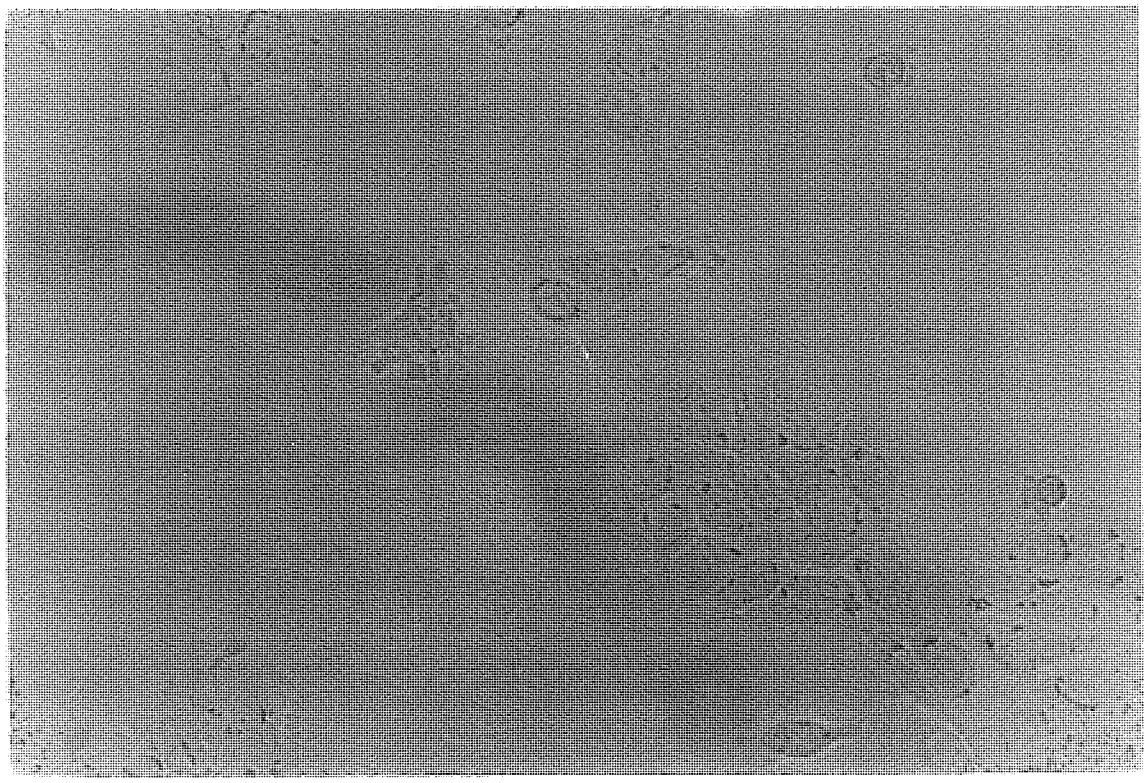

After the cell suspension was added to wells layered with concentrations of PLETESA higher than 0.5%, it was observed that bubbles became suspended in the medium (the bubbles having an approximate diameter of 25μm), Plate 5.4. The bubbles became progressively smaller over time. Cells exhibited a rounded morphology after 1h although cell spreading on the well plate surface improved with time. And compared more favourably than that observed after exposure to 0.1% PLETESA. Further investigation revealed that structures could be seen within the bubbles, Plate 5.5

At 6h it was observed that increasing the concentration of PLETESA from 0.3% to 1% progressively improved cell adhesion. This trend was repeated at 22h, however, when viewed after 22h it was seen that the cell multiplication appeared to not improve past a plateau reached with 0.5% PLETESA. Filopodia on cells also seemed to be progressively more numerous and more elongated at concentrations of PLETESA higher than 0.3%.

Plate 5.4 CMT64/61 cells 6h after addition of cells to well plate layered with 1% PLETESA (magnification X100)

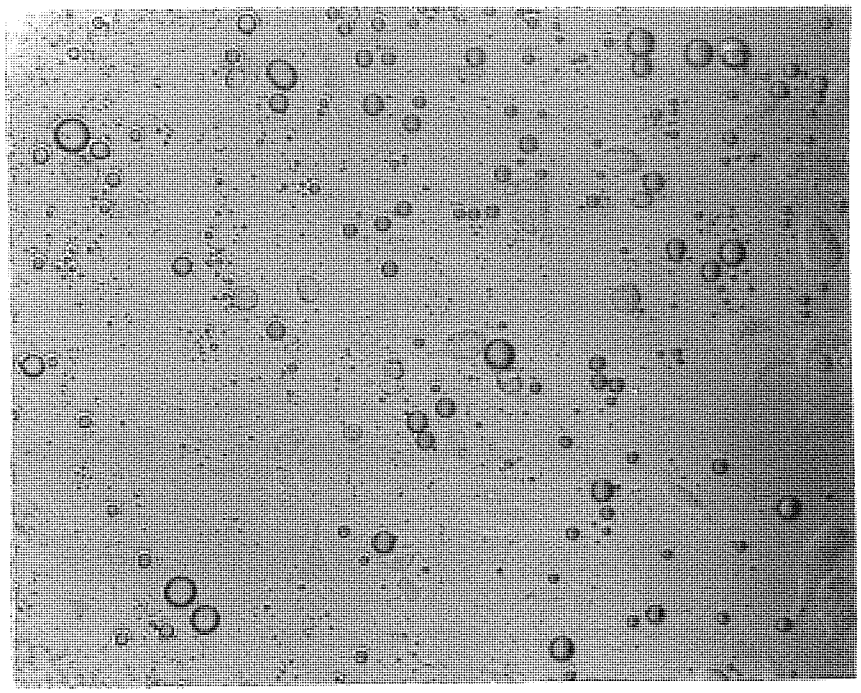

Plate 5.5 Bubbles seen in medium 18h after addition of cells to well plate layered with 0.1% PLETESA (magnification X200)

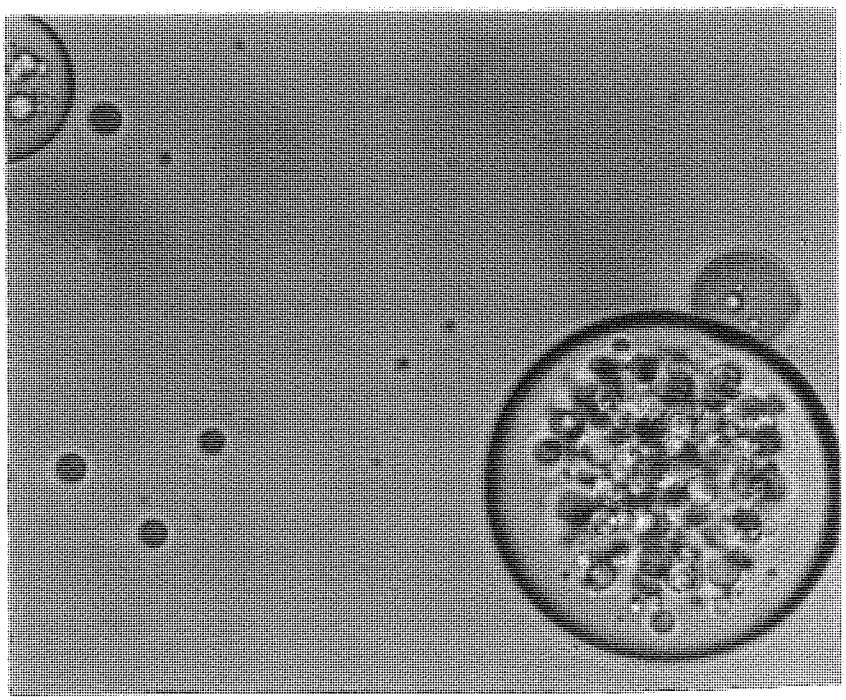

5.5 Discussion

5.5.1 Exposure of Surfactant to CMT64/61 Cells

It might have been expected that saline containing samples would have a slightly reduced cell growth rate due to the dilution of growth factors. This was indeed the case with the cell growth lower than in the control samples. However, the differences in cell growth with medium containing saline and medium were not significant.

Although pMA/STY and pMA/STY sp^2 were copolymers theoretically the same sample (one made in house the other purchased commercially) during use an odour reminiscent of toluine was noted with the commercially derived pMA/STY. If toluine contaminants were present in the sample this may have been inhibitory to cell adhesion and cell growth and could explain the differences in cell numbers between pMA/STY and pMA/STY sp^2.

The surfactants may possibly have had the ability to denature the enzymes in the trypsin solution. If this was mirrored in the viability one would expect that the samples would show low viability as cells with cell membranes fractured by the surfactant denaturing cell membrane proteins. It was seen during counting of the cell numbers that at higher concentrations of pMA/STY sp^2 there was an increased amount of cellular debris present. Rather than leaving a cell with a fragmented membrane which would have been recorded as non-viable the action of the surfactant and trypsin appear to cause cells to totally fragment. Surfactant may act as a membrane destabilizing influence disrupting and fragmenting cell membrane integrity. After exposure to high concentrations of pMA/STY sp^2 and treatment with trypsin a fragmentation of cells was seen. This would explain the very low cell numbers recovered from samples. Considering the results displayed with Figure 5.4 it would appear that the surfactants acted on cell multiplication in a concentration dependent manner. Where the cell numbers are inversely proportional to a concentration of surfactant. By increasing the concentration of surfactant there is a progressive degradation of the cellular membrane of cells exposed to the surfactant.

The trypsin used to strip cells off TCPS derived from a porcine pancreatic source. Tyrpsinogen is a proteolytic enzyme acting on lysyl and arginyl bonds of peptide chains and can hydrolyse esters and amides. With trypsinogen there could have been the possibility of contaminants of proteases, elastases, chymotrypsinogen, lipase and ribonucleases, all of which would allow the breakdown of extracellular matrix and cell membrane proteins.

When culturing cells there is generally thought to be no problem with the sub-culture of cells when viabilities above 70% are observed. It should be remembered though that the viability measured by Trypan Blue Exclusion Dye is an over estimate the number of cells still viable at 24h would be lower. The viability observed with alveolar cells was typical of that expected of lung cells when measured with Trypan Blue.

To determine cell viability more accurately the MTT assay could be employed. This test does not require cells to be stripped so that the cells are separate and thus the

effect of typsin in denaturing fragmenting cell membranes would be avoided. The MTT is also a more accurate measure of cell viability and would give a better estimate of the real viability of the cells present.

The change in pH due to the addition of the test solutions containing surfactant appeared to be within the buffering capacity of the medium.

5.5.2 Layering of PLETESA

In preparing a layer of polymer on which to grow cells on it was thought that methanol from a methanolic mixture would evaporate from the well plate during air drying leaving no residues. Results indicated that wellplates exposed to methanol allowed cells to grow at the same rate as untreated control wellplates, this confirmed that no cytotoxic materials appear to have been left as a residue.

When using a concentration of 0.1% PLETESA to coat a wellplate, the PLETESA may have covered the functional hydroxyl groups left on TCPS during gas plasma treatment to promote cell adhesion. The improved cell adhesion seen with 1% compared to 0.1% PLETESA may possibly be due to the more rugose surface which may have resulted with the increased amount of PLETESA used to coat the bottom of the well. 0.1% PLETESA only produced a thinly coated layer on the bottom of the well where functional groups from the gas plasma treatment were covered with the amide groups from PLETESA. However, with higher concentrations of PLETESA, the surface became more rugose and with a corresponding increase in surface energy this may have improved cell adhesion until a limit was reached where the increase in surface energy did not improve cell adhesion. The increase of cell adhesion was reached with a PLETESA concentration of 0.5%.

The cells observed with extended filopodia were possibly a strategic action by the cells aiming at assisting in adhering to a surface that was made less adhesive due to the layering of PLETESA if the layering was complete. Although rugose, the lack of hydroxyl groups (covered by PLETESA) required cells to adhere to amide functional groups presented by PLETESA. As these amide functional groups are weaker in their adhesive power, in order for the cells to remain attached they would have extended filopodia to adhere to more amide groups extending the cell over a larger area. When hydrolysed, PLETESA would have a negative and positive charge and this would facilitate adhesion to cell surfaces carrying an overall negative charge. The hydrolysis of PLETESA is likely as the medium used contained esterase enzymes which would hydrolyse the amide containing backbone of PLETESA. Thus the cell adhesion potential of PLETESA may only be temporary and dependent on the rate of hydrolysis of PLETESA by esterase enzymes. The change in morphology with cells exposed to pMA/STY sp^2 and pMA/STY could possibly be due to the surfactant acting on the cell membrane altering the conformation and possibly denaturing cell membrane proteins. The cell membranes being less stable shrunk and relied more on focal contacts anchoring the cells to the surface of the TCPS. Alternatively, if the layering of PLETESA was not complete the cells could have been attaching to those areas of TCPS that were not layered, hence the cells would appear to be stretched out. However, it would be expected that at higher concentrations of PLETESA the tendency for TCPS to be uncoated would be less. Fewer cells would be able to attach

to uncoated TCPS, the majority of cells would appear rounded (adhered to the PLETESA but not spread out) and a few cells that were be able to attach to unlayered areas would appear to be stretched out. However, the appearance of all the cells was uniform.

The bubbles in suspension with 1% PLETESA were probably the result of PLETESA having eluted into solution from the layer of dried polymer from the base of the well plate. This was supported by the fact that no bubbles were seen with solutions containing saline solution, medium, pMA/STY or pMA/STY sp^2. The decease in size of the bubbles could be explained by the PLETESA slowly settling down to coat the sides of the well. The breaking and rejoining of bubbles of PLETESA would indicate that the membrane of the bubbles exhibited low interfacial tension with the surrounding medium.

The bubbles of PLETESA could be acting in a manner analogous to crown ethers by taking up cations into the centre of a molecular complex. PLETESA amide heads could attach to cations in solution and form a shell. The tails of PLETESA join with other tails leaving a shield of spare PLETESA heads sticking out into the solution. This can attract further cations that join to the exposed amide heads of PLETESA. Ca^{2+} and Mg^{2+} cations are the most likely candidates in Waymouth medium, In addition, the medium contains the positively charged amino acids of L-histidine and L-lysine that could be taken up into the centre of the PLETESA bubbles.

5.6 Further Consideration

One way of determining the effect of PLETESA on cell adhesion would be to seed polystyrene with PLETESA. If the untreated polystyrene showed an improved cell adhesion when coated with PLETESA then this would be an indication that PLETESA improved cell adhesion to a material. Scanning electron microscopy could then be used to scan the surface of gas plasma treated polystyrene, untreated polystyrene and polystyrene layered with PLETESA, to determine whether the surface could be seen to be more rugose at the macroscopic level.

Atomic force microscopy also enables differences to be determined in the surface morphology by applying a very small mechanical force to the surface while scanning across the surface of the material. Atomic force microscopy does not damage specimens by using energetic electrons that are needed in producing scanning electron microscope images.[90] However, if PLETESA had affected the surface adhesive properties through a change in the overall electrostatic charge of the surface, this would not be seen by a SEM or by atomic force microscopy.

It would be interesting to determine whether the same cellular response to adhesion with PLETESA was found when using other cell lines. The alveolar cell line was used because the target for PLETESA was the alveolar cells. However, if PLETESA was used as a delivery system in other locations of the body then other cell lines such as BHK-21 cells may be used to determine the likely cytotoxicity of PLETESA *in vivo*.

5.7 Fluorescent Probe Conjugation to PLETESA

To determine if PLETESA was incorporated in the cell membrane of alveolar cells one could use a fluorescent probe attached to PLETESA conjugated to albumin. If the conjugated PLETESA probe was able to enter cells to attach to membranes it may be possible to confirm that PLETESA may be used as a drug delivery system.

In addition, it would be interesting to freeze dry a sample of bubbles of PLETESA. By use of a microtome it may be possible to observe the structure of such bubbles too see if they possessed any defined cross sectional arrangement.

5.8 Conclusions

All artificial lung surfactant analogues were found to be non cytotoxic yet the analogues did decrease cell proliferation when tested at higher concentrations. PLETESA had the least effect on cell numbers and pMA/STYsp^2 the most pronounced cellular inhibitory response. At the expected concentration of use the effect of the artificial lung surfactant analogues is likely to be minimal.

The mode of action in decreasing cell proliferation appears to be through membrane destabilization. At higher concentrations some instances of an abnormal fibroblast morphology were also seen.

Layering tissue culture well plates with PLETESA allowed cells to adhere in a concentration dependent manner until a limit was reached possibly due to inhibitory effects of rugosity and of the polar component of surface energy.

Bubbles of PLETESA can be created when the polymer dissolves in a solution of Waymouth medium. The bubbles appear to have a secondary structure possibly caused by complexing with cations or positively charged amino acids present in the growth medium.

CHAPTER SIX
Concluding Remarks on Cell Adhesion

6.1 Overview

The aim of this thesis is to report the behaviour of mammalian cells when placed in contact with synthetic polymers which have the potential for application to the human body. The thesis has addressed the cell adhesion properties and cytotoxicity of a number of hydrogels, as well as comparing closely related polymers to determine which hydrogels would fulfill their desired biomedical purpose. However, one must consider that the Trypan Blue Dye Exclusion techniques used to determine cytotoxicity may provide only a best estimate of cellular viability. Alternative cytotoxicity assays, such as the MTT assay, may provide more accurate cytotoxicity results and could be used to complement and confirm the results of the cytotoxicity assays undertaken in this work.

Investigation of the suitability of hydrogels for use as core and skirt components of a keratoprosthetic device has identified some interesting properties of the hydrogels tested. For example, a smooth hydrogel surface is generally non cell adhesive, as is a very rough hydrogel surface, the later will also allow a limited cell adhesion and proliferation. However, a slightly roughened surface generally achieves substantial cell adhesion and proliferation.[91] In addition, the investigation of cell adhesion on hydrogels with pores, fibres and whiskers has shown some promising developments as to how to achieve a more cell adhesive polymer. Pores appear to shield cells contained within from external shearing forces and provide a safe anchorage for cell multiplication. The pore size that enables improved cell adhesion of fibroblast cells ranges from 10μm to 50μm and corresponds to that reported by other researchers.[17,22,92,93,94] Fibres such as those comprised of calcium sodium or hydroxyapatite whiskers are also advantageous for cell adhesion and appear to allow cells to spread within the protective network of the fibres. It cannot be over emphasized that for the periphery of the keratoprosthetic skirt to maintain a secure integrated fit within the hosts tissue, the hydrogels used must allow cellular integration to occur and enable the corneal epithelium to grow over the hydrogel surface. It is hoped that the research on the initial cell adhesion of these hydrogels will give insights as to which polymers would be ideal to promote cell adhesion. Furthermore the formulation of composite materials with fibers may extend the suitability of hydrogels for *in vivo* materials that require both the flexibility offered by hydrogels, yet, also require greater strength that cannot be supplied by the hydrogel alone.[18,35,95,96]

The use of *in vitro* cell culture techniques to determine early biodegradation profiles of PHB-HV polysaccharide containing blends provides a sensitive technique to complement the physical techniques employed for the measurement of degradation. This technique achieves a greater sensitivity compared with other physical methodologies used to determine early degradation and will complement the research carried out to determine the degradation patterns of PHB-HV blends over time in physiological conditions. The discovery of a substrate in which a polysaccharide elutes out of PHB-HV may have applications in biodegradable wound dressings and implants. The ultimate aim of the research into PHB-HV blends is the development of a synthetic architecture that will maintain structural integrity, yet, over time will degrade and allow the replacement of synthetic materials by natural materials. The next stage in the development of a

biodegradable wound dressing is to determine whether the fibrous PHB-HV has sufficient flexibility, strength and non-antigenicity for use *in vivo*.[29] In addition, the combination of PHB-HV with polycaprolactone may extend the physical properties and may possibly enable further application of the polymer blends.[48] The degradation of an apparently solid material is a cautionary example to researchers illustrating how materials inserted *in vivo* may degrade over time and could possibly weaken to such as extent as to lead to implant failure.[50] Care should be taken to investigate the long term degradation profile of a material unless it is comparatively easy to replace periodically without any risk to the surrounding tissue of post operative tissue necrosis.[17,20,21]

A protein coat of a material may dramatically alter cell adhesion and can act as "conditioning" to promote cell adhesion.[43,44] The study of how differences in contact lens materials and wear regimes can influence the adsorbance of vitronectin provides some evidence of the propensity of different hydrogel materials to adsorb protein. In addition, the adsorbance of protein may be at different levels on different locations of a contact lens e.g. anterior versus posterior surfaces. This research may provide supporting evidence to indicate that increased levels of vitronectin may have the potential to increase ocular inflammation.

Not only was the cytotoxicity of the artificial lung surfactant analogue PLETESA tested, the surfactant analogue was also studied in its effect on cell adhesion with a layer of PLETESA coated onto a substrate. The discovery of multilaminar liposomes of PLETESA may be considered for additional research to determine the potential of the multilaminar liposomes as a drug delivery system.

6.2 Limitations of cell culture

There are a number of limitations associated with *in vitro* cell culture techniques. A single monolayer of cells will have different requirements and characteristics when compared to a multicellular formations of cells.[97] The *in vitro* environment will not duplicate the complex structural and biochemical interactions found *in vivo*, as biological processes will only occur at the cellular level. For example, nutrient and gaseous exchange *in vitro* are dependent upon diffusion, whereas *in vivo*, complex transport mechanisms are used to exchange nutrients as well as transport away waste products. This highlights the problem of clearance mechanisms, *in vitro* cell culture is essentially a closed system e.g. test substances may become toxic or concentrated only after metabolism by the liver. It must therefore be shown that drugs reaching cells *in vitro* are in the same form as those reaching cells *in vivo*. If a substance is not cytotoxic until metabolized in a particular tissue *in vivo*, the toxic form of the material will not be encountered *in vitro*. In addition, there can be significant differences in drug exposure time, rate of change of concentration, cell metabolism, tissue penetration, clearance, and excretion. For example, the dosage of a seemingly innocuous material may reach higher, possibly cytotoxic concentrations, if the body sequesters the material in a particular tissue. As there is only one type of cell grown *in vitro* at any one time, there can be no selective concentration of a substance within such a tissue type.

The development of organ culture techniques has enabled complex multicellular arrangement composed of different cell types to be tested *in vitro*. However, organ

culture will still only measure short term cytotoxicity as a single organ lacks the life support systems found *in vivo* and is unlikely to survive for anything other than a short period. *In vivo*, different organs specialize in their function, yet, act together to operate as a functional unit. The technique of organ culture has limited reproducibility, the size of organs will vary just as animals differ in size, thus a cytotoxic dose in one animal may not have the same result in another animal because of the difference in the size of the organ.

Although SEM techniques provide qualitative and quantitative analysis of samples with excellent high magnification images of cells, there are still a number of limitations in useage of this technique. In the first instance, SEM techniques are ultimately destructive, once prepared for SEM, the sample cannot be recovered and used again without the possibility of contamination from heavy metals and cytotoxic fixation agents. To achieve a high quality of preservation samples must be handled with care, fixed cells even after coating with heavy metals are still extremely fragile and are liable to be lost from the sample if the SEM stub is handled roughly.

Fixation and preservation may produce artifact images because the preservation and fixation protocols can change the cells' structure. For example, glutaraldehyde is used for cell fixation but without an additional osmium tetroxide treatment, cells can exhibit residual elasticity that may lead to the cells becoming rounded in morphology and lose their fine membrane detail.[98] Even the solvents used in critical point drying can extract lipids from cells and lead to shrinkage and loss of fine cellular detail.[43-44] SEM cell samples are not only subject to artifacts caused by chemicals, physical preservation methods may also alter their appearance. Water evaporation during critical point drying subjects samples to simultaneous crushing and tearing forces.[99] Unless there is a close adherence to the standard operating procedure the deviations from normal temperature and pressure can subject a sample to excessive deformation forces. Even using standard operation, cells can be subjected to considerable deformation, up to 20% linear deformation and 50% volume reduction.[44] Such deformation can change the appearance of cells from fibroblastic morphology to a rounded morphology, thereby leading the researcher to the wrong conclusion on the suitability of a polymer to adhere cells. Once an optimal preservation protocol is identified the protocol should not be deviated from if comparisons are to be made. Furthermore, if different protocols are used by different researchers, the comparison of should be viewed with caution.

One also has to consider that a SEM image covers only a small field of view. Individual samples may vary considerable in topography, cell density and cell preservation. The observer must not be biased in their selectivity, an average view of the sample must be taken and not merely that which best fits a particular theory. Futhermore, the information that the SEM micrographs provide should not be extrapolated, the images represent but a single image in time.[45] There is also the matter of analysis of SEM micrograph images. Fortunately fibroblastic cell morphology is quite easy to recognize, however, there is the question as to whether a spherical structure is a dead cell or merely debris and dust?[100]

In vitro cell culture requires aseptic operation, cell lines are easily contaminated by microorganisms and this contamination will negate the results of the assays

undertaken. Fortunately, hydrogels can be autocalved, however, care must still be taken that the numerous manipulations involved in cell culture do not introduce contamination. The original mammalian cell lines used as the cell source needs to be regularly examined to determine whether the cell line is contaminated prior to use. The presence of effectively dead cells at the end of an assay, as a result of microbial contamination, may be wrongly interpreted as indicative of a cytotoxic material.

Many materials can be sterilized with autoclave treatment, although, there remain certain materials that are not able to withstand autoclave treatment. To wash such materials with detergent and then incubate them with antibiotics may resolve this problem and remove the possibility of contamination but there is still the risk of contamination if the penetration of antibiotics is incomplete.[101] The issue of infection is an important consideration for materials designed for *in vivo* usage, as traumatized tissues are an ideal substrate for bacterial colonization and growth.[95] Inflamed tissues not only allow loss of protein and fluid but the cytolytic products of the inflammatory system may lead to tissue necrosis around an implant and lead to the eventual failure of the implant.[102]

It must be considered whether polymers produce the same cell colonization and cytotoxicity results in the short term. It has been reported that many non-cell adhesive materials will temporarily adhere cells, however, the effect is short lived and cells become eventually rounded and migrate where possible to a more suitable substrate.[103-104]

The Trypan Blue Dye Exclusion cytotoxicity test used to determine viability only takes into consideration the short term viability of cells and is prone to over estimates of the viability of the cell population, as cells frequently go into a decline that would not be detected by a short term assay (40% of the population may not be viable after 24h).[9] Short term tests only demonstrate whether cells are dead at the time of the assay. Trypan Blue Dye relies on membrane integrity to determine viability, where damaged membranes take up the dye which is impermeable to viable cells, although a cell may have an intact cell membrane the cell may be non viable. Also it would be unlikely that the uptake of the dye would be one hundred percent efficient. An alternative test to determine cell viability, such as the MTT assay, will measure the metabolic activity of the cell.[105] By measurement of the cell populations average metabolic activity a more accurate indication of the growth phase and general health of cells can be obtained. One way to determine the long term viability of a cell population is to recover the cells after the assay where the cell population is harvested and used to subculture a new generation of cells. The future cell populations can then be measured for any decline in growth rate and cell viability. If a substance is not cytotoxic and yet, inhibits or lessens the generation of cellular progeny then the monitoring of later sub-cultures of cells should identify the decline in cell growth.

The sub-culture of cells favours the isolation of cell sub-populations that are faster growing and are more adapted to *in vitro* conditions. Eventually the cells selected will be from only a small sub-population of the original cell line and the cells may have adapted to *in vitro* conditions to such as extent that they are atypical of the original cell line. Cells used in assays also need to be used at the same stage in their

growth phase e.g. if cells are harvested during the declining lag phase, the multiplication will be less rapid compared with that found in cells taken when in an exponential growth phase.[9] While *in vitro* tests give a quantitative evaluation over short periods of time and can replace to some extent *in vivo* testing in initial studies they are not a complete substitution for animal trials.

A toxic response *in vitro* can only be measured in terms of cell survival or metabolic alteration. Whereas *in vivo* the tissue may have an alternative response including, an inflammatory reaction or fibrosis. The lack of an immune system *in vitro* limits *in vitro* studies of inflammatory response to the release of immune system products from only one type of cell, such as PMN cells.

One must therefore ask is there any relevance in comparing *in vitro* studies to *in vivo* environments? Although cell culture methods can be presented in a skeptical light, their use to determine cytotoxicity and material biocompatibility is a great improvement on the adoption of a trial and error methodology. Cell culture is a valuable technique to employ in the assistance of the investigation of potentially biocompatible synthetic polymers for *in vivo* applications. As the *in vitro* techniques can provide an indication on how materials will behave *in vivo* and a fair correlation between *in vivo* and *in vitro* biocompatibility results for at least some prosthesis materials has been reported.[106] Early use of *in vitro* cell culture methods at the design and development stage of prosthetic devices may give an indication of the possible effect that the synthetic polymer employed will have when exposed to cells *in vivo*. This may eliminate unsuitable polymers before animal trials commence, by the provision of information in regard to how cells react with a synthetic polymer surface and eluted monomers. At the design and development stage it is better to try and fail many times, than to continue with fewer yet more comprehensive trials that have no guarantee of achieving the design criteria. While at later stages of development reduction in the number of unsuitable materials tested will allow more time and resources to be devoted to those materials that do fulfil the design criteria.

APPENDIX I

Cell Numbers Recovered from PHB-HV Degraded Samples (Chapter 3)

Table 6.1 Cell adhesiveness and cytotoxicity of BHK-21 cells seeded onto 12% HV PHB-HV 10% Dextrin blends (5 replicates)

Description	Mean Cell Value ($x10^5$ cells/ml) ± SD	Viability (%)	SEM
Undegraded	1.15±0.23	99	
7 days	1.51±0.51	99	
22 days	1.36±0.35	99	***
62 days	0.95±0.30	100	***
112 days	0.58±0.13	98	***
250 days	0.73±0.19	98	****

Table 6.2 Cell adhesiveness and cytotoxicity of BHK-21 cells seeded onto 12% HV PHB-HV 10% Dextran blends (5 replicates)

Description	Mean Cell Value ($x10^5$ cells/ml) ± SD	Viability (%)	SEM
Undegraded	1.19±0.34	98	
7 days	1.56±0.27	98	
22 days	1.20±0.20	98	****
62 days	1.82±0.24	99	**
112 days	1.64±0.21	99	****
250 days	1.25±0.22	96	*

Table 6.3 Cell adhesiveness and cytotoxicity of BHK-21 cells seeded onto 12% HV PHB-HV 10% Amylose blends (5 replicates)

Description	Mean Cell Value ($x10^5$ cells/ml) ± SD	Viability (%)	SEM
0 days	2.37±0.88	97	
7 days	1.71±0.27	98	****
7 days	1.50±0.30	96	
112 days	1.36±0.54	92	
180 days	1.24±0.32	94	
250 days	1.27±0.58	99	

Table 6.4 Cell adhesiveness and cytotoxicity of BHK-21 cells seeded onto 20% HV PHB-HV 10% Dextrin blend (5 replicates)

Description	Mean Cell Value ($x10^5$ cells/ml) ±	Viability (%)	SEM
Undegraded	1.46±0.25	98	**
7 days	1.07±0.19	98	**
62 days	3.17±0.32	99	***
112 days	1.16±0.18	100	****
180 days	1.11±0.27	98	****
250 days	1.04±0.20	100	****

APPENDIX II

Vitronectin Mediated Cell Adhesion (Chapter 4)

Table 6.5 The effect of adhesive proteins on cell adhesion to Group I contact lenses (6 replicates)

Vitronectin (μg/ml)	Mean cells per view ± S.D.
0	4±3
2	6±3
5	13±5
9	24±13
10	33±15
Fibronectin (μg/ml)	Mean cells per view ± S.D.
3	3±2
6	1±1
13	4±4
25	8±4
Lysozyme (μg/ml)	Mean cells
5	12±19
10	17±22

Table 6.6 The effect of anti-vitronectin and anti fibronectin antibodies on Acuvue (Group IV) contact lenses doped with fibronectin and vitronectin

Vitronectin	Fibronectin	Antibody	Mean cells per view ± S.D.	Statistical Significance
N	Y	None	5±6	N/A
N	Y	Anti-Fn	1±2	P<0.001
N	Y	Anti-Vn	3±2	P=0.065
Y	N	None	3±3	N/A
Y	N	Anti-Fn	2±2	P=0.456
Y	N	Anti-Vn	1±2	P<0.001

Table 6.7 Cell adhesion to worn Precision UV (FDA Group II) contact lenses (6 replicates)

Modality of wear	Side Measured	Mean cells per view ± S.D.
Unworn	N/A	8±4
Worn	Anterior	13±7
Worn	Posterior	32±20

Table 6.8 Cell adhesion to worn Surevue (FDA Group IV) contact lenses (6 replicates)

Modality of wear	Side Measured	Mean cells per view ± S.D.
Unworn	N/A	5±4
Worn	Anterior	7±4
Worn	Posterior	21±9

APPENDIX III

Cell Numbers Recovered from CMT64/61 Cells Exposed to Artificial Lung Surfactants (Chapter 5)

Table 6.9 Quantity of cells recovered from CMT/61 cells exposed to surfactant displayed as a proportion of 100 (control = 100)

Sample	0%	Saline	0.001%	0.01%	0.1%	1%
PMA/STY	100	94	76	73	10	10
PMA/STY sp^2	100	94	36	30	23	7
PLETESA	100	105	116	95	44	12

Table 6.10 Quantity of cells recovered from CMT/61 cells exposed to surfactant ($x10^5$ cells/ml) with ± Standard Deviation.

Sample	0%	Saline	0.001%	0.01%	0.1%	1%
PMA/STY	1108±94	1044±83	838±37	810±68	115±80	106±7
PMA/STY sp^2	1108±94	1044±83	400±28	333±11	253±34	74±10
PLETESA	851±173	894±103	987±60	865±44	372±43	106±7

APPENDIX IV - Materials

Anti-human fibronectin polyclonal antibodies derived from rabbit (Sigma F3648)

Anti-human vitronectin polyclonal antibodies derived from rabbit (Life Technologies 12114-013)

3T3 Swiss mouse embryo fibroblast cell line (European Collection of Animal Cell Cultures ECACC 88031146)

BHK-21 (Clone 13) baby hamster kidney cells (ECACC 850111433)
Cell culture flasks (Corning 25111-75)

NCTC Clone L929 mouse areolar cells (ECACC 88102702)

CMT64/61 Mouse alveolar cell line (European Collection of Animal Cell Cultures ECACC 86082105)

Dulbecco's Modified Eagle medium (Life Technologies 41966-029)
Fibronectin (Sigma F4759)
Foetal bovine serum EC approved (Life Technologies 10106-078)
Freon 113 1,1,2-Trichlorotrifluoroethane (Taab F012)
Fungizone (Life Technologies 15290-180)
Gentamycin (Sigma G1272)
Glutaraldehyde 25% (Taab Laboratories G005)
Glutaraldehyde 25% (aq) solution grade I (Sigma G-5882)
L-glutamine (Sigma G7513)
HEPES buffer 1M (Sigma H00887)
Lysozyme from chicken egg white (Sigma L-6876)
Magnesium chloride (BDH 26123)
Manganese chloride (BDH 10152)
Methanol (Aldrich, methyl alcohol anhydrous 99%+)
Phosphate buffered saline (Sigma P-4417)
Sp^2 maleic anhydride styrene (Speciality polymers)
24 Tissue culture polystrene wellplate (Corning 25820)
Trypan blue stain 0.4% (Sigma T8154)
Trypsin/EDTA 0.25% (Sigma T4049)
Tween 20 (Sigma P2287)
Vitronectin human plasma (Calbiochem 681105)
Waymouth's MB752/1 medium (Life Technologies 31220-023)

References

1. Tateishi, T., Ushida, T., Aoki, H., Ikada, Y., Nakamura, M., Williams, D.F., Clark, B., Stookey, G., Christel, P. and Pizzoferrato, 1992, A round-robin test for standardization of biocompatibility test procedure by cell culture method. Biomaterial-Tissue Interfaces P.J. Doherty *et al.* (Eds) Advances in Biomaterials 10, Elsevier Science Publishers page 89.
2. Thomas, K. D., Biological interactions with synthetic polymers. 1988, PhD Thesis, University of Aston, Birmingham.
3. Minett, W.T., 1986, Cell adhesion on synthetic polymer substrate. PhD Thesis, University of Aston, Birmingham.
4. Altankov, G. and Groth, T.H., 1994, Reorganization of substratum-bound fibronectin on hydrophilic and hydrophobic materials is related to biocompatibility. J. Mat. Sci. Mat. in Medicine. **5**, 732-737.
5. Fitton, H., 1993, Cells, Surfaces & Adhesion. PhD Thesis, University of Aston, Birmingham.
6. Richter, E., Fuhr, G., Muller, T., Shirley, S., Rogaschewski, S., Reimer, K and Dell, C., 1996, Growth of anchorage-dependent mammalian cells on microstructures and microperforated silicon membranes. J. Mat. Sci: Mat. in Medicine **7**, 85-97.
7. Kishida, A., Iwata, H., Tamada, Y. and Ikada, Y., 1991, Cell behaviour on polymer surfaces grafted with non-ionic and ionic monomers. Biomaterials, **12**, 786-792.
8. Springer, E.L, Hakett, A.J and Nelson-Rees, W.A., 1976, Alteration of the cell membrane architecture during suspension and monolayer culturing. Int. J. Cancer **17**, 407-413.
9. Freshney, R.I., (Ed) 1994, Cell culture of animal cells 3rd Edition. Wiley-Liss (NY).
10. Gumbiner, B.M., 1996, Cell Adhesion: The molecular basis of tissue architecture and morphogenesis. Cell. **84**, 345-357.
11. Lauffenburger, D.A. and Horwitz, A.F., 1996, Cell migration: A physically integrated molecular process. Cell **84**, 359-369.
12. Robertis De, E.D.P. and Robertis, E.M.F De Jr., 1987, Cell and Molecular Biology 8th Edition. Lea and Febiger, Philadelphia.
13. Holland, S.J., Jolly, A.M., Yasin, M. and Tighe, B.J., 1987, Polymers for biodegradable medical devices II. Hydroxybutyrate-hydroxyvalerate copolymers: hydrolytic degradation studies. Biomaterials **8**, 289-295.
14. Lydon, M.J., Minett, T.W. and Tighe, B.J., 1985, Cellular interactions with synthetic polymer surfaces in culture. Biomaterials **6**, 396-402
15. Britsh Standard BS EN 30993-5: 1994 ISO 10993-5: 1992, Biological evaluation of medical devices. Part 5. Tests for cytotoxicity, *in vitro* methods, British Standards Institution.
16. Roux, H., Duval, J.L., Sigot-Luizard, M.F. and Sigot, M., 1992, Assessment of the cytocompatibility of biomaterials by analysis of cellular viability in a Coulter multisizer multichannel analyzer. Biomaterial-Tissue Interfaces P.J. Doherty *et al.* (Eds) Advances in Biomaterials 10 Elsevier Science Publishers, page 81.

17. Leibowitz, H.M., Trinkaus-Randall, V., Tsuk, A.G. and Fransblau, C., 1994, Progress in the development of a synthetic cornea. Progress in Retinal and Eye Research, **13**, 2, 605-621.
18. Trinkaus-Randall, V., Capecchi, J., Sammon, L., Gibbons, D., Leibowitz, H.M. and Franzblau, C., 1990, In vitro evaluation of fibroplasia in a porous polymer. Invest. Ophthalmol. Vis. Sci. **31**, 1321-1326.
19. Chirila, T.V., 1994, Modern artificial corneas: the use of porous polymers. TRIP. **2**, 9, 296-300.
20. Kirkham, S.M., and Dangel, M.E., 1991, The keratoprosthesis: Improved biocompatibility through design and surface modification. Ophthalmic Surg. **22**, 8, 455-461.
21. Kenyon, K.R., Berman, M., Rose, J. and Gage, J., 1979, Prevention of stromal ulceration in the alkali burned rabbit cornea by glued on contact lens. Evidence for the role of PMN leukocytes in collagen degradation. Invest. Ophthalmol. Vis. Sci. **18**, 570-587.
22. Dohlman, C.H., 1983, Biology of complications following keratoprosthesis. Cornea **2**, 175-176.
23. Dohlman, C.H., Schneider, H. and Doane, M.G., 1974, Prosthokeratoplasty. Am. J. Ophthalmol. 77, 5, 694-700.
24. Castroviejo, R., Cardona, H. and DeVoe, A.G., 1969, Present status of prosthokeratoplasty. Am. J. Ophthalmol. **68**, 613.
25. Marchi, V., Ricci, R., Pecorella, I., Ciardi, A. and Tondo, U., 1994, Osteo-Odonto-Keratoprosthesis. Cornea, **13**, 2, 125-130.
26. Blencke, B. A., Hagan, P., Bromer, H. and Deutscher, K., 1978, Study on the use of glass cramics in osteo-odonto-keratoplasty. Ophthalmologica, **176**, 105-112.
27. Doane, M.G., Dohlman, C.,H. and Bearse, G., 1996, Fabrication of a keratoprosthesis. Cornea, **15**, 2, 179-184.
28. Imai, Y. and Masuhara, E., 1982, Long-term *in vivo* studies of poly(2-hydroxyethyl methacrylate). J. Biomed. Mater. Res. **16**, 609-617.
29. Corkhill, P.H., Hamilton, C.J. and Tighe, B.J., 1989, Synthetic hydrogels VI. Hydrogel composites as wound dressings and implant materials, Biomaterials **10**, 3-10.
30. Downes, S., Braden, M., Archer, R.S., Patel, M., Davy, K.W.M. and Swai, H., 1994, Modifications of polymers for controlled hydrophilicity: The effect on surface properties, Surface Properties of Biomaterials, Edited R.West and G. Batts (Proceedings of the International Symposium on Surface Properties of Biomaterials, Manchester, UK May 1992, Butterworth-Heinemann Ltd. Pages 11-23.
31. Wan, H., Williams, R.L., Doherty, P.J. and Williams, D.F., 1997, A study of cell behaviour on the surfaces of multifilament materials. J. Mat. Sci: Mat. Medicine **8**, 1, 45-51.
32. Lydon, F.J., 1994, Novel hydrogel copolymers and semi-interpenetrating polymer networks. PhD Thesis, University of Aston, Birmingham.
33. Sitlinger, M., Bujia, J., Rotter, N., Reitzel, D., Minuth, W.W. and Burmester, G.R., 1996, Tissue engineering and autologous transplant formation practical approaches with resorbable biomaterials and new cell culture techniques. Biomaterials, **17**, 237-242.
34. Horbett, T.A. and Schway, M.B., 1988, Correlations between mouse 3T3 cell spreading and serum fibronectin adsorption on glass and

hydroxyethylmethacrylate-ethylmethacrylate copolymers. J. Biomed. Mat. Res. **22**, 763-793.

35. Wisman, C.B., Pierce, W.S., Donachy, J.H., Pae, W.E., Myers, J.L. and Prophet, G.A., 1982, A polyurethane trileaflet cardiac valve prosthetic *in vitro* and *in vivo* studies. Trans. Am. Soc. Artif. Intern. Organs, **28**, 164-168.Yasin, M. and Tighe, B.J., 1993, Strategies for the design of biodegradable polymer systems: Manipulation of polyhydroxybutyrate-based materials. Plastics, Rubber and Composites Processing and Applications **19**, 1, 15-27.
36. Herold, M., Lo, H.R. and Reul, H., 1987, Polyurethane in Biomedical Engineering II. Planck, H., Syre, I., Dauner, M., and Egbers, G., (Eds), Amsterdam, Elsevier Sciences pages 231-256.
37. Jansen, J. and Reul, H., 1992, A synthetic three leaflet valve. J. Med. Eng. Technol. **16**, 27-33.
38. Hoffman, D., Sisto, D., Yu, L.S., Dahm, M. and Kloff, W.J., 1991, Evaluation of a polyurethane mitral valve prosthesis. Trans. Am. Soc. Artif. Intern. Organs, **37**, M354-M355.
39. Hennig, E. and Bucherl, E.S., 1984, Polyurethane in Biomedical Engineering I. Planck, H., Syre, I., and Egbers, G., (Eds) Amsterdam, Elsevier Sciences pages 109-134.
40. Freshney, R.I., (Ed) 1994, Cell culture of animal cells 3rd Edition. Wiley-Liss New York.
41. Lydon, M.J. and Clay, C.S., 1985, Substratum topography and cell traction on sulphuric acid treated bacteriological-grade plastic. Cell Biol. Int. Reps. **9**, 10, 911-921.
42. Doherty, P.J., Willians, R.L. and Willains, D.F., (Eds) 1992, Biomaterial-Tissue Interfaces. Proceedings of the Ninth European Conference on Biomaterials, Chester, UK September 1991, Elsevier, Amsterdam page 23.
43. Allen, T.D., 1983, The application of scanning electron microscopy to cells in culture: selected methodologies. SEM, **4**, 1963-1972.
44. Boyde, A., 1978, Pros and cons of critical point drying and freeze drying for SEM. SEM, **2**, 303-304.
45. Sjostrand, F.S., 1967, Electron microscopy of cells and tissues I. Academic Press, New York.
46. Richter, E., Fuhr, G., Muller, T., Shirley, S., Rogaschewski, S., Reimer, K. and Dell, C., 1996, Growth of anchorage-dependent mammalian cells on microstructures and microperforated silicon membranes. J. Mat. Sci: Mat. Med. **7**, 85-97.
47. Atkins, T.W. and Tighe, B.J., 1996, Preliminary *in vitro* cytotoxicity screening of a bead-formed macroporous hydrophilic polymer matrix. J. Biomater, Sci, Polymer Edn, **7**, 9: 759-768.
48. Yasin, M. and Tighe, B.J., 1993, Strategies for the design of biodegradable polymer systems: Manipulation of polyhydroxybutyrate-based materials. Plastics, Rubber and Composites Processing and Applications **19**, 1, 15-27.
49. Tighe, B.J., Franklin, V., Graham, C.D., Mann, A. and Guillon, M., 1996, Vitronectin adsorption in contact lens surfaces during wear: locus and significance. Second International conference on the Lacrimal Gland, Tear Film and Dry Eye Syndromes: Basic Science and Clinical Relevance, Bermuda November 1996.
50. Yasin, M., Holland, S.J., Jolly, A.M. and Tighe, B.J., 1989, Polymers for biodegradable medical devices VI. Hydroxybutyrate-hyroxyvalerate

coplymers: accelerated degradation of blends of polysacchardies. Biomaterials **10**, 400-412.
51. Holland, S.J., Yasin, M. and Tighe, B.J., 1990, Polymers for biodegradable medical devices VII. Hydroxybutyrate-hydroxyvalerate copolymers: degradation of copolymers and their blends with polysaccharides under *in vitro* physiological conditions. Biomaterials **11**, 206-215.
52. Yasin, M. and Tighe, B.J., 1993, Strategies for the design of biodegradable polymer systems: Manipulation of polyhydroxybutyrate-based materials. Plastics, Rubber and Composites Processing and Applications **19**, 1, 15-27.
53. Steele, J.G., Johnson, G., McFarland, C., Dalton, B.A., Gengenbach, T.R., Chatelier, R.C., Underwood, P.A. and Griesser, H.J., 1994, Roles of serum vitronectin and fibronectin in initial attachment of human vein endothelial cells and dermal fibroblasts on oxygen- and nitrogen- containing surfaces made by radiofrequency plasmas. J. Biomat. Sci.: Polymer Edn. **6**, pages 511-532.
54. Preissner, K.T., 1991, Structure and biological role of vitronectin. Annu. Rev. Cell Biol. **7**, 275-310.
55. Reilly, T.M., Lorelli, S.K., Pierce, S.M., Spitz, S.M. and Walton, H.L., 1993, Monoclonal antibodies against a recombinant form of plasminogen activator inhibitor-1: Effects on tissue plasminogen activator neutralizing and vitronectin binding properties. Fibrinolysis **7**, 373-378.
56. Sack, R.A., Underwood, P.A., Tan, K.O., Sutherland, H. and Morris, C.A., 1993, Vitronectin possible contribution to the closed-eye external host-defence mechanism. Ocular Immunology and Inflammation. **1**, 4, 327-336.
57. Sigurdardottir, O. and Wilman, B., 1992, Studies on the interaction between plasminogen activator inhibitor-1 and vitronectin. Fibronolysis. **6**, 27-32.
58. Steele, J.G., Dalton, B.A., Johnson, G. and Underwood, P.A., 1995, Adsorption of fibronectin and vitronectin onto Primaria™ and tissue culture polystyrene and relationship to the mechanism of initial attachment of human vein endothelial cells and BHK-21 fibroblasts. Biomaterials, **16**, 1057-1067.
59. Sigurdardottir, O. and Wiman, B., Studies on the interaction between PAI-1 and vitronectin. Scandinavian Journal. Clin. Lab. Invest. **52**,2, 107.
60. Steele, J.G., Johnson, G. and Underwood, P.A., 1994, Role of serum vitronectin and fibronectin in adhesion of fibroblasts following seeding onto tissue culture polystyrene. J. Biomed. Mat. Res. **26**, 861-884.
61. Sack, R.A., Underwood, A., Tan, K.O. and Morris, C., 1994, Vitronectin in human tears-protection against closed eye induced inflammatory damage. Lacrimal Gland Tear Film and Dry Eye Syndromes. (Ed) D.A. Sullivan, Plenum Press, New York, pages 345-349.
62. Sack, R.A., Tan, K.O. and Tan, A., 1992, Diurnal tear cycle: evidence for a nocturnal inflammatory constitutive tear fluid. Opthalmol. Vis. Sci, **33**, 626-640.
63. Tan, K.O., Sack, R.A. and Holden, B.A., 1993, Temporal sequence of changes in tear protein composition following eye closure. Opthalmol. Vis. Sci, **34** (suppl), 1468.
64. Sack, R.A., Tan, K.O., Chuck, J., Holden, B.A. and Vannas, A., 1992, Eye closure induces activation of tear plasminogen and complement systems. Opthalmol. Vis. Sci, **33** (suppl), 849.
65. Vannas, A., Sweeney, D.F., Holden, B.A., Sapyska, E.M. and Vaheri, A., 1992, Plasmin activity with contact lens wear. Curr. Eye Res, **11**, 243-251.

66. Hermann, M., Jaconi, M.E., Dahlgren, C., Waldvogel, F.A., Sendahl, O. and Lew, D.P., 1990, Neutrophil bactericidal activity against Staphylococcus aureus adherent to biological surfaces. Surface-bound extracellular matrix protein activate intracellular killing by oxygen-dependent and –independent mechanisms. J. Clin. Invest, **86**, 942-951.
67. Parker, C.J., Frame, R.N. and Elstad, M.R., 1988, Vitronectin (S-protein) augments the functional activity of monocyte receptors for IgG and complement C3b. Blood, **71**, 86-93.
68. Underwood, P.A., Steele, J.G. and Dalton, B.A., 1993, Effects of polystyrene surface chemistry on the biological activity of solid phase fibronectin and vitronectin analysed with monoclonal antibodies. J. Cell Science. **104**, 3, 793-803.
69. Vaheri, A., Bizik, J., Salonen, E.M., Tapiovaara, H., Siren, V., Myohanen, H. and Stephens, R.W., 1992, Regulation of the pericellular activation of plasminogen and its role in tissue-destructive process. Acta. Ophthalmol, **70**, 202, 34-41.
70. Minarik, L. and Rapp, J., 1989, Protein deposits on individual hydrophilic contact lenses: effects of water and ionicity, CLAO Journal, **15**, 3, 185-188.
71. Baines, M.G., Cai, F. and Bechman, H.A., 1990, Adsorption and removal of protein bound to hydrogel contact lenses. Optom. Vis. Sci, **67**, 807-810.
72. Bohnert, J.L., Horbett, T.A., Ratner, B.D. and Royce, F.H., 1988, Adsorption of proteins from artificial tear solutions to contact lens materials. Invest. Ophthalmol. Vis. Sci, **29**, 362-374.
73. Sack, R.A., Jones, B., Antignani, A., Libow, R. and Harvey, H., 1987, Specificity and biological activity of the protein deposited on the hydrogel surface. Invest. Ophthalmol. Vis. Sci. **28**, 842-849.
74. Groth, T., Zlatanov, I. and Altankov, G., 1994, Adhesion of human peripheral lymphocytes on biomaterials preadsorbed with fibronectin and vitronectin. J. Biomater. Sci. Polymer Edn, **8**, 729-739.
75. Underwood, A., Steele, J. and Dalton, A., 1993, Effects of polystyrene surface chemistry on the biological activity of solid phase fibronectin and vitronectin, analysed with monoclonal antibodies. J. Cell Science, **104**, 793-803.
76. Robertson, B., Van Golde, L.M.G. and Batenburg, J.J., 1992, (Eds). Pulmonary surfactant from molecular biology to clinical practice. Elsevier, Amsterdam, page 295.
77. Robertson, B., Van Golde, L.M.G. and Batenburg, J.J., 1992, (Eds). Pulmonary surfactant from molecular biology to clinical practice. Elsevier, Amsterdam, page 56.
78. Robertson, B., Van Golde, L.M.G. and Batenburg, J.J., 1992, (Eds). Pulmonary surfactant from molecular biology to clinical practice. Elsevier, Amsterdam, page 20.
79. Tonge, S.R., 1994, Hypercoiling & Hydrophobically Associating Polymers, PhD Thesis, University of Aston, Birmingham.
80. Wright, J.R. and Clements, J.A., 1987, Metabolism and turnover of lung surfactant. Am. Rev. Respir. Dis., **136**, 426-444.
81. Waver, T.E., Sarin, V.K., Sawtell, N.,Hull, W.M. and Whitsett, J.A., 1988, Identification of surfactant proteolipid SP-B in human surfactant and fetal lung. J. Appl. Physiol., **65**, 982-987.

82. Shimizu, H., Miyamura, K. and Kuroti, Y., 1991, Appearance of surfactant proteins, SP-A and SP-B in developing rat lung and the efects of *in vivo*, dexamethasone treatment. Biochim. Biophys. Acta, **1081**, 53-60.
83. Katyal, S.L., Singh, G., Ryan, L. and Gottron, S., 1988, Hydrophobic surfactant-associated proteins: electrophoretic and immunologic analyses and cellular localization in human lung. Exp. Lung Res., **14**, 655-669.
84. Robertson, B., Van Golde, L.M.G. and Batenburg, J.J., 1992, (Eds). Pulmonary surfactant from molecular biology to clinical practice. Elsevier, Amsterdam, pages 283-290.
85. Robertson, B., Van Golde, L.M.G. and Batenburg, J.J., 1992, (Eds). Pulmonary surfactant from molecular biology to clinical practice. Elsevier, Amsterdam, pages 19-28.
86. Robertson, B., Van Golde, L.M.G. and Batenburg, J.J., 1992, (Eds). Pulmonary surfactant from molecular biology to clinical practice. Elsevier, Amsterdam, pages109-152.
87. Bangham, A.D., 1987, Lung Surfactant: how it does and does not work. Lung, **165**, 17-25.
88. Robertson, B., Van Golde, L.M.G. and Batenburg, J.J., 1992, (Eds). Pulmonary surfactant from molecular biology to clinical practice. Elsevier, Amsterdam, page 609.
89. Tear-Centre Study Group, 1987, Tear-Centre trial of artificial surfactant (artificial lung expanding compound) in very premature babies. Br. Med. J. **294**, 991-996.
90. Jenny, C. and Vanasupa, L., 1996, AFM of biocompatible polymers. Microscopy and analysis, July, page 46.
91. Manly, R.S., 1970, Adhesion in biological systems. Academic Press, New York.
92. Trinkaus-Randall, V., Johnson-Wint, B., Banwatt, R.S., Gibbons, D., Capecchi, J. and Leibowitz, H.M., 1992, Matrix metalloprotein involvement in corneal healing. Invest. Ophthalmol. Vis. Sci., **33**, 983.
93. Legeais, J.M., Renald, G., Savoldelli, M. and Keller, N., 1988, Etude de la colonisation tissulaire du polytetrafluoroethylene expanse en vue de son utilisation comme support de keratoprothese. J. Ophthalmologie, **11**, 727-732.
94. Legeais, J.M., Renald, G., Parel, J.M., Serarevic, O., Mei, M.M. and Pouliquen, Y., 1994, A new fluorocarbon polymer for keratoprosthesis: Cellular ingrowth and transparency. Exp. Eye Res., **58**, 41-51.
95. Pintucci, S., Pintucci, F., Cecconi, M. and Calazza, S., 1995, New Dacron tissue colonisible keratoprosthesis: Clinical experience. Br. J. Ophthalmol, **79**, 825-829.
96. Kain, H.L.and Throft, R.A., 1987, A new approach to keratoprothesis prosthetics. Invest. Ophthalmol. Vis. Sci., **28**, (suppl), 229.
97. Bell, E., 1995, Tissue Engineering: Deterministic models for tissue engineering. J. Cellular Engineering, **1**, 28-34.
98. Arro, E., Collins, V.P. and Brunk, U.T., 1981, High resolution SEM of cultured cells: preparatory procedures. SEM, **2**, 159-168.
99. Cohen, A.L.,1979, Critical point drying-principles and procedures. SEM, **2**, 303-323.
100. Phillips, D.M., 1978, SEM for detection of mycoplasma contamination of cell cultures. SEM, **2**, 785-790.

101. Crawford, G.J., Chirila, T.V., Vijayasekoun, S., Dalton, P.D. and Constable, I.J., 1996, Preliminary evaluation of a hydrogel core-and-skirt keratoprosthesis in the rabbit cornea. J. Refractive Surgery, **12**, 525-529.
102. Gallico, G., 1990, Biologic skin substitutes. Clinics in Plastic Surgery, **17**, 3, 519-526.
103. Shay, J.W. and Walker, C., 1980, Introduction to cells in culture as studied by SEM. SEM, **2**, 171-178.
104. Carter, S.B., 1967, Hapotaxis and the mechanism of cell motility. Nature, **213**, 256-261.
105. Mosmann, T., 1983, Rapid colorimetric assay for cellular growth and survival. Application to proliferation and cytoxicity assays. J. Immunol. Methods, **65**, 55-63.
106. Marois, Y., Guidoin, R., Roy, R., Vidovsky, T., Jakubiec, B., Sigot-Luizard, M., Braybrook, J., Mehri, Y., Laroche, G. and King, M., 1996, Selecting valid *in vitro* biocompatibility tests that predict *in vivo* healing response of synthetic vascular prosthesis. Biomaterials, **17**, 1835-1842.